YOLLA SUBSURFACE DEVELOPMENT PLAN

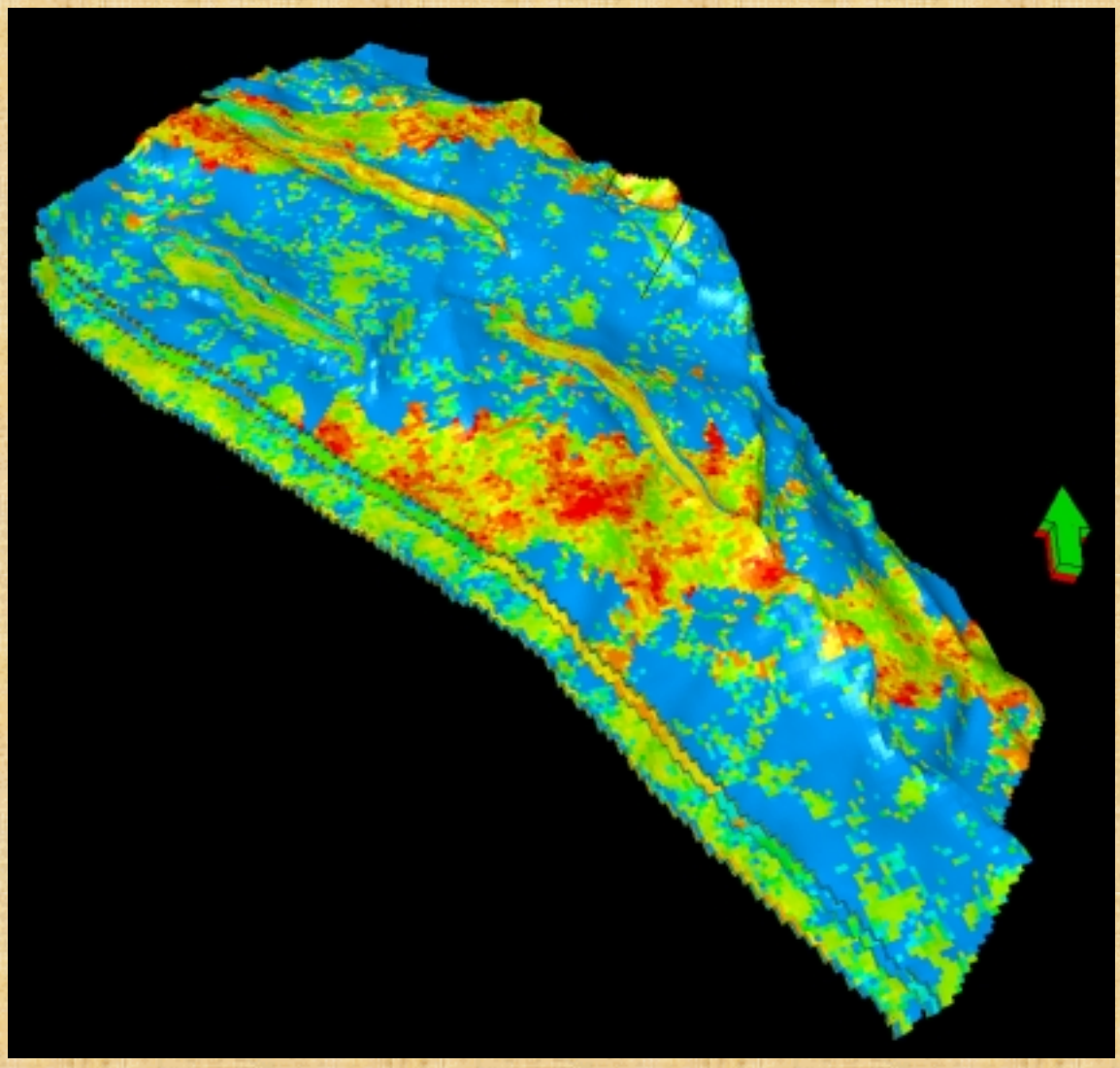

T/RL1: YOLLA GAS FIELD

Prepared by
Chung Chen
Stuart Tye
Randall Taylor
Mark Mussared

Origin energy
delivering the goods

Sept. 2001

EXECUTIVE SUMMARY

The T/RL1 Joint Venture proposes to develop the Yolla Gas Field to supply gas to customers in Victoria under gas sale agreements finalised in July 2001. Financial closure and regulatory approvals are targeted in 2002. First gas deliveries are scheduled for early 2004. Facilities construction would occur during 2003 and early 2004, and would include a wellhead platform installed over the field late in 2003.

The gas sale agreements call for annual deliveries of 20 PJ, which translates to an average field offtake rate of 72 MMscfd. The production and gas processing facilities are being designed to be capable of up to 84 MMscfd to allow for downtime and a small amount of overcapacity

The P50 gas reserves of the Yolla field are estimated at 337 bcf which will yield 256 PJ of sales gas. This estimate of reserves is identical to that of Malkewicz, Hueni and Associates (MHA) which undertook a reserves review in 2000. A field life of 16 years is forecast; 11 years at the plateau rate, and 5 years on decline. The production forecast for the most likely case is contained in Table 1.1.

The optimal subsurface development plan consists of four directional development wells drilled from the central platform location, into the gas reservoirs of the Intra-EVCM formation encountered by Yolla-1, at depths between 2700 metres and 3000 metres.

The objectives of the subsurface development plan are:

- Maximum economic recovery of Intra-EVCM reservoir raw gas reserves
- Evaluation of the individual performance of each of the 3 major sands in reserves recovery and deliverability
- Maintain field deliverability as long as possible above the contract rate
- Delay drilling of subsequent development wells as long as possible
- Appraise the Top-EVCM reservoir in 1 or more development wells

The optimal sequence for development drilling and compression in the most likely case has been determined as follows:

- An initial 2 wells drilled by a jackup rig over the wellhead platform after its installation late in 2003. These wells target locations in the main body of the Yolla field to the west and south of Yolla-1.
- A further 2 wells drilled by a jackup rig over the platform after approximately 7 years dependant on reservoir performance. These second phase wells target locations in the eastern portion of the field in areas potentially isolated from the first two wells by volcanic dykes.
- Wellhead compression added in year 9 of field life to reduce wellhead pressure and increase overall recovery.

Initial minimum flowing wellhead pressure will be 1200 psi (8270 kPa). Following the addition of compression, wellhead flowing pressures will reduce to 725 psi (5000 kPa).

The optimal tubing size has been determined to be 5 ½" OD allowing maximum deliverability per well and also the ability to lift liquids down to rates of less than 10 MMscfd.

All wells would be completed in such a way as to allow monitoring of the performance of individual sands. Detailed completion design is the subject of a separate drilling study, but the options being considered include a multi-tandem completion with multiple packers and sliding sleeves, and a monobore design with zone changes affected using casing patches and sequential perforating.

The production strategy is to produce each of the 3 major reservoir units separately for a period averaging 2 years in each of the first 2 wells over the first 6 years of field life. Bottomhole pressure surveys will be taken in each well at least annually to determine the decline curve of each layer. In this way, the volume of OGIP connected to each well in each layer can be determined, to evaluate the total volume of connected OGIP and the degree to which the eastern areas of the field are contributing. The timing of the second 2 wells will depend on the performance of the first 2 wells. They will be added in time to maintain deliverability above 84 MMscfd.

Apart from variation in OGIP, the main parameters with the potential to affect recovery of gas from the field are:

- Poorer than expected reservoir connectivity resulting from reservoir sand heterogeneity
- Volcanic dykes in the eastern areas of the field possibly forming barriers to flow

Modelling of these outcomes indicates that the subsurface development proposed would still achieve recoveries above the P90 level of 262 bcf (200 PJ) estimated by MHA.

TABLE 1.1

(Recoveries: 95% C3, 100% C4 and C5+)

Case: **Simulation Most Likely Case - Proved plus Probable OGIP, Reserves.**

OGIP **504 bcf** **P50**
Reserves **256 PJ**

Year	Sales PJ	Raw Production bcf	Cum Production bcf	Depletion %	CGR stb / mmscf	LPG t/mmscf	Condensate mstb	LPG ktonnes
			0.0	0%	46.7	3.016	0.0	0.0
1	20.0	26.3	26.3	5%	46.7	3.016	1227.3	79.3
2	20.0	26.3	52.6	10%	46.7	3.016	1226.7	79.3
3	20.0	26.3	78.8	16%	44.9	3.016	1179.6	79.3
4	20.0	26.3	105.1	21%	43.2	3.016	1135.6	79.3
5	20.0	26.3	131.4	26%	41.7	3.016	1095.2	79.3
6	20.0	26.3	157.7	31%	40.3	3.016	1058.4	79.3
7	20.0	26.3	184.0	37%	39.0	3.016	1025.5	79.3
8	20.0	26.3	210.2	42%	37.9	3.016	996.7	79.3
9	20.0	26.3	236.5	47%	37.0	3.016	972.2	79.3
10	20.0	26.3	262.8	52%	36.2	3.016	952.3	79.3
11	20.0	26.3	289.1	57%	35.7	3.016	937.2	79.3
12	19.6	25.7	314.8	62%	35.3	3.016	907.7	77.6
13	7.5	9.8	324.6	64%	35.2	3.016	346.0	29.7
14	4.6	6.0	330.6	66%	35.1	3.016	211.1	18.1
15	3.0	4.0	334.6	66%	35.1	3.016	139.6	12.0
16	1.9	2.5	337.2	67%	35.1	3.016	89.5	7.7
Total	**256**	**337.2**					**13,500.5**	**1,016.9**

LPG yield:	Av. Raw Content bbls/mmscf	Recovered bbls/mmscf
C3	24.5	23.3
C4	12.4	12.4
Total	36.9	35.7
Total - tonnes/mmscf		**3.016**

Table of Contents

Page No.

List of Figures

1 INTRODUCTION

The Yolla Gas Field is located in T/RL1 in the Bass Basin, 120km offshore from Tasmania and 220km SSE of Melbourne in a water depth of 80m. The field is a large northwest-southeast trending anticlinal feature which has been compartmentalized by major faults.

Two wells have been drilled in the Yolla Field. Yolla 1 was drilled in June 1985 and encountered gas in both the top of the Eastern View Coal Measures (EVCM) and also in the Intra-EVCM. Gas Pay was encountered in five separate zones within the latter interval and this has been the principal focus for potential appraisal and development.

A 3D seismic survey was shot over the Yolla Field in mid 1994 with the aim of enabling more accurate depth mapping for the purpose of reserves estimation and appraisal/development planning. These data were subsequently reprocessed in early 2000. Updated depth maps were produced in December 2000 and January 2001 and form the basis for the latest field review contained herein.

The last reserves audit by Boral Energy Resources Ltd was conducted in July 1999. This audit was undertaken as a result of discrepancies identified in the depth mapping used in previous reserves calculations. Subsequent to this work, Malkewicz Hueni Associates (MHA) was contracted by Origin Energy Resources Ltd to perform a review of reserves in the intra-EVCM reservoirs (2700 to 3000 m RT approximately). This study reviewed all core, log, DST, RFT, fluid property and petrophysical data and provided a probabilistic estimate of reserves for both the Yolla Main and Yolla North Blocks. Origin Energy subsequently adopted the gas reserve volumes calculated by MHA as it's booked reserves for the field, and have been referenced in subsequent gas sales contract negotiations.

Origin Energy and the Yolla Joint Venture now propose to develop the Yolla Gas Field to supply gas to customers in Victoria. Engineering and Environmental work is currently underway which will lead to a development plan and budget for consideration for approval by the Joint Venture, and which forms the basis of an EES/EIS process for gaining the necessary environmental regulatory approvals

As part of the total approvals process, this report provides the subsurface development plan for the Yolla Gas Field. The report reviews the ultimate recoverable reserves, evaluates the optimum development scheme of well locations and timing, and investigates the potential impact of varying reservoir parameters on the field performance under this scheme. The study was conducted in 4 phases:

1. Field seismic reinterpretation, mapping and depth conversion following the seismic reprocessing completed early in 2001.
2. Geological modelling for OGIP determination and input to the reservoir modelling
3. Eclipse reservoir simulation modelling to determine the optimum well completion strategy and drainage locations and to provide production, well timing and compression timing forecasts.
4. Development of preliminary well drilling paths and formation top prognoses for input into the development drilling budget costings.

2 YOLLA 3D INTERPRETATION AND DEPTH MAPPING

2.1 Time Structure Mapping

The reprocessed Yolla 3D Seismic Survey was loaded into Schlumberger's Geoframe software and interpreted using the IESX and Geoviz modules. Eight horizons were interpreted as shown in Figure 2.1 and Table 2.1. The upper horizons were used for the interval velocity depth conversion.

Horizon Interpreted	Seismic Character	Purpose
Water Bottom (WB)	Strong Peak	Interval velocity depth conversion
Lower Mid Miocene (LMM)	Strong Peak	Interval velocity depth conversion
Top Volcano (V)	Strong Peak	Interval velocity depth conversion
Base Volcano (BV)	Strong Peak	Interval velocity depth conversion
Near top EVCM	Strong Trough	Secondary target
Middle M.Diversus (MDIV)	Strong Peak	Used to constrain picks on deeper horizons
Top 2718 Sand	Weak Peak	Uppermost sand of the main reservoir section
Top 2809 Sand	Weak Peak	Most prominent event within main reservoir section

Table 2.1: Horizons interpreted as a part of the remapping of the Yolla Field.

2.2 Well Ties

Synthetic seismograms were generated with the "Geoframe Synthetic" software and used to tie the well data into the 3D grid. A composite traverse between the wells shows the final tie of the Gamma ray logs to the seismic data (Fig. 2.2).

Time Interpretation

Time structure maps were produced for all horizons shown in Table 2.1. Picks were interpreted on every 5th inline and cross-lines were interpreted as required. Auto-tracking was used to fill in the remaining lines in the 3D grid. Time picks for the 2809 sand to the north of the field could not be made due to a deterioration in data quality, however this region is outside the area of the gas accumulation. Time maps for the main three target horizons are shown in Figures 2.3 to 2.5.

2.3 Dykes and Sills

The Yolla 3D region is intersected by a number of prominent dykes and several smaller ones that disrupt the stratigraphy. These features are prominent on the variance-cube time-slices, on which they can be seen to strike approximately N-S, (Fig. 2.6). The dykes are interpreted to be the primary source of the mid-Tertiary volcanism and also to be the source of a number of sills that have intruded the Eastern View Coal Measure

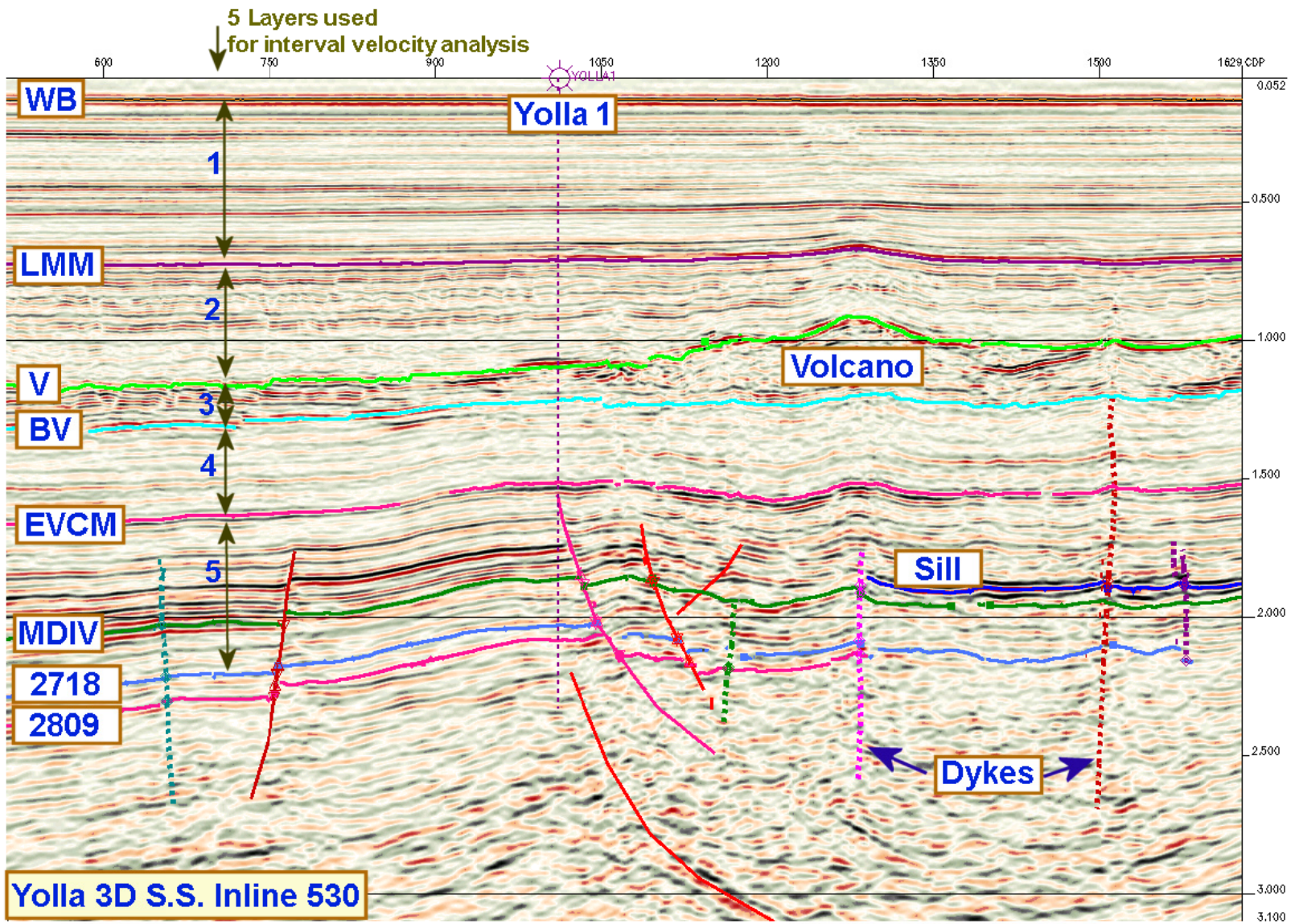
5 Layers used
for interval velocity analysis
600
750
900
1050
1200
1350
1500
1629 CDP
YOLLA1
Yolla 1
WB
LMM
V
BV
EVCM
MDIV
2718
2809
1
2
3
4
5
Volcano
Sill
Dykes
Yolla 3D S.S. Inline 530
0.052
0.500
1.000
1.500
2.000
2.500
3.000
3.100

Figure 2.1

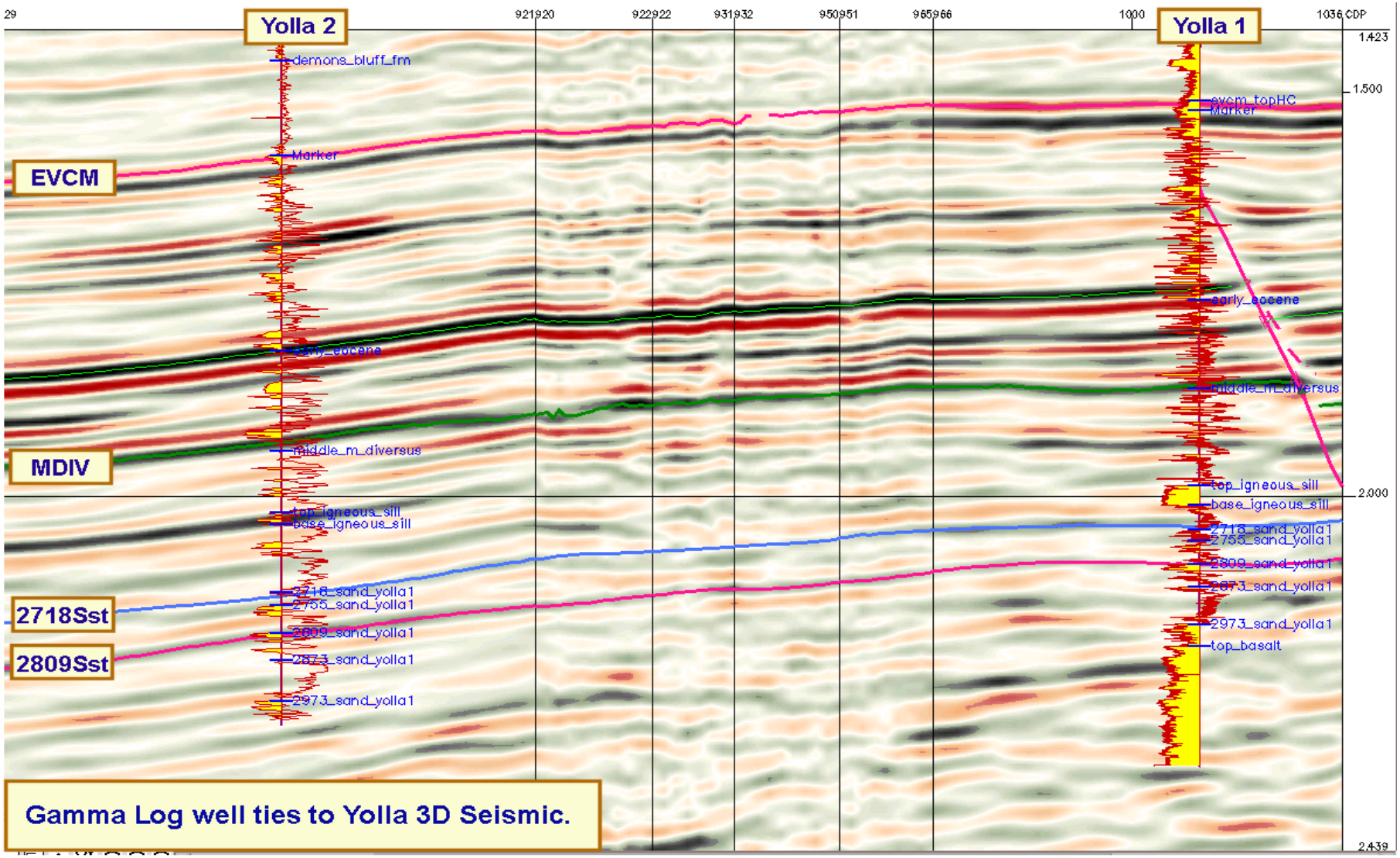

Figure 2.2

Gamma Log well ties to Yolla 3D Seismic.

Yolla Gas Field T/RL1

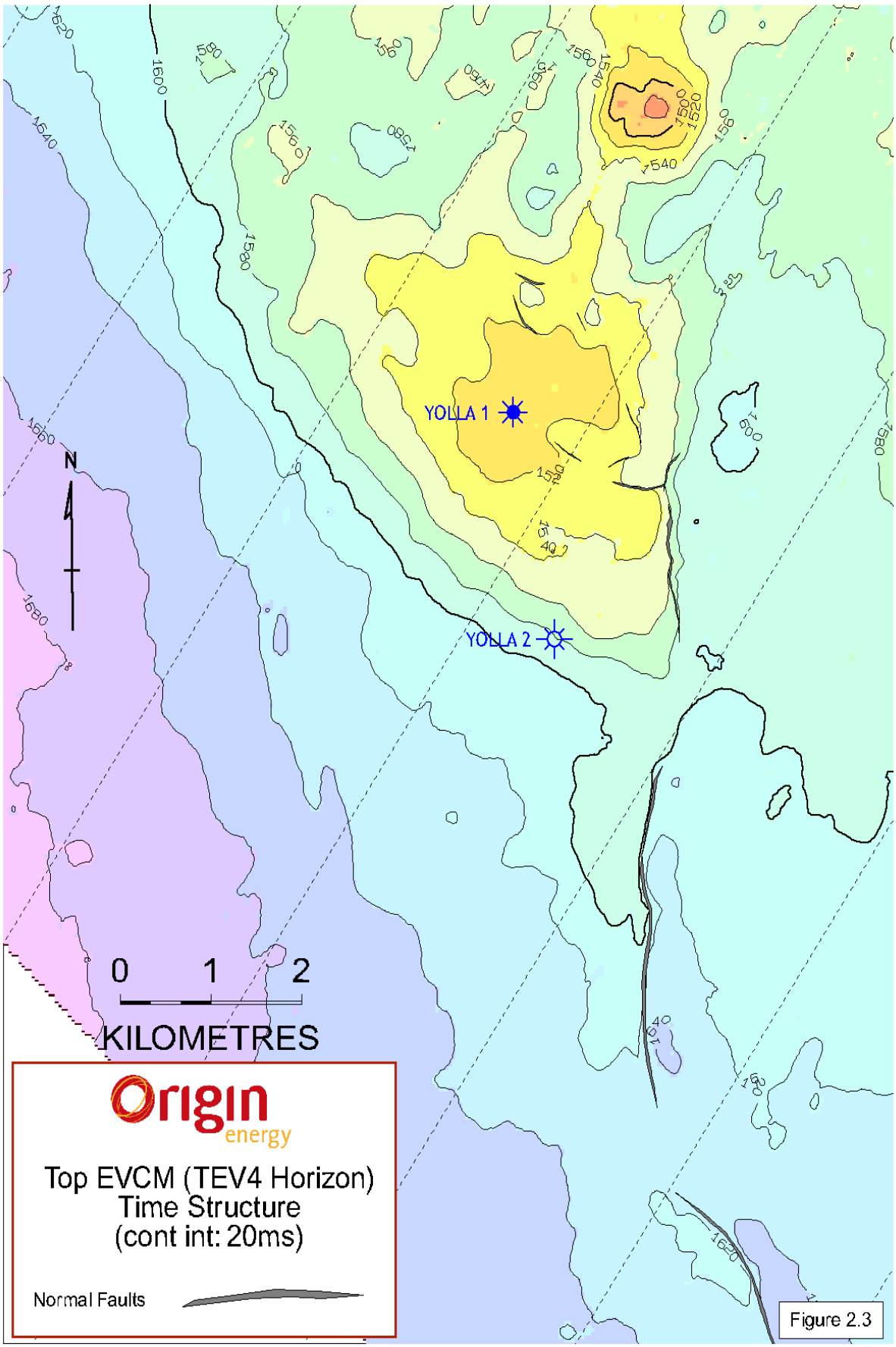

Figure 2.3

Yolla Gas Field T/RL1

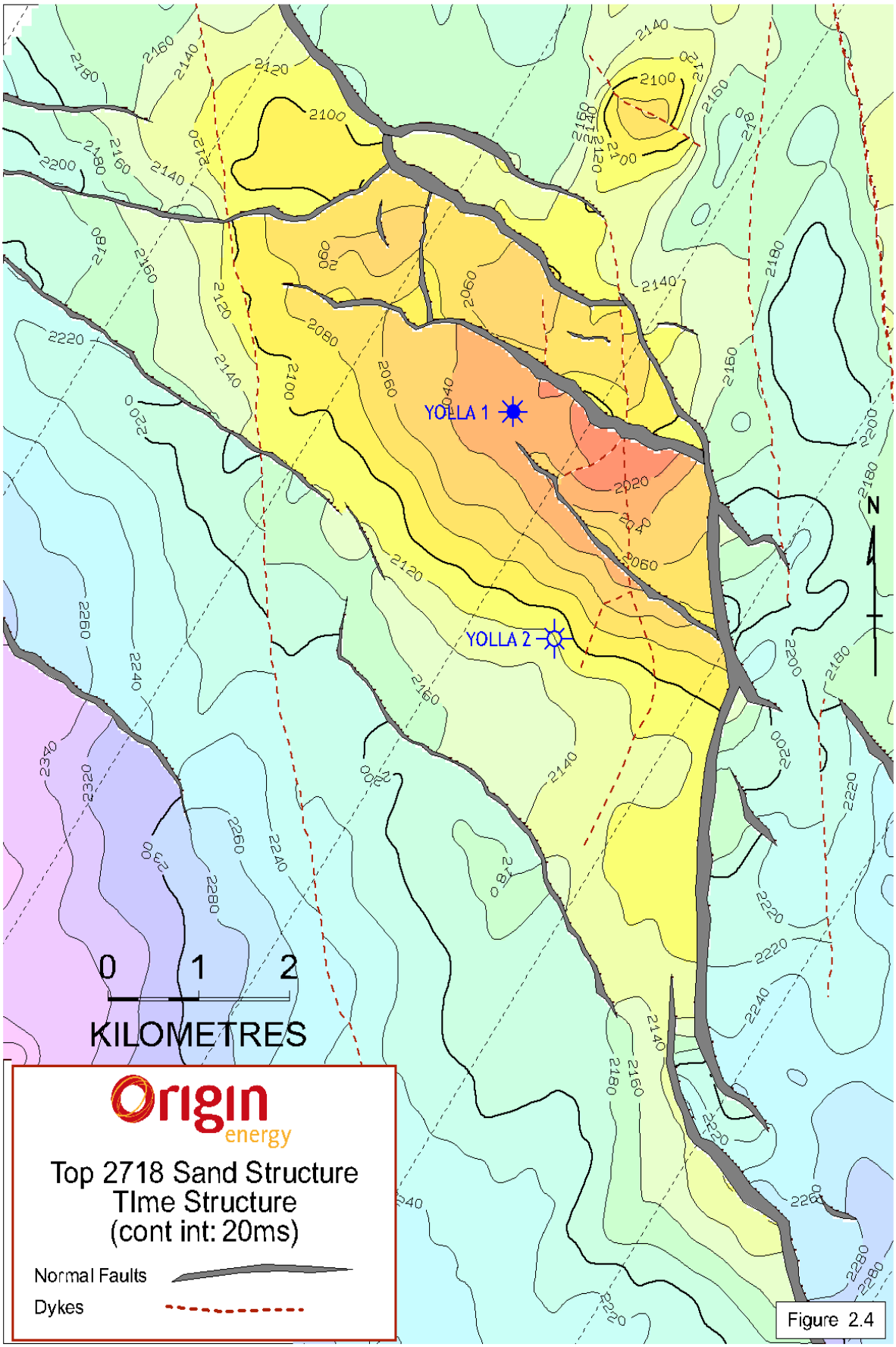

Figure 2.4

Yolla Gas Field T/RL1

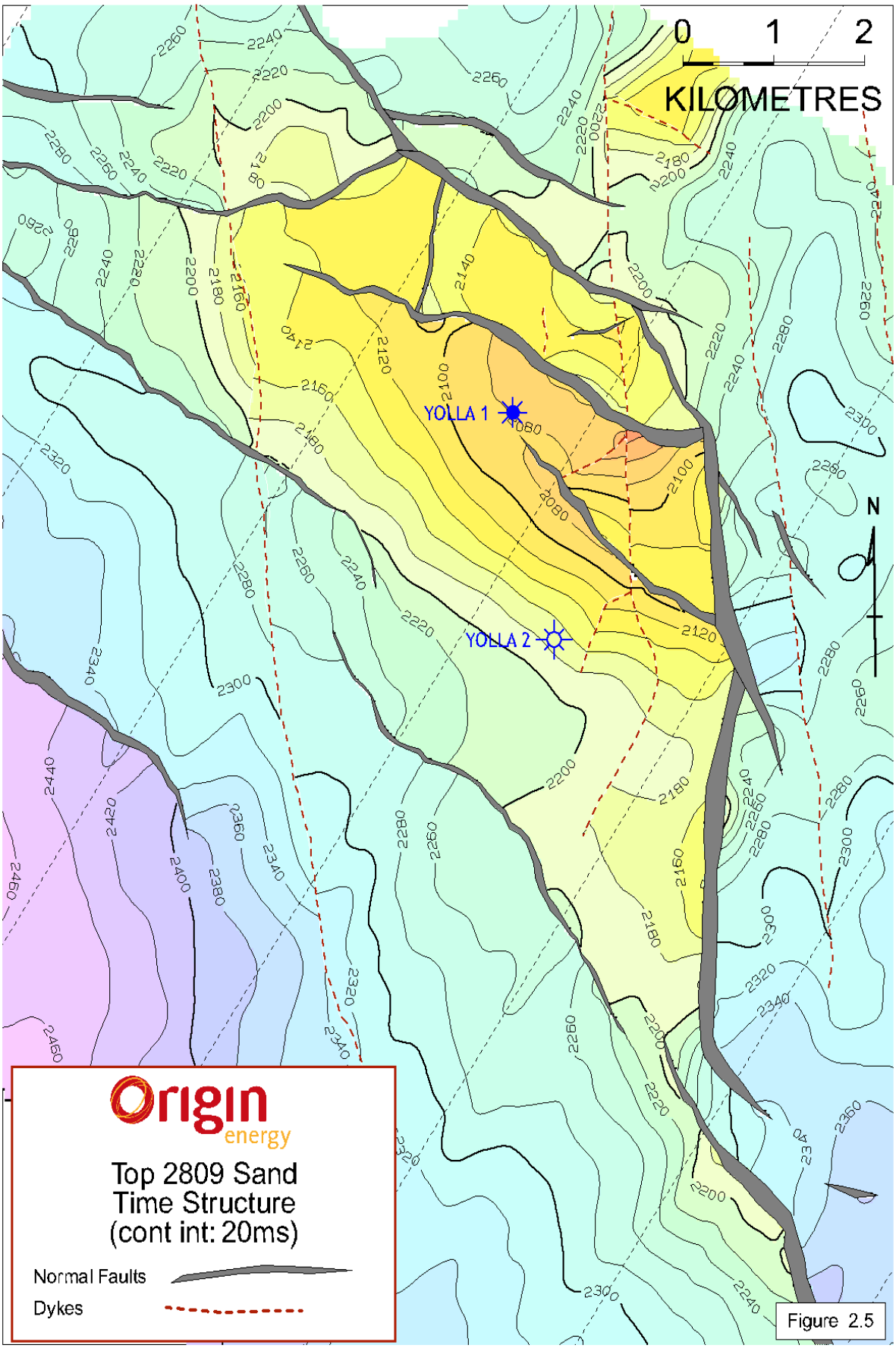

Figure 2.5

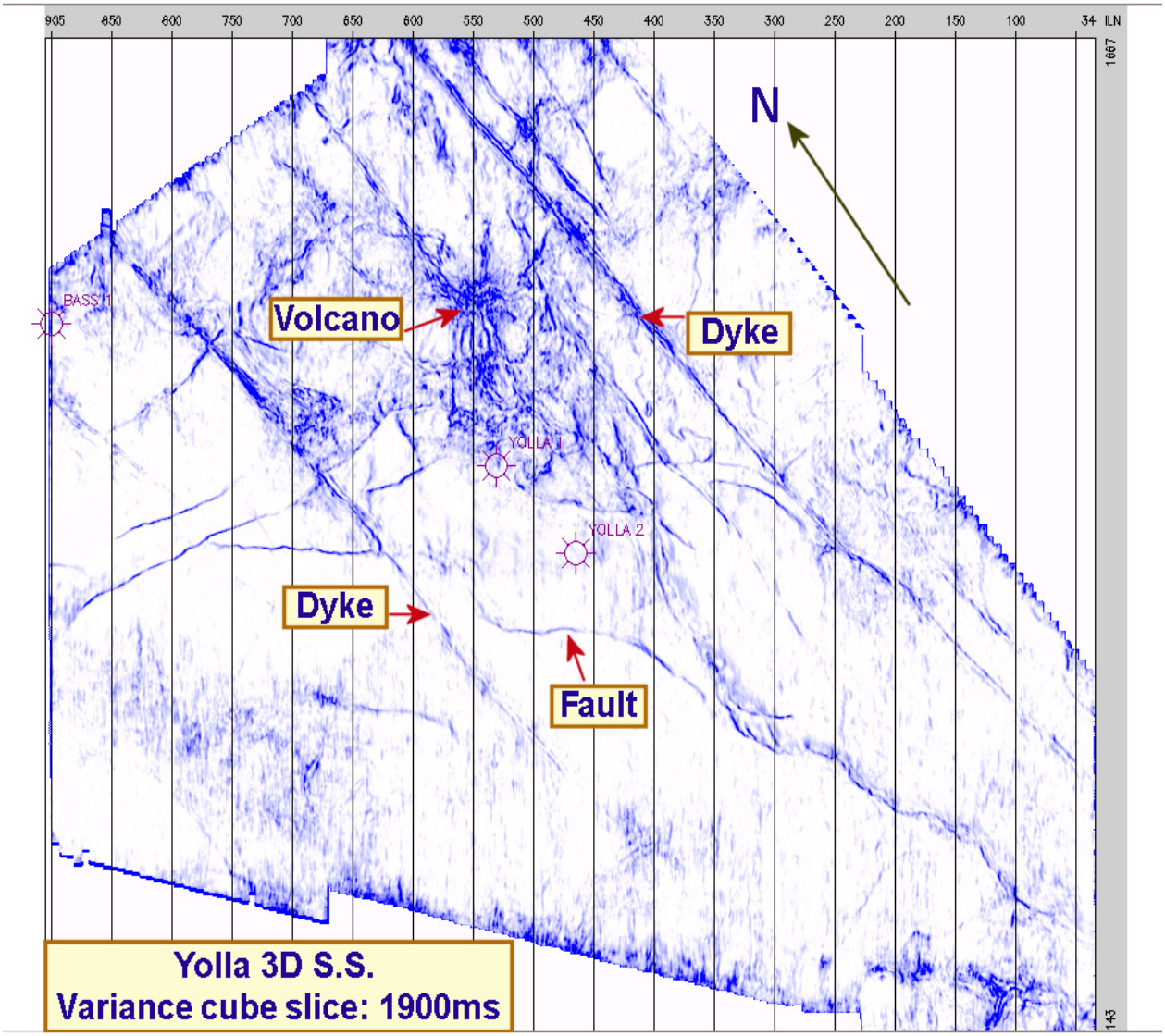
905
850
800
750
700
650
600
550
500
450
400
350
300
250
200
150
100
34
ILN
1667
143
N
BASS 1
Volcano
Dyke
YOLLA 1
YOLLA 2
Dyke
Fault
Yolla 3D S.S.
Variance cube slice: 1900ms

Figure 2.6

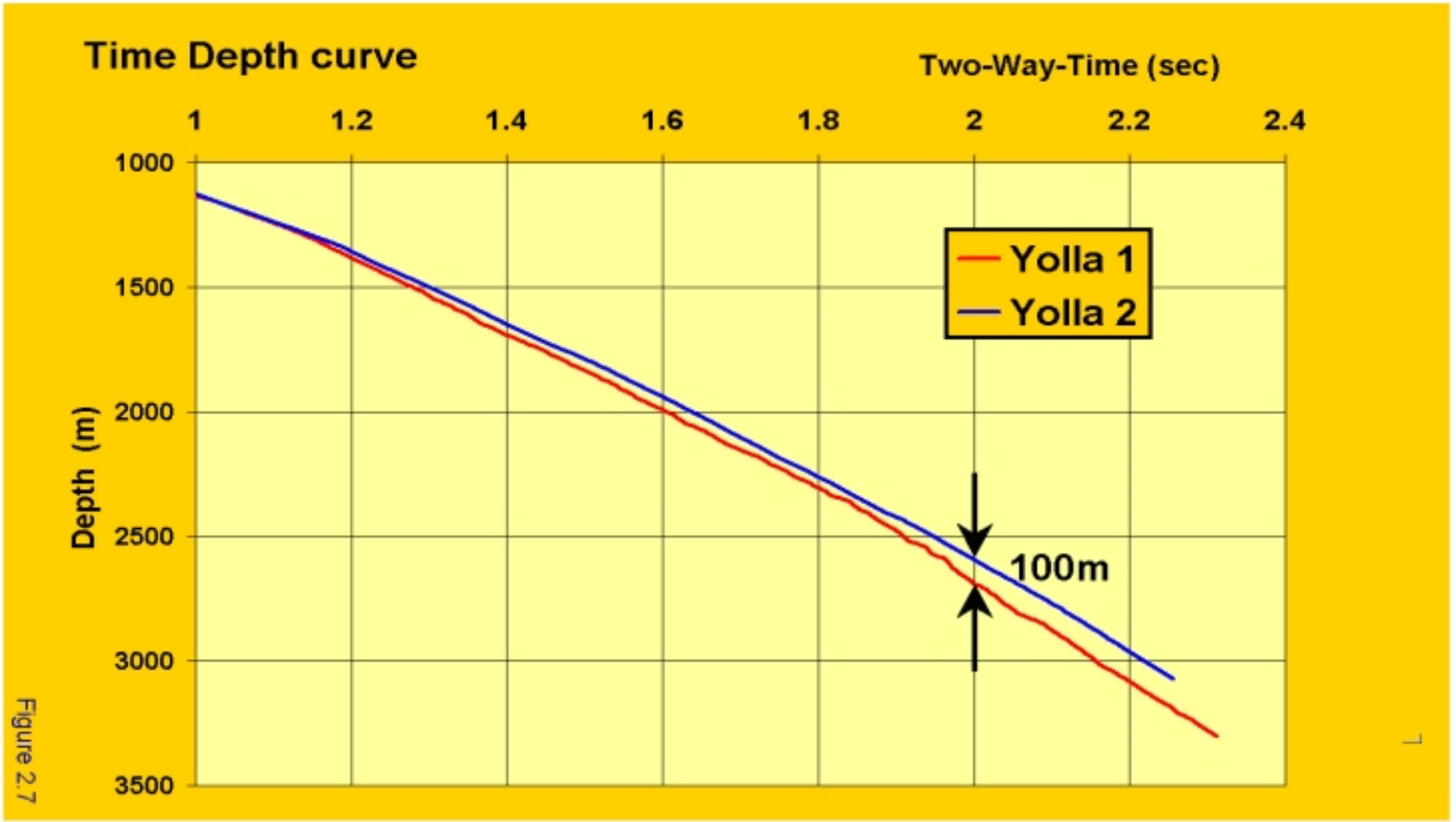
Time Depth curve
Two-Way-Time (sec)
1
1.2
1.4
1.6
1.8
2
2.2
2.4
1000
1500
2000
2500
3000
3500
Depth (m)
Yolla 1
Yolla 2
100m

Figure 2.7

sequence, (Fig. 2.1). Several smaller dykes are interpreted to intersect the fault block containing the gas reservoirs. These may be partial barriers to the transmissibility of gas and have therefore been included in the interpretation and subsequent reservoir modelling.

Sub-Seismic Sills

While no major sills are currently recognized from the seismic to significantly effect the main reservoir section, the wells do contain a number of thin sills within the reservoir section, that are either below or close to the limits of seismic resolution. These thin sills have the potential to locally adversely modify the reservoir through the effects of heating. Further analyses such as Acoustic Impedance (AI) inversion of the seismic data is recommended to help avoid some of these features prior to the final well design. One such feature that needs further investigation may occur in the vicinity of the proposed Yolla 3 (section 5.1.1).

2.4 Depth Conversion Methodology

As shown in Figure 2.1 and 2.5, a volcano lies immediately adjacent to the Yolla Gas field. This feature, together with a number of dykes and sills has a major influence on seismic velocities over the structure. The time depth curves from the check-shot surveys of Yolla 1 and 2 show a strong divergence, indicating that the interval velocities are highly laterally-variant, (Fig. 2.7). It is for this reason, together with the sparse well control, that a horizon-based velocity analysis approach was taken to the depth conversion.

CMP gathers from 33 2D lines were extracted from the 3D survey and used for horizon based stacking and interval velocity analysis. Twenty in-lines and 13 cross-lines were extracted. The gathers had all pre-processing steps applied, up to but excluding DMO. They were loaded into Paradigm Geophysical's "Power2D" module to perform the analyses. Full details of the depth conversion methodology may be found in the Yolla 3D 2000 reprocessing interpretation report (Taylor, in prep). A brief explanation of the method used is included below.

Horizon based velocity analysis

Both Horizon Stacking Velocity Analysis (HSVA) and Interval Velocity Analysis (IVA) were used to derive velocity information for depth conversion. The HSVA velocities were used for an average velocity depth conversion and the IVA velocities were used for an interval velocity depth conversion.

HSVA is simply regular stacking velocity applied along an interpreted time horizon. It can be scaled to approximate average velocity. HSVA analysis was done for the EVCM and 2718 horizons.

IVA is akin to HSVA but computes the semblance for a range of velocities in a target layer defined by 2 interpreted horizons. It is a layer stripping process that builds up a velocity model for successive layers from the top down. Ray-tracing is used to account for non-hyperbolic move-out. Its ability to derive the velocity field for a given layer relies on the accuracy of the velocity field derived in the overlying section. The

method employed was the coherency inversion technique, as implemented in Paradigm Geophysical's "Power2D" module.

IVA was applied to the 5 layers bounded by the horizons shown in Figure 2.1. This was done for each of the 33 2D lines extracted from the 3D survey. For each successive layer, the interval velocity semblances on all lines were interpreted simultaneously, to produce a consistent grid of velocity picks, before proceeding to analyse the next layer. This was an important step as it minimised any systematic line to line errors.

2.5 Depth Conversion

The main method of depth conversion was an interval velocity approach using map-migration to convert successive layers to depth. The maps produced using this technique were the P50 case for volumetric estimates, (Figs. 2.8 to 2.10). A vertical-stretch type interval velocity depth conversion was also produced, (ie interval velocities without map-migration). A third depth conversion using average velocities based on the HSVA velocity picks was also produced but is regarded as the least accurate because of a tendency to overly smooth velocities across the faults.

All velocity maps were calibrated to check-shot velocities in the wells. For the upper horizons the well Bass 1 was included together with Yolla 1 and 2. For each layer, the seismically derived velocities were scaled by a constant factor to approximately tie the check-shot velocities, then map-migrated to depth. A hand contoured mistie map was then used to flex the grids to exactly tie the wells.

The overall effect of the volcano on the velocity field can be seen by examining the final average velocity map produced by dividing the final depth conversion of the 2809 sand by the two-way-time map, (Fig. 2.11). It shows that the volcano has a large bearing on the velocities with the average velocity decreasing in a concentric manner away from the centre of the volcano. This is a reasonably plausible given the expected effect of volcanic activity and is therefore taken as support for the veracity of the depth conversion.

2.6 Depth Uncertainty

For each horizon, all methods of depth conversion produced fairly similar maps. The average velocity derived depth maps had a slightly larger closure at the EVCM and a slightly smaller closure at the 2718 and 2809 sands compared to the maps derived from map migration.

To generate upside and low-side cases for the volumetrics, a depth percentage error estimate was determined from the range of velocity picks reasonably interpreted from the HSVA and IVA semblance profiles. This figure was determined to be +/-0.3 % at around 2-3km from the wells, with zero percent error at the well locations. A percent error map was generated by hand contouring around the wells, (Fig. 2.12). A slightly larger gradient in error was contoured in the direction of the volcano.

Upside (P10) and low-side (P90) depth maps for the 2809 sand were produced by applying the uncertainty map to the final 2809 sand depth map. These are shown as

Figures 2.13 and 2.14. Note that all three methods of depth conversion produced maps within the P10 to P90 range.

Yolla Gas Field T/RL1

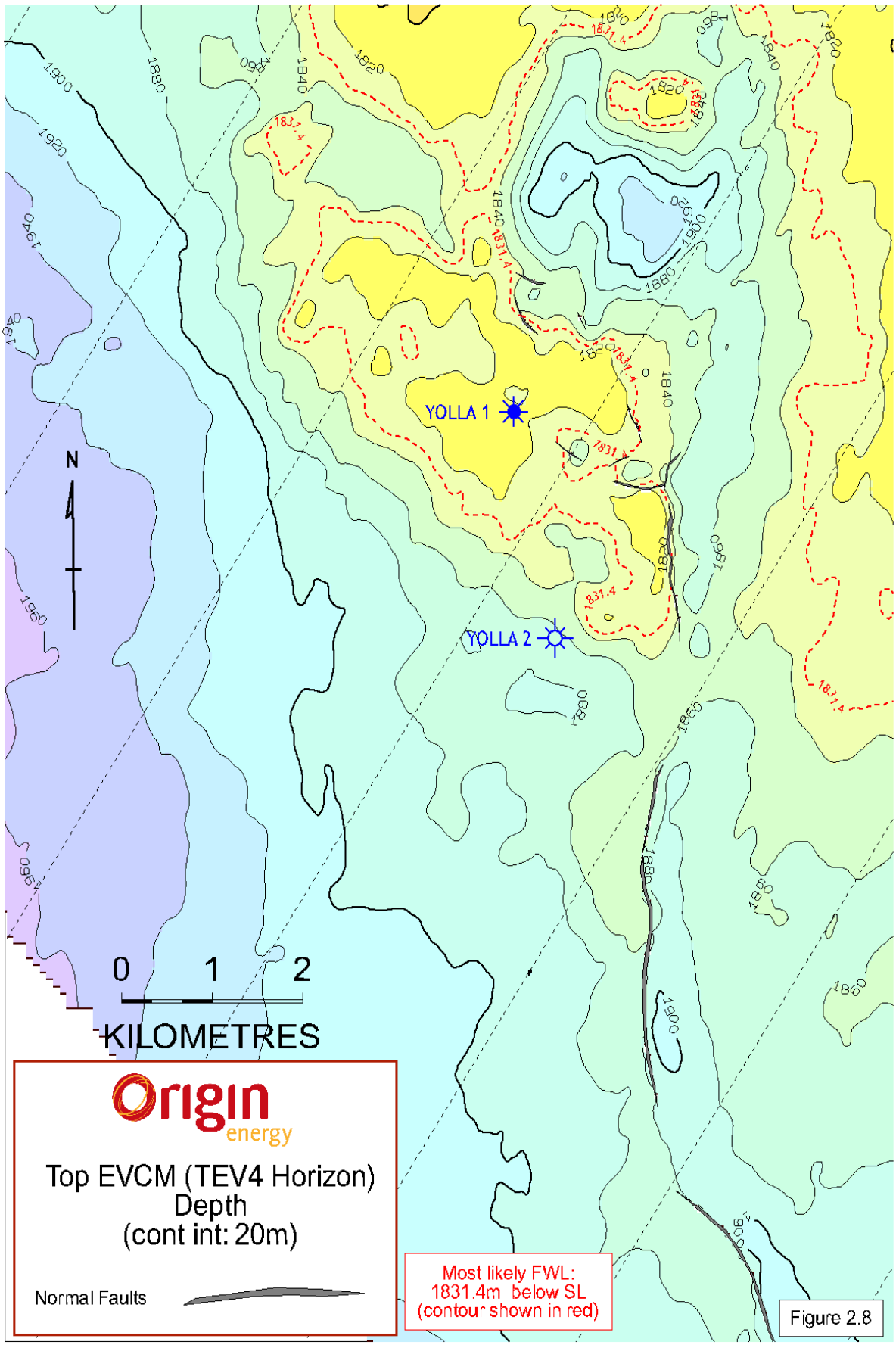

Figure 2.8

Yolla Gas Field T/RL1

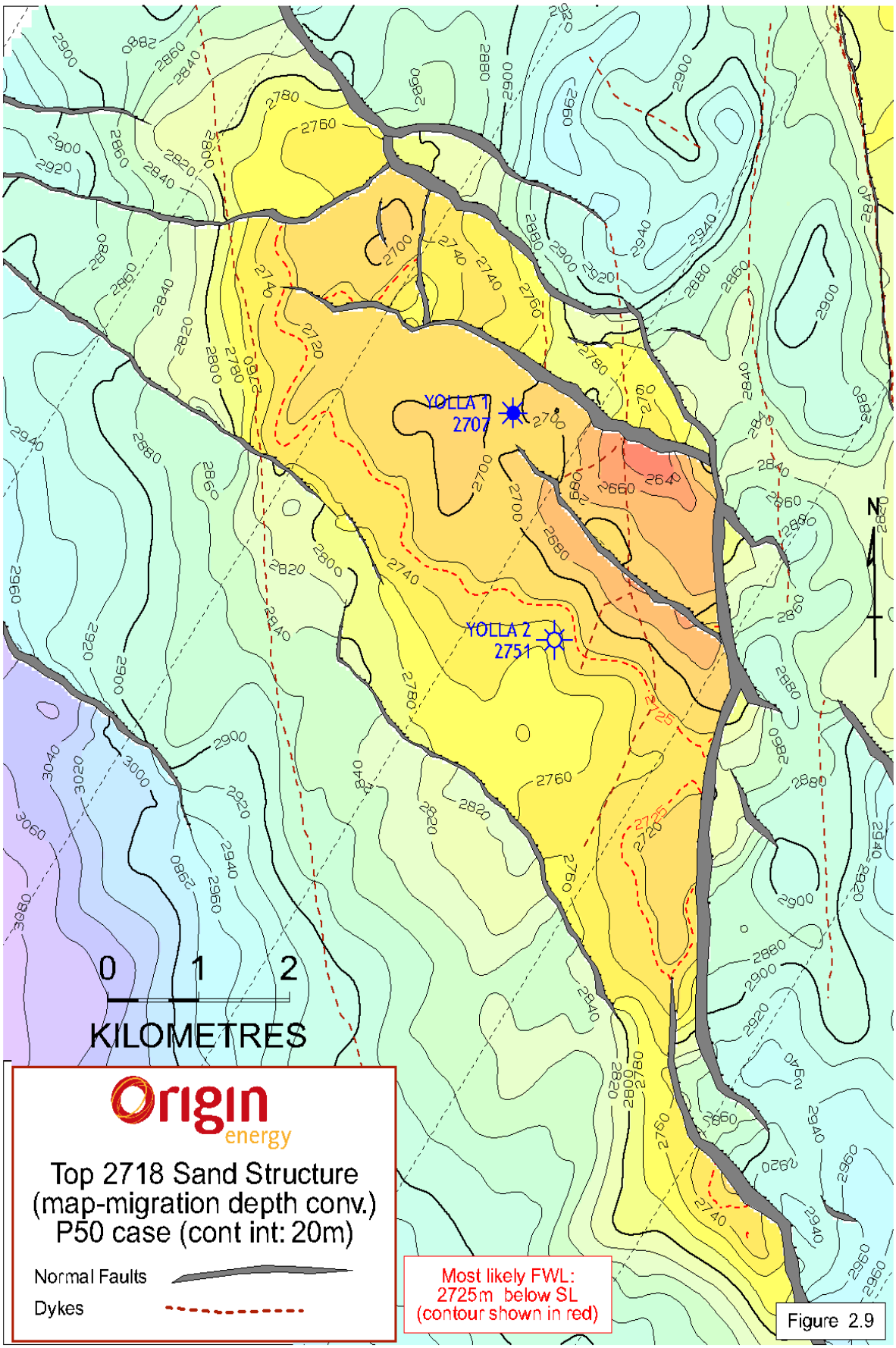

Figure 2.9

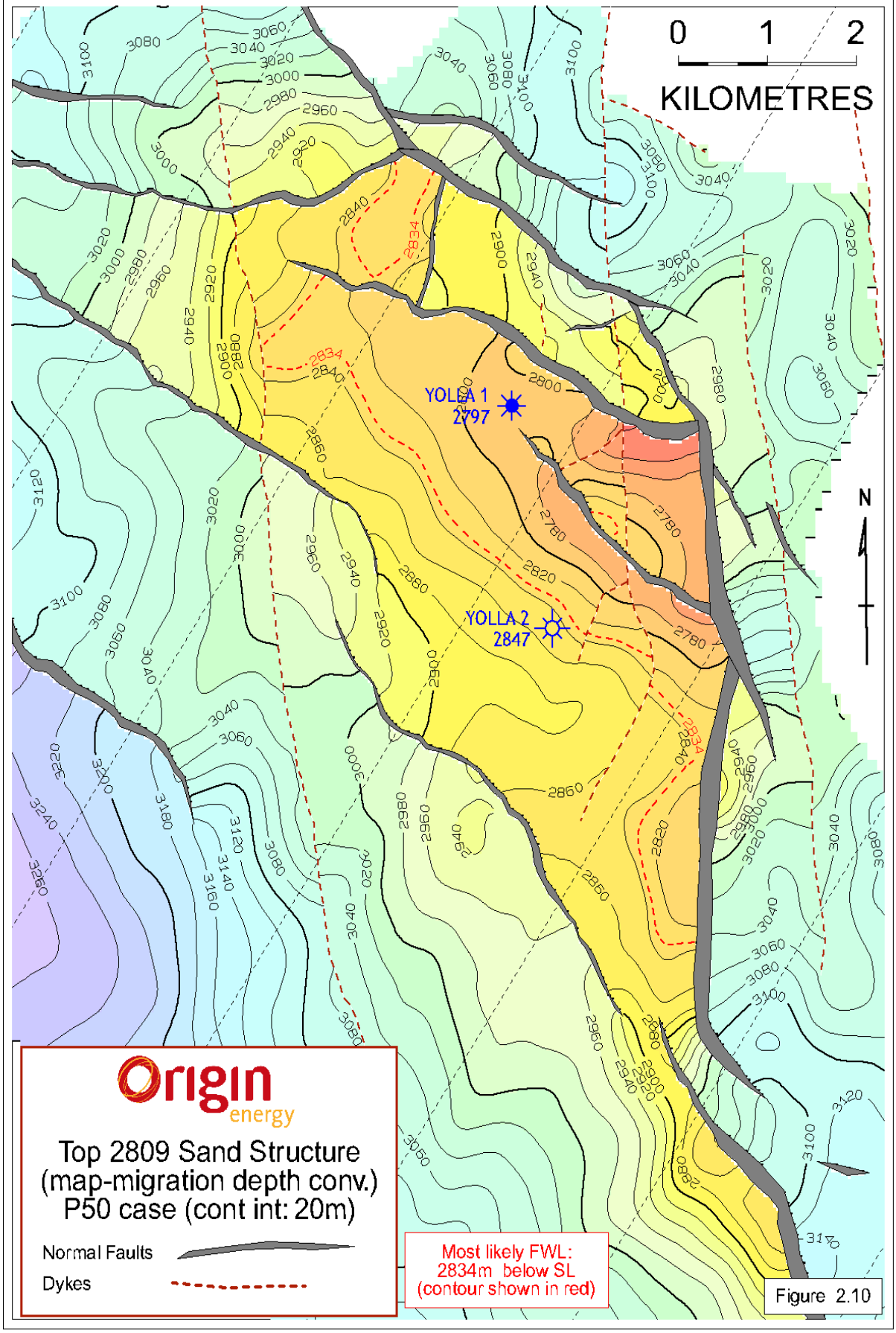
Yolla Gas Field T/RL1
0 1 2
KILOMETRES
N
YOLLA 1
2797
YOLLA 2
2847
Origin energy
Top 2809 Sand Structure
(map-migration depth conv.)
P50 case (cont int: 20m)
Normal Faults
Dykes
Most likely FWL:
2834m below SL
(contour shown in red)
Figure 2.10

Yolla Gas Field T/RL1

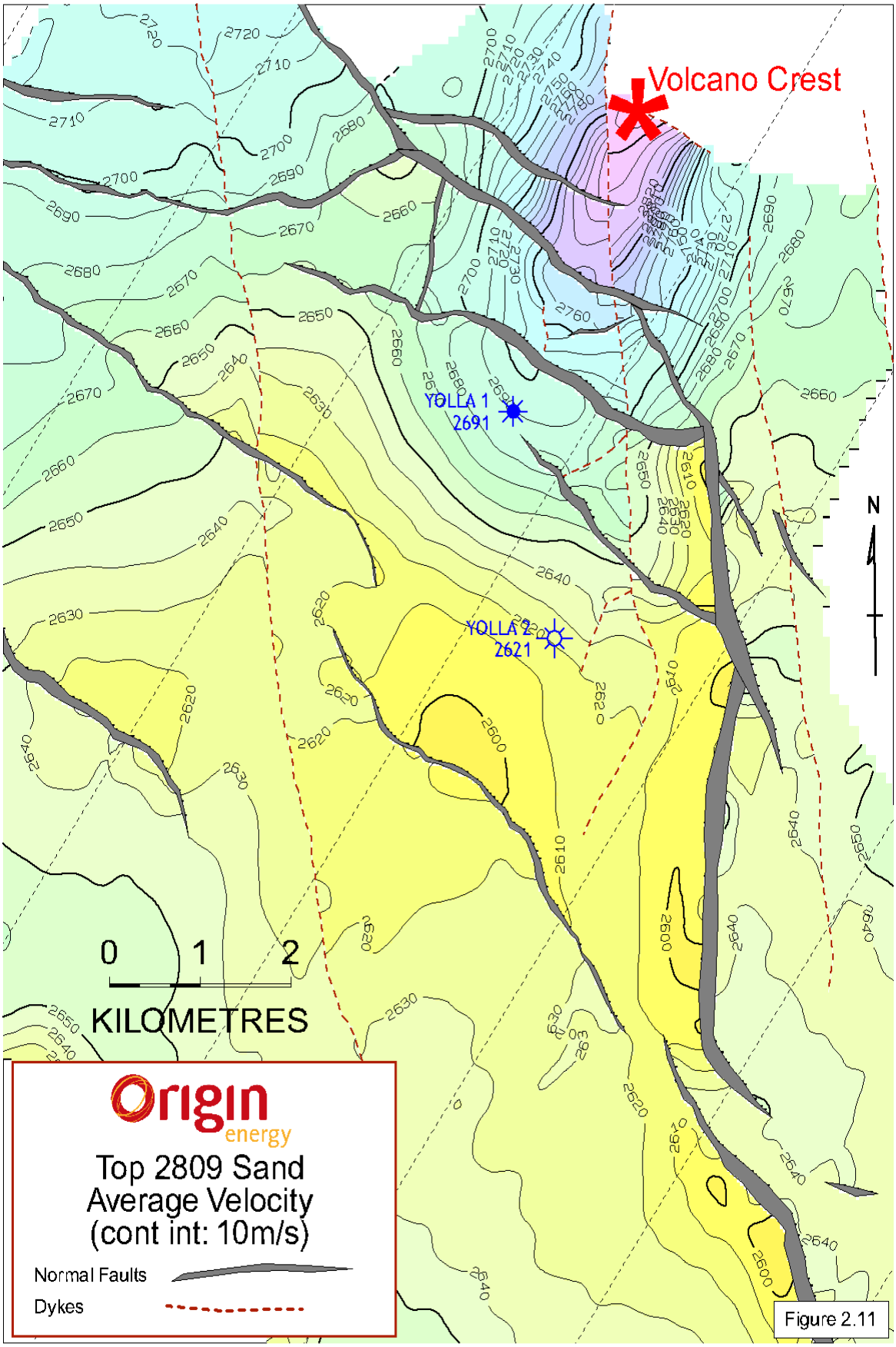

Figure 2.11

Yolla Gas Field T/RL1

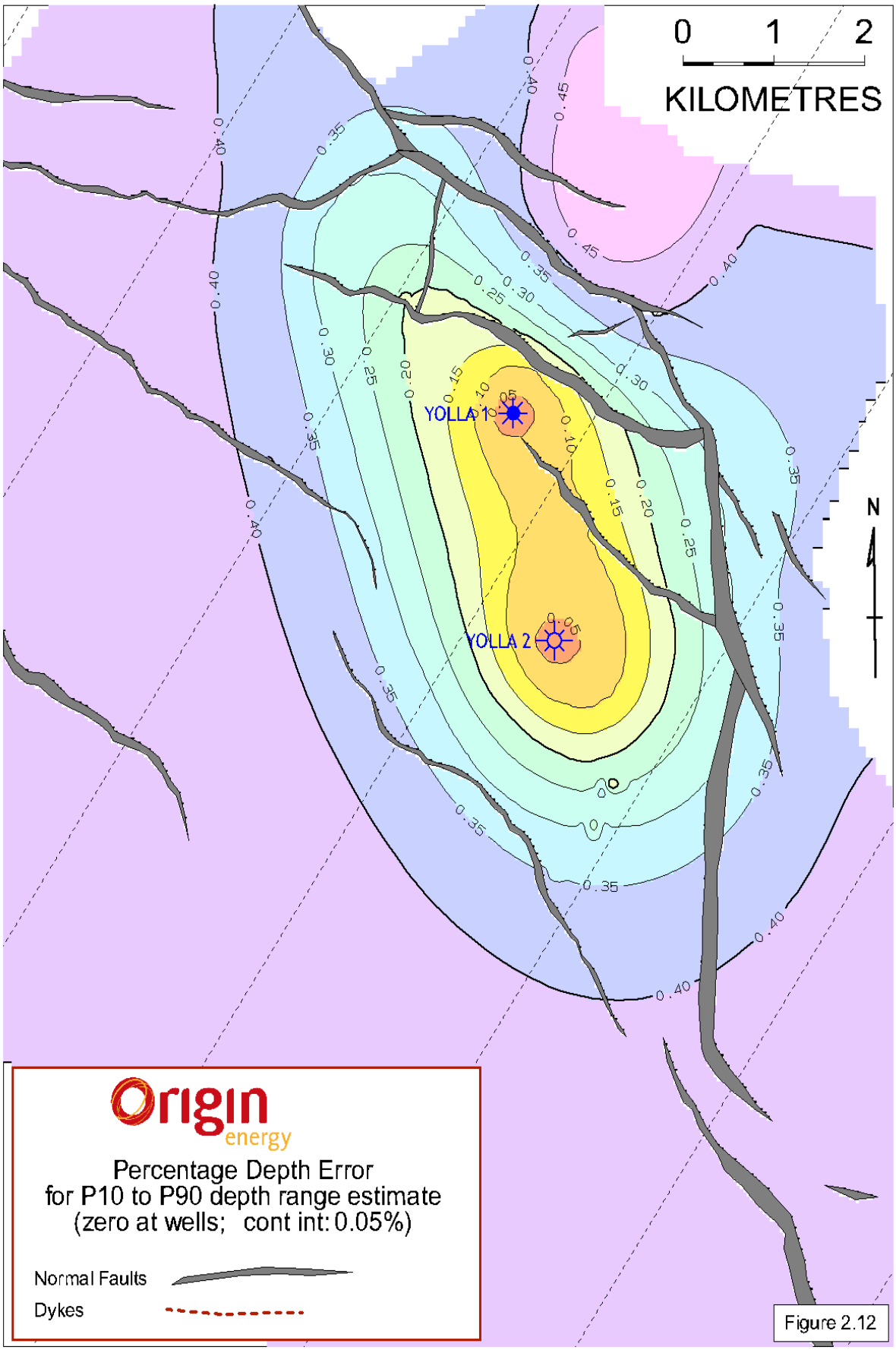

Figure 2.12

Yolla Gas Field T/RL1

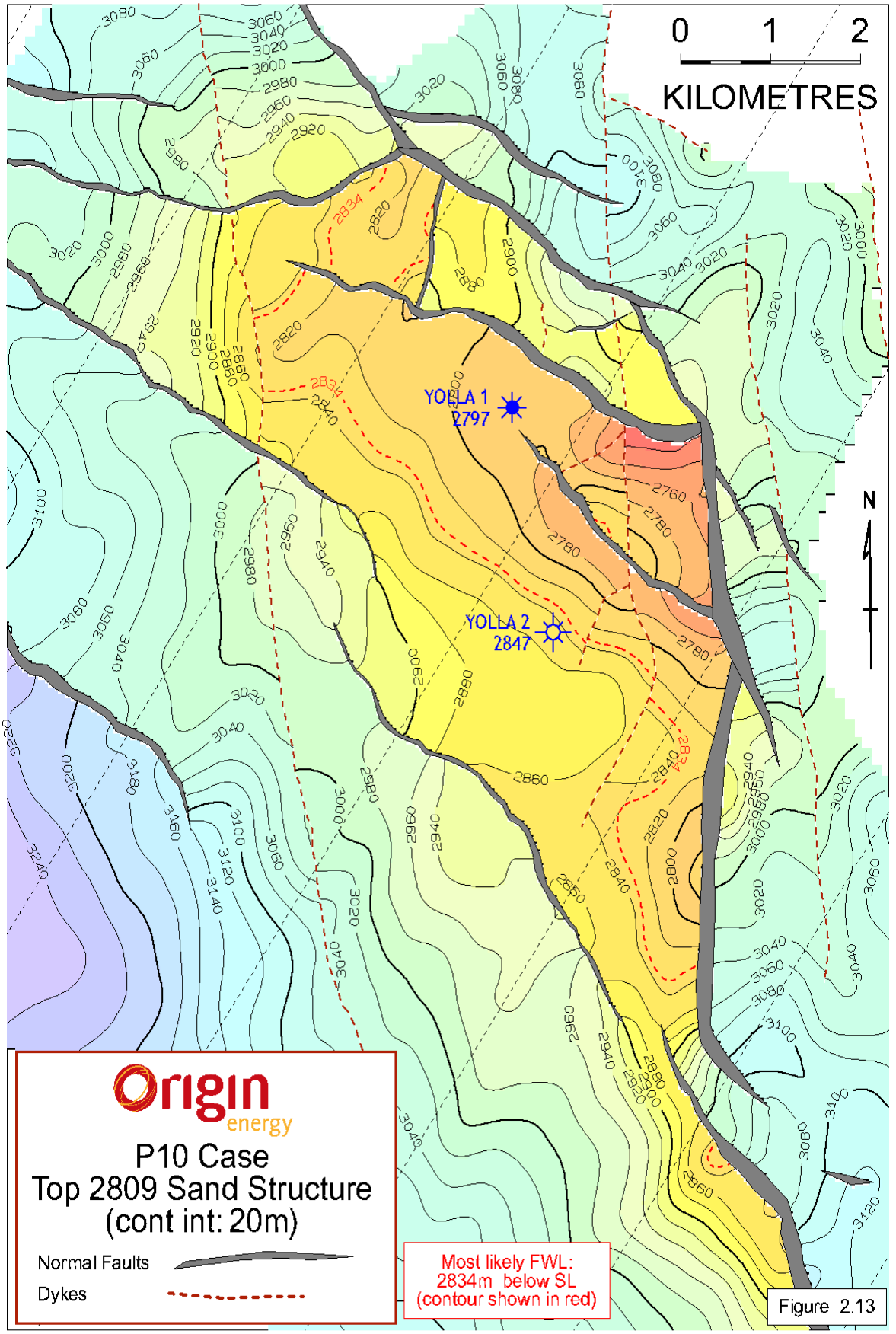

Figure 2.13

Yolla Gas Field T/RL1

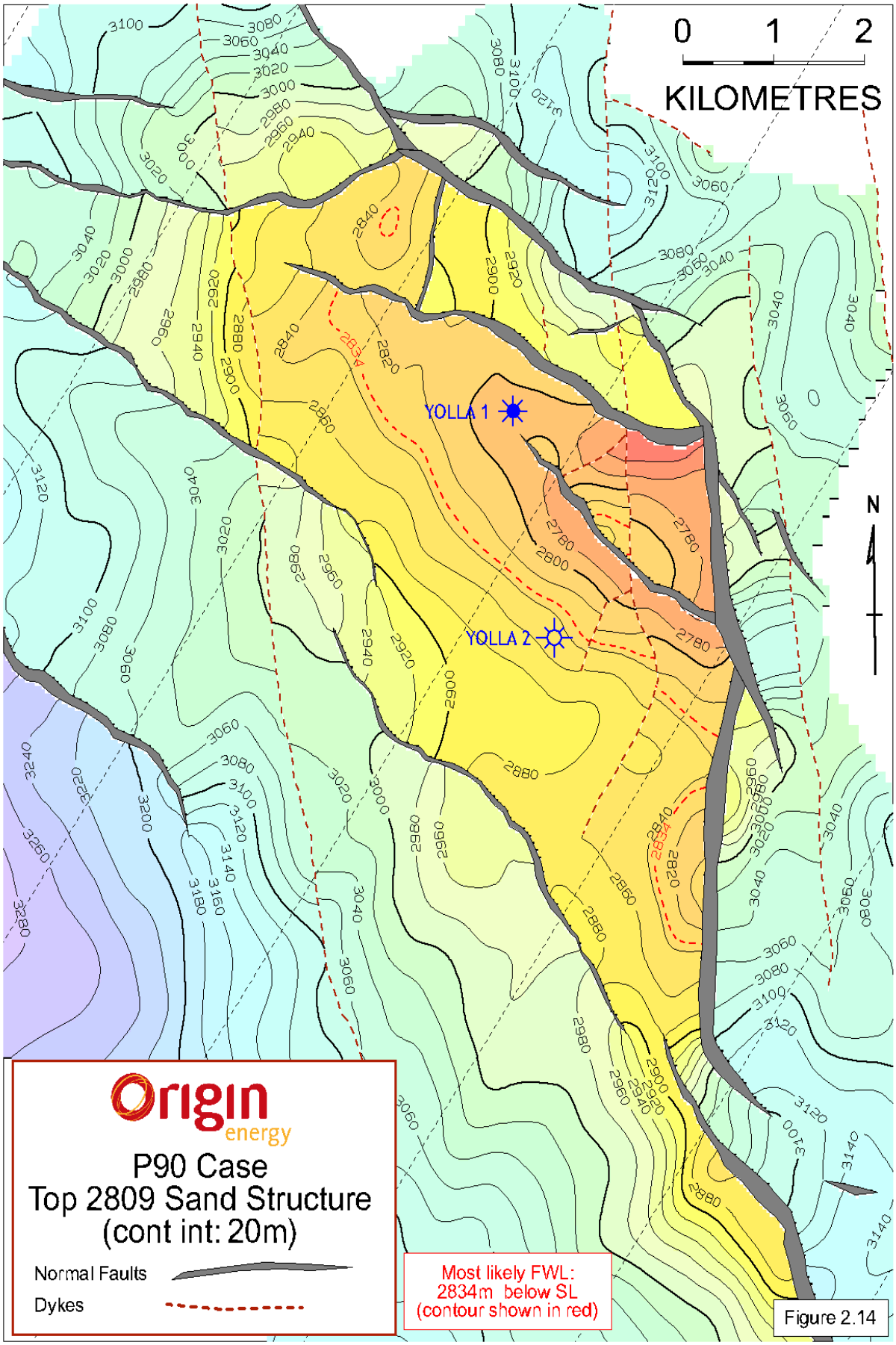

Figure 2.14

3 GEOLOGICAL MODELLING

3.1 Overview of Methodology

The purpose of the 3D geological modeling (Fig. 3.1) was to provide an accurate geologically-based upscaled grid for Eclipse simulation modeling. Grids were constructed within Technoguide's Petrel™ 3D geological modeling package. Petrel was also used to upscale the geological model for input into Eclipse.

Horizon grids were imported as Z-map files for the Top 2718 and Top 2809 sands (see section 2.). These maps formed the basis for the structural and stratigraphic model. Faults were constructed from fault polygons that were also imported from Petrosys for these 2 horizons.

A fine-scale grid with horizontal dimensions of 80 x 80m was constructed for the Yolla Field. The vertical sub-layer thickness was set at approximately 1m for the reservoir units i.e. 2718, 2755, 2809, 2952 and 2973 sands (see section 3.4 for discussion on stratigraphy).

Porosity logs were upscaled to the vertical grid resolution and formed the basis for subsequent property modeling. Water saturation was modeled within Eclipse. For OGIP comparison in Petrel however, a saturation algorithm was used. Permeability was calculated from porosity using an equation determined from core data.

A fluvial facies model was built for the main 2755, 2809 and 2973 units. Facies were interpreted from core data (where available) and by log character where absent. Reservoir facies parameters were determined from palaeogeographic models and published literature. The facies model was subsequently populated with porosity values using a sequential gaussian simulation based on the porosity distribution present within each specific interpreted facies at the 2 wells. The porosity grids for the minor 2718 and 2952 sands were populated using a stochastic sequential gaussian algorithm with no facies control (see section 3.7).

Multiple realizations of the model were run in order to provide sensitivity cases for reservoir simulation. The modeling attempted to match the OGIP determined from probabilistic calculations i.e. for the most likely model an OGIP of 500 bcf was matched (see Table 3.1). Matching was achieved by adjusting the parameters and/or proportion of facies for each specific zone. On this basis, models with variable sand trends and structural models were constructed. OGIP was later adjusted within Eclipse to match the bcf figure of the Probabilistic estimate.

All geological models were then upscaled to a coarser grid size prior to importing into Eclipse for reservoir simulation.

As a quality control check for the volumetric analysis, the volume contained between the 2834 level and the 2809 seismic horizon was calculated in both Petrel and Petrosys. A value of 336 km^2/m was determined by both methods.

GEOLOGICAL MODELLING METHODOLOGY

Reservoir Simulation

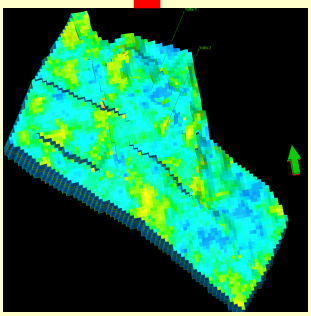

Upscaling

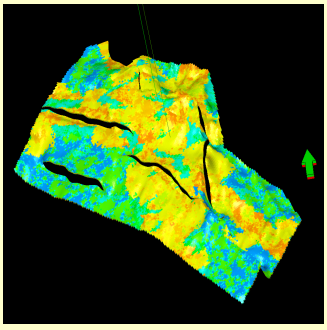

Property modelling

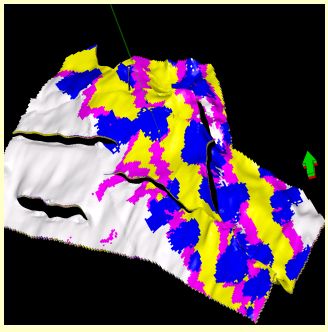

Facies modelling

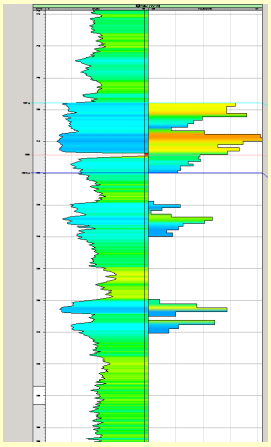

Log upscaling

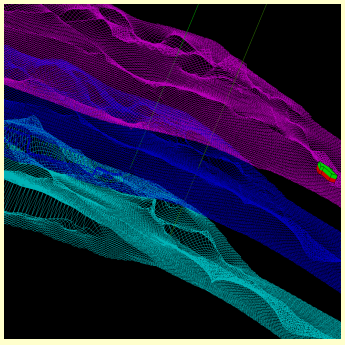

Grid building

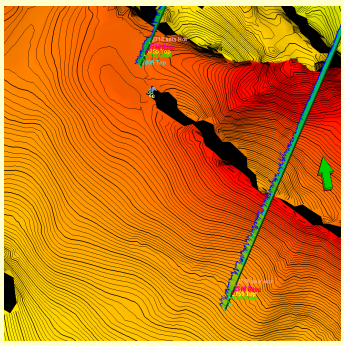

Import Data

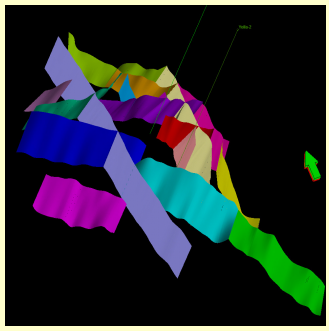

Structural modelling

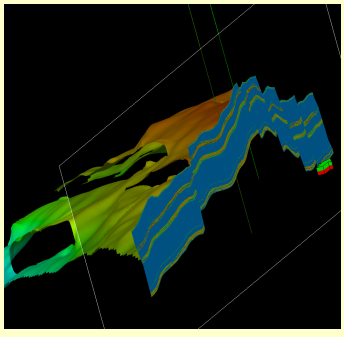

Stratigraphic modelling

Figure 3.1: Summary diagram of geological modelling methodology

3.2 Probabilistic Volumetric Estimate

Prior to undertaking the geological modeling a revised probabilistic estimate of reserves was determined. Gross rock volumes (GRVs) were calculated within Petrel for the respective most likely, high side and low side models. Reservoir parameters and fluid contacts used in this analysis were those used in the previous MHA reserves study (2000). OGIP was calculated probabilistically using REP reserves estimation software. All sub-totals and totals were probabilistically consolidated. The volumes calculated in this work formed the basis for the subsequent geological modeling and reservoir simulation. Calculated OGIP estimates are summarized in Table 3.1 below and are within 4% at the mean and P50 level:

	ORIGIN 2001				MHA 2000			
bcf	P90	P50	P10	Mean	P90	P50	P10	Mean
Yolla Main (OGIP)	342.0	448.0	569.0	452.0	-	-	-	428
Yolla North (OGIP)	31.1	50.6	76.4	52.5				57
Total (OGIP)	393	500	621	504	377	483	601	486.8

Table 3.1: Summary of OGIP calculated for the Yolla Field based on recent Origin reserves review. This review used GRVs derived from the Petrel model and properties determined by MHA.

MHA reserves figures have been used as the basis for economic analysis and contractual negotiations. As the above Origin volumetrics essentially confirm the MHA figures the former have been used in forming the development plan. The minor differences between the figures can be attributed to the remapping of the field post-reprocessing.

3.3 Structural Model

The structural model was constructed in Petrel using fault polygons imported as xyz ASCI files from Petrosys. The cross-cutting relationship between faults and the dip of fault planes has been preserved (Fig. 3.2). Dykes have also been included within the model (Fig. 3.2) and have been distinguished from faults. This allowed the transmissibility of these features to be varied within the simulation model. The pillar gridding process created cells with 80 x 80m areal dimensions. The main Yolla bounding fault (Dorothy) was defined as a structural trend in this process in order to assist in refining and improving the gridding process.

3.4 Stratigraphic Model

Five reservoir zones (Fig. 3.3) have been modelled for the purposes of the reservoir simulation. These are termed the 2718, 2755, 2809, 2952 and 2973 units. By far the most volumetrically significant units in terms of OGIP are the 2755, 2809 and 2973 units. Based on the facies interpretation (see section 3.7) it was decided to split the 2809 unit into 2 sub-zones. The depth defining the contact between the 2 sub-zones is 2814.2m SS in Yolla-1 and 2861.2 m SS in Yolla-2. The 2844 and 2873 units were not

Structural Model

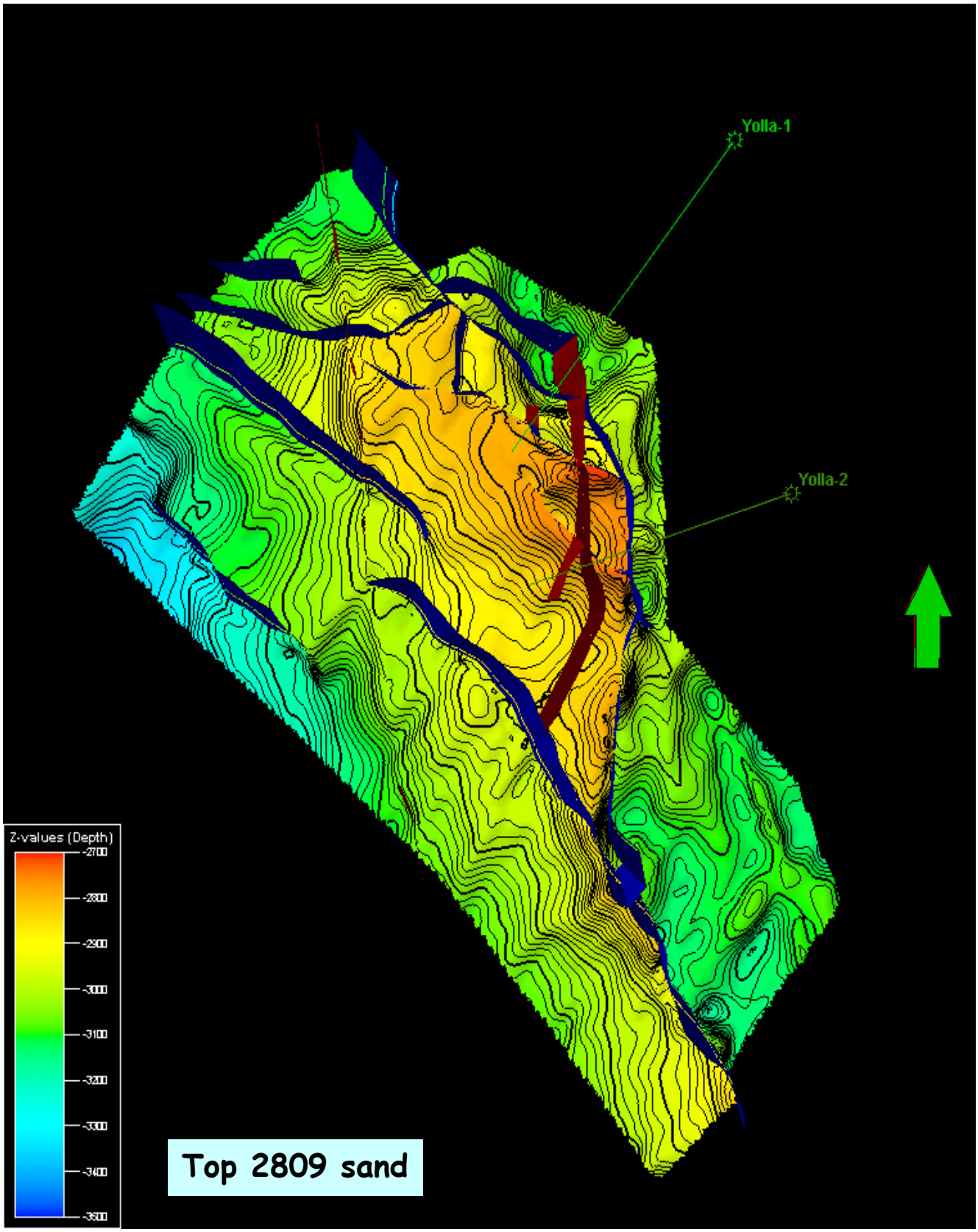

Faults

Dykes

Figure 3.2: Structural model which formed the basis for a number of the geological models constructed within Petrel. Interpreted horizons and fault polygons were imported as Z-map files from Petrosys.

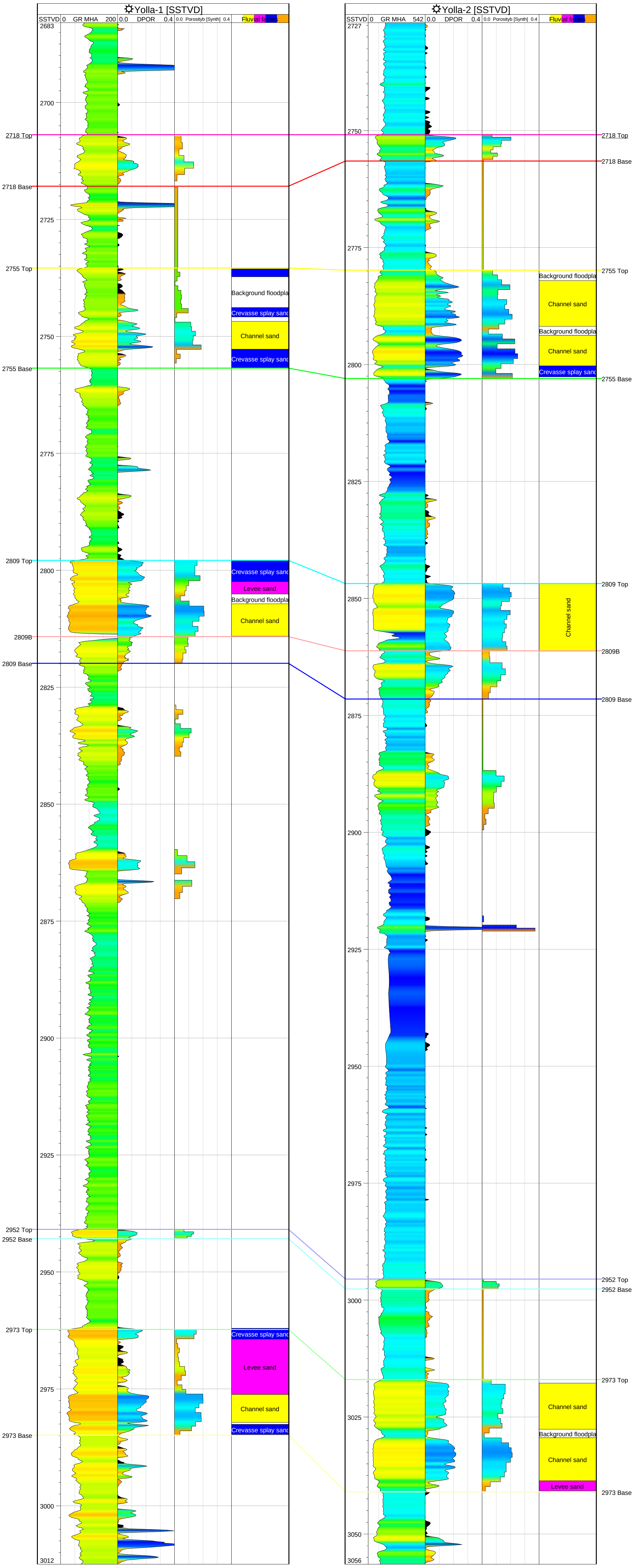

Figure 3.3: Cross-section through Yolla 1 and Yolla 2 showing, GR, porosity and upscaled porosity log.

modeled as a part of this study as they are interpreted to be water-saturated (MHA 2000).

The Top 2718 sand and Top 2809 sand depth grids were imported into Petrel from Petrosys for 3D geological modeling. The base of the 2718 unit was constructed as conformable to the Top 2718 horizon. All other horizons were created as conformable surfaces to the 2809 sand and were tied to the respective well tops using a smoothing algorithm. Well tops used in this process are presented in Table 3.2.

Stratigraphic surface	Yolla-1(mSS)	Yolla-2 (mSS)
2718 Top	2706.9	2750.88
2718 Base	2717.9	2756.5
2755 Top	2735.4	2779.8
2755 Base	2756.8	2803.0
2809 Top	2797.9	2846.8
2809 Base	2819.9	2871.5
2844 Top	2828.9	2886.8
2844 Base	2839.9	2899.5
2873 Top	2859.9	2916.55
2873 Base	2870.4	2921.8
2952 Top	2940.9	2995.5
2952 Base	2942.9	2997.6
2973 Top	2962.3	3017.0
2973 Base	2984.9	3041.0

Table 3.2: Well Picks for Yolla-1 and Yolla-2.

3.5 Fluid Contacts

MHA (2000) reviewed the fluid contacts based on the available MDT and RFT data. The contact levels determined in this previous study have been used herein and are presented as Table 3.3.

Sand	LKG (Minimum)	Most Likely GWC	Maximum GWC
2718	2711	2727	2822
2755	2803	2834	2834
2809	2813	2834	2834
2952	2942.5	2997	3004.7
2973	2983.5	2997	3004.7

Table 3.3: Reservoir fluid contacts used in evaluation (from MHA 2000). Depths in mSS.

The reader is referred to the MHA (2000) report for further justification of fluid contacts. That report is contained as an attachment to this document.

3.6 Reservoir Properties

Porosity curves calculated by MHA (2000) were used in the modeling. This was based on Neutron-Porosity cross-plotting techniques. The high resolution porosity curves were then arithmetically upscaled to approximately 1m resolution prior to porosity modeling.

Permeability was calculated from porosity based on core data (Fig.3.4). The following algorithm was used:

If porosity < 0.17.5 % then perm = $(0.0000001e^{125.85})$
If porosity >= 0.17.5 % then perm = $(0.1531e^{45.002})$

As stated previously, for the purposes of the simulation, water saturation was modeled within Eclipse. For OGIP calculation within the geological modeling process, the following algorithm was used to convert porosity to water saturation:

$Sw = 0.0482 \times Porosity^{-0.9982}$

This is the identical approach taken by MHA (2000). It was determined by MHA that porosity and water saturation could be related by the bulk volume water relationship.

3.7 Facies Modeling

The 2755, upper 2809 and 2973 sands have been interpreted as fluvial reservoirs. Well log interpretation forms the basis of the facies model and is included in Figure 3.3. The facies interpretation is also supported by the Yolla-2 FMI interpretation (Z & S 1998) and core data (only available for 2973 sand in Yolla 2). The lower part of the 2809 sand is interpreted as prograding mouthbar/shoreface facies based on the upward-coarsening log character. This zone has therefore been modeled separately from the upper part of this zone. The interpretation is based primarily on log character. The 2755, 2809 and 2973 units were divided into 4 facies (Fig. 3.3):

- Channel
- Levee
- Crevasse splay
- Background or floodplain

Facies interpretation was difficult in most cases, particularly when distinguishing between crevasse splay, levee and channel facies. Input parameters for channel dimensions were based on the methodology outlined by Bridge and Tye (2000) and are presented in Table 3.4 for each of the reservoir zones. These parameters form the basis for the facies model, stochastically populated between the wells. Similar parameters were defined for both levee and crevasse splay sand bodies (Fig. 3.5 & 3.6).

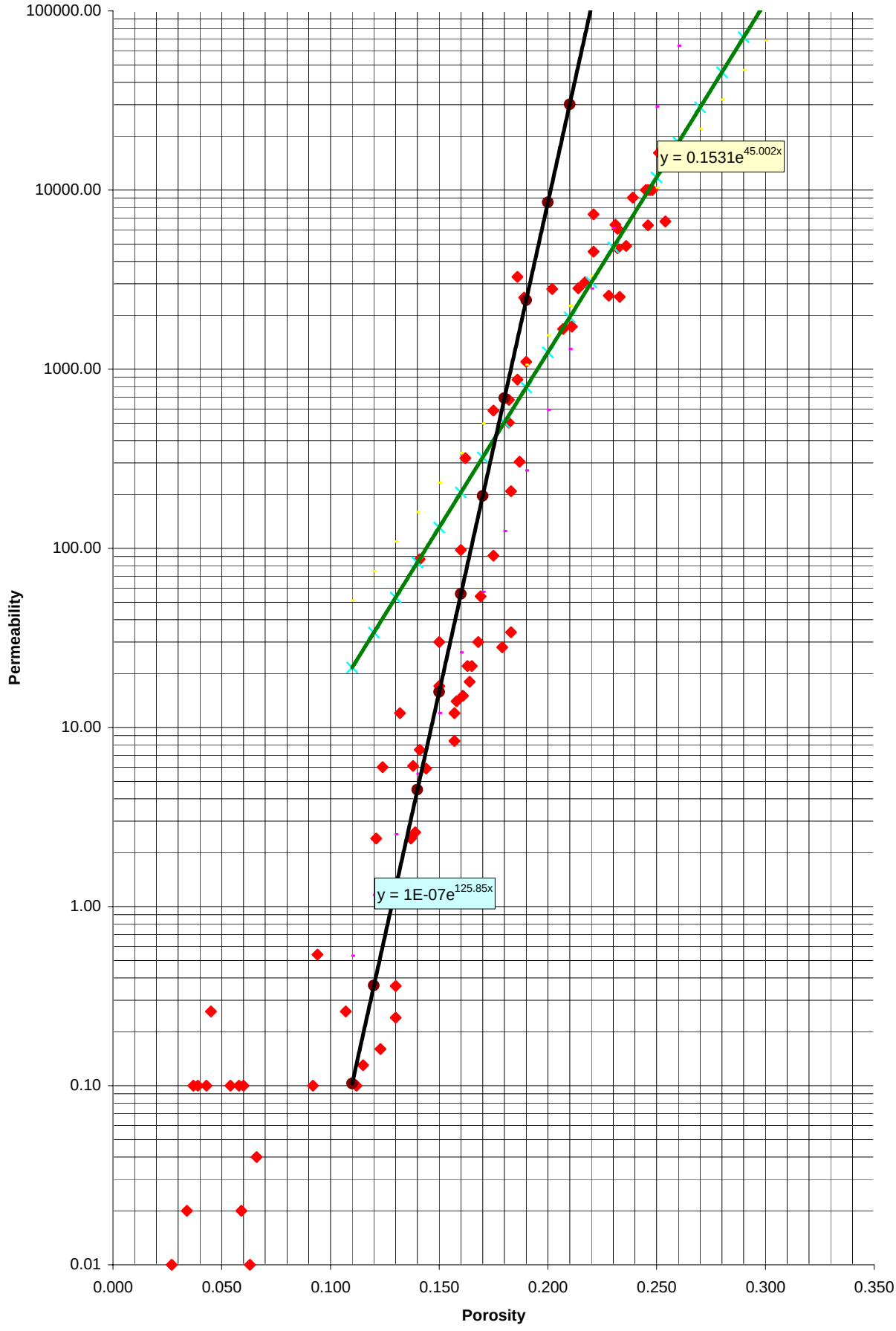

Figure 3.4: Plot of core data from Yolla-2 with trendline and equations used for Porosity to Permeability conversion.

Facies Model – 2973 Sand

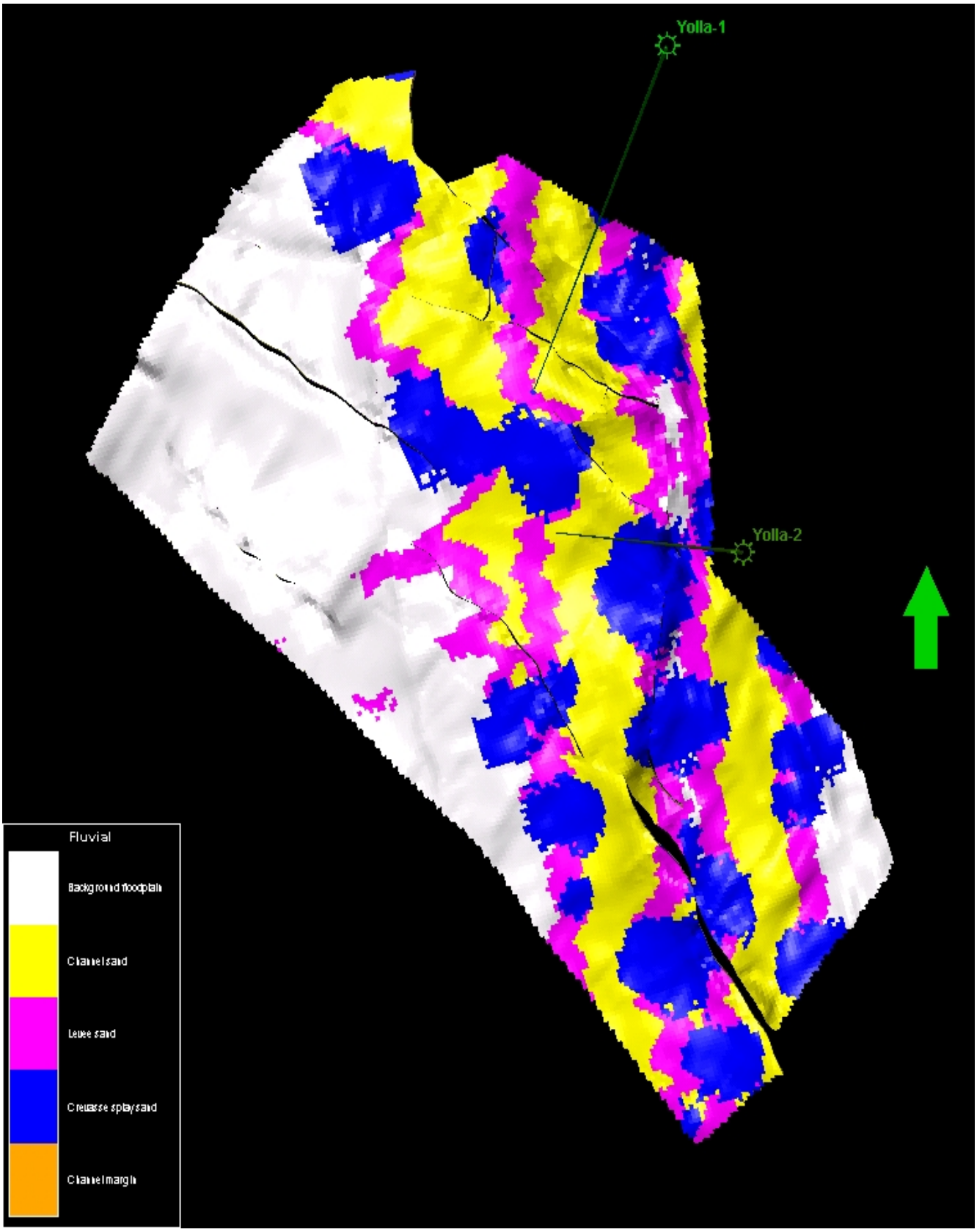

Figure 3.5: Example of stochastic facies model used to populate geological model with porosity.

Based on palaeogeographic and FMI interpretation (Z & S 1998) a broad south-east to northwesterly trend has been assumed for the fluvial systems and this has been built into the stochastic model (see Table 3.4).

An example of the resultant facies model is presented in Figure 3.5. This model was subsequently used to condition the property modeling (section 3.8).

Sand	Model	Direction of channel axis (from north)			Sandbody Thickness			Width/Depth ratio			Max No. Channels
		Min	ml	max	min	Ml	Max	Min	Ml	max	
2755	P90	-45	-30	-15	1	3	8	50	150	200	45
	P50	-45	-30	-15	2	5	12	100	150	250	50
2809	P90	-45	-30	-15	1	3	8	50	150	200	35
	P50	-45	-30	-15	2	6	10	100	200	300	50
2973	P90	-45	-30	-15	1	3	8	50	150	200	40
	P50	-45	-30	-15	2	6	10	100	200	300	40

Table 3.4: Channel sand body parameters for P90 and P50 facies models.

The 2718, lower part of the 2809 sand and the 2952 sand are interpreted as prograding mouthbar/shoreface deposits and, as such, were not modeled as fluvial reservoirs. Given the relative small thickness of these zones and the sheet-like nature of the interpreted depositional environment it was decided not to build a facies model. Instead, porosity was modeled directly, using a stochastic sequential gaussian algorithm (see below).

Sand	Model	Width of levee deposit			Height above channel top			Depth below channel top		
		min	ml	max	Min	Ml	Max	min	Ml	Max
2755	P90	80	120	160	0.1	0.1	0.1	0.2	0.3	0.4
	P50	160	240	320	0.1	0.1	0.1	0.2	0.3	0.4
2809	P90	80	120	160	0.1	0.1	0.1	0.2	0.3	0.4
	P50	160	240	320	0.1	0.1	0.1	0.2	0.3	0.4
2973	P90	80	120	160	0.1	0.1	0.1	0.2	0.3	0.4
	P50	160	240	320	0.1	0.1	0.1	0.2	0.3	0.4

Table 3.5: Levee body parameters for P90 and P50 facies models.

Sand	Model	Width			Thickness next to channel (relative to channel thickness)		
		min	Ml	Max	min	Ml	Max
2755	P90	125	500	1000	0.1	0.25	0.5
	P50	250	500	1000	0.1	0.25	0.5
2809	P90	125	500	1000	0.1	0.25	0.5
	P50	250	500	1000	0.1	0.25	0.5
2973	P90	125	500	1000	0.1	0.25	0.5
	P50	250	500	1000	0.1	0.25	0.5

Table 3.6: Crevasse splay body parameters for P90 and P50 facies models.

3.8 Property Modeling

The purpose of the property modeling stage was to populate the grid with porosity values based upon the reservoir section intersected in Yolla-1 and Yolla-2. The major challenge with property modeling the Yolla Field is to create a realistic grid based on the sparse data coverage (i.e. 2 wells). It was decided that the best method in this situation was a stochastic sequential gaussian simulation method. This method relies on a variogram model to populate the grid as opposed to straight deterministic or Kriging methods, which are more prone to produce "bulls eyes" in a situation with few data points.

The property models for the 2755, upper 2809 and 2973 units were conditioned to the facies grid. In this process the algorithm populates the facies with porosity based upon the distribution intersected in a specific facies at the wells e.g. If the porosity distribution for the interpreted channel facies at Yolla-1 and Yolla-2 was 13 to 24% then this range would be used to populate the channel facies grid cells between wells. A distance of 500m was estimated as the range for the variogram used in the gridding process. As a QC procedure, the distribution of porosity across the total grid was then compared with the distribution of porosity within the wells in an attempt to match the real data as closely as possible. Histograms of porosity distribution and porosity maps of selected sub layers for the three units are shown in Figures 3.6, 3.8 and 3.10. The permeability grid was derived from the porosity grid using the aforementioned equation (section 3.6) and is presented as Figures 3.7, 3.9 and 3.11 for the same selected sub layers. These porosity and permeability maps show only one sub-layer of the total zone. The porosity distribution changes vertically throughout each zone as the facies and properties are populated stochastically. A porosity grid cross-section through 3 of the zones is presented in Figure 3.12.

As discussed above, no facies models were constructed for the 2718, lower 2809 and 2973 zones. The same stochastic sequential gaussian simulation was used but was not conditioned to another variable. The grid was populated with porosity based on the porosity distribution for the whole zone. A range of 500m was estimated for the variogram used in this procedure. The porosity distributions for selected layers for the three zones are shown in Figures 3.13 to 3.15.

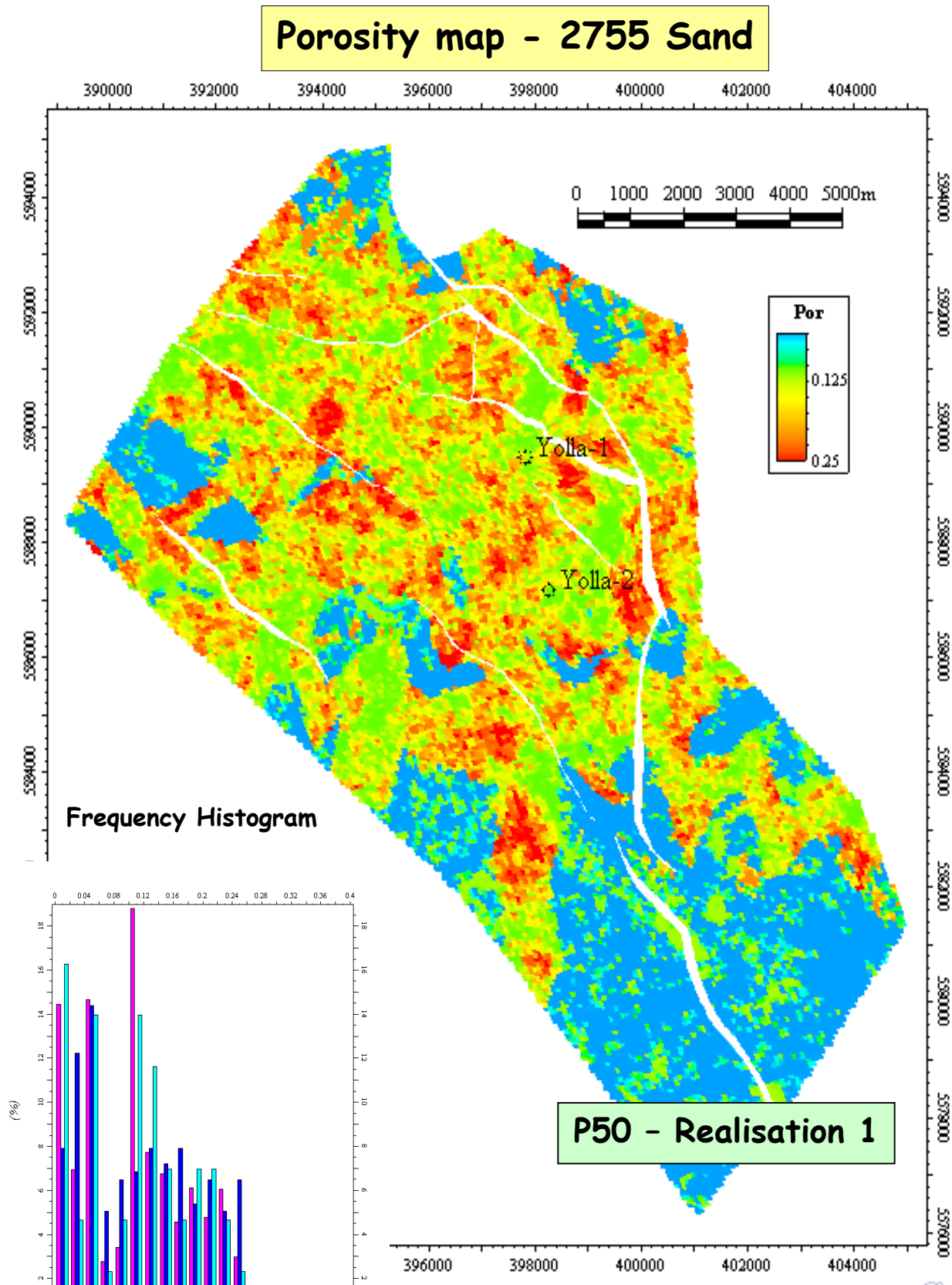

Figure 3.6: Porosity map of selected sub layer in 2755 sand for P50 realisation 1 model. Histogram shows comparison of porosity distribution at wells with the total grid distribution.

Produced with Petrel

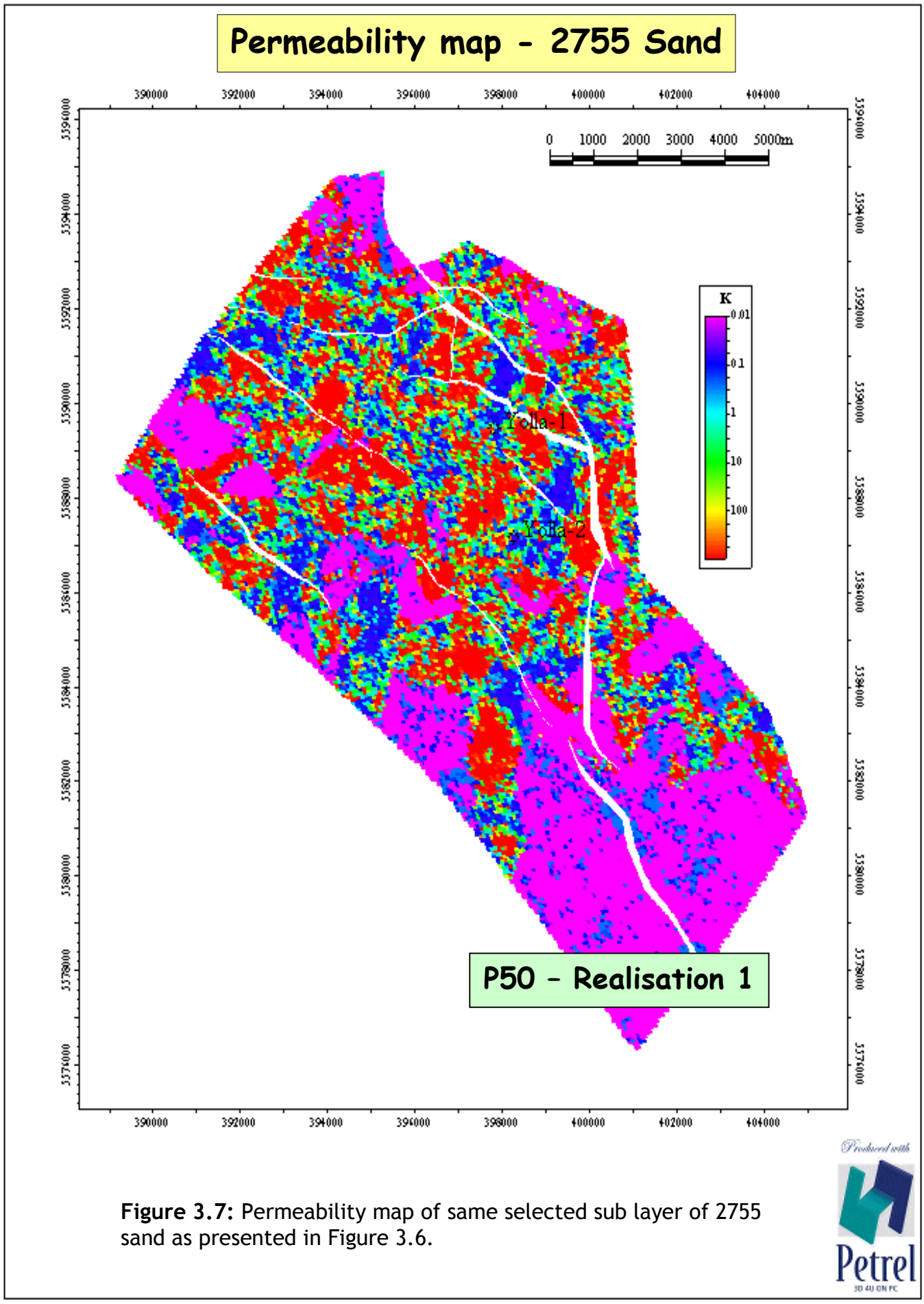

Figure 3.7: Permeability map of same selected sub layer of 2755 sand as presented in Figure 3.6.

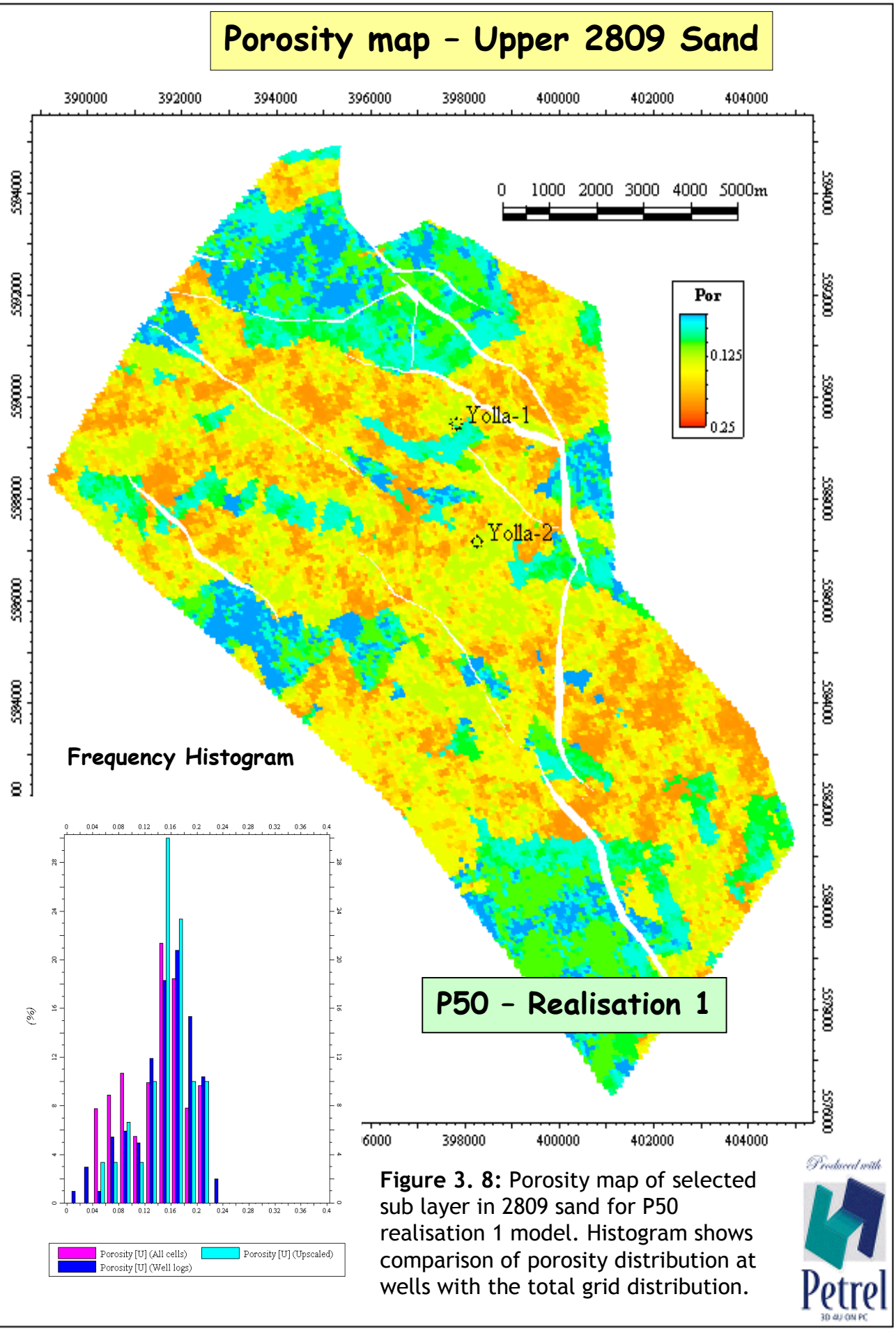

Figure 3. 8: Porosity map of selected sub layer in 2809 sand for P50 realisation 1 model. Histogram shows comparison of porosity distribution at wells with the total grid distribution.

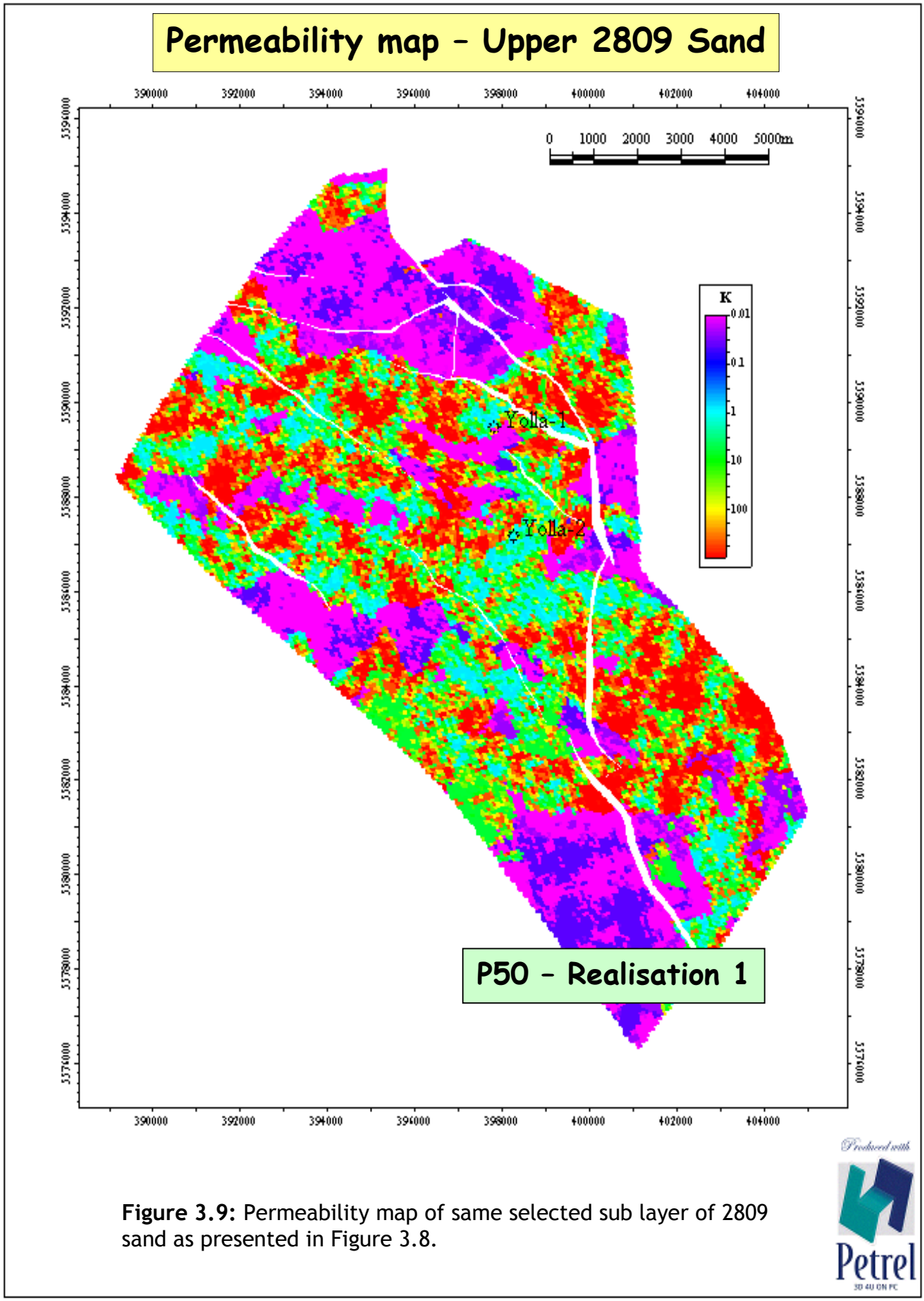

Figure 3.9: Permeability map of same selected sub layer of 2809 sand as presented in Figure 3.8.

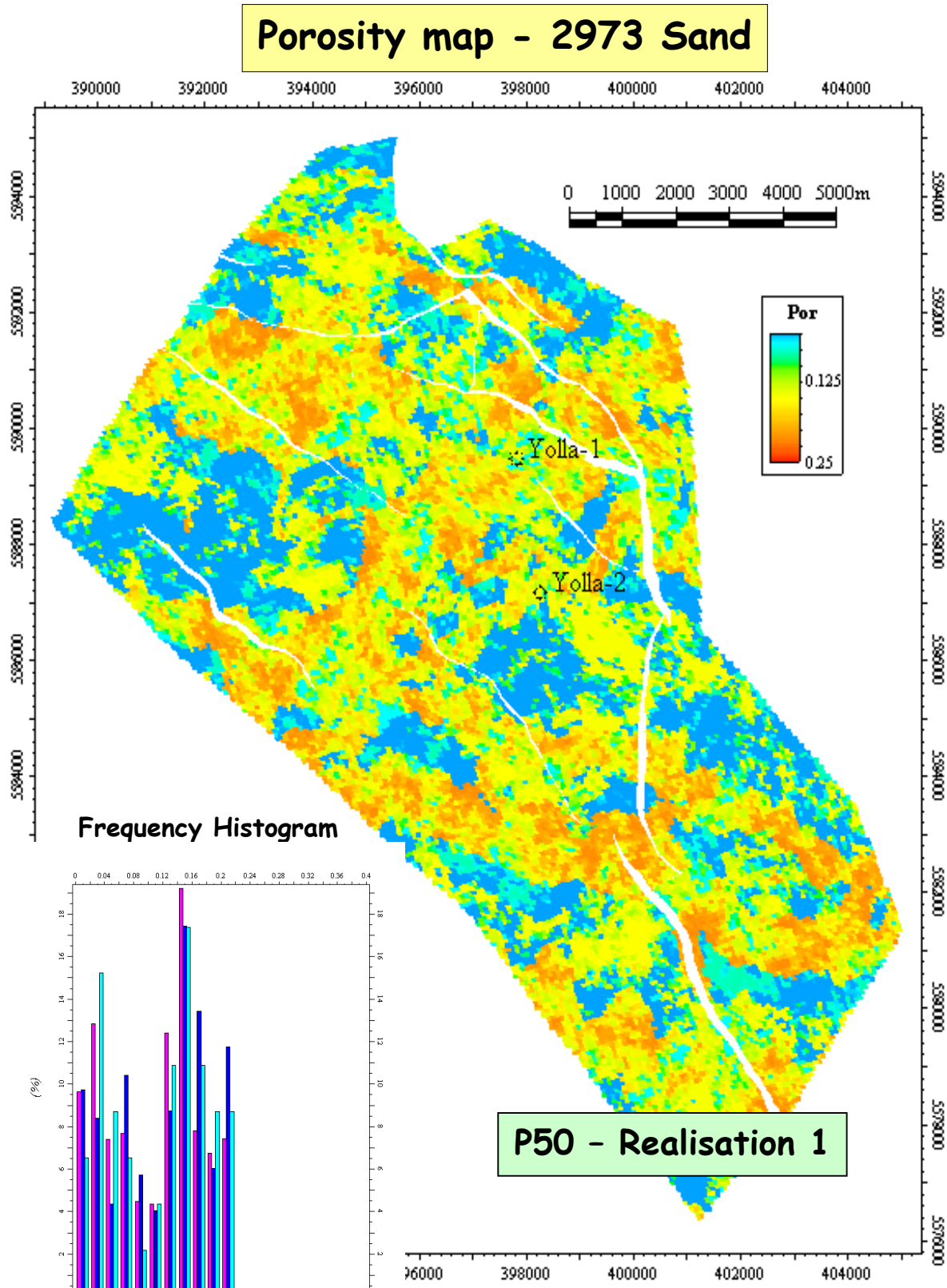

Figure 3. 10: Porosity map of selected sub layer in 2973 sand for P50 realisation 1 model. Histogram shows comparison of porosity distribution at wells with the total grid distribution.

Produced with Petrel

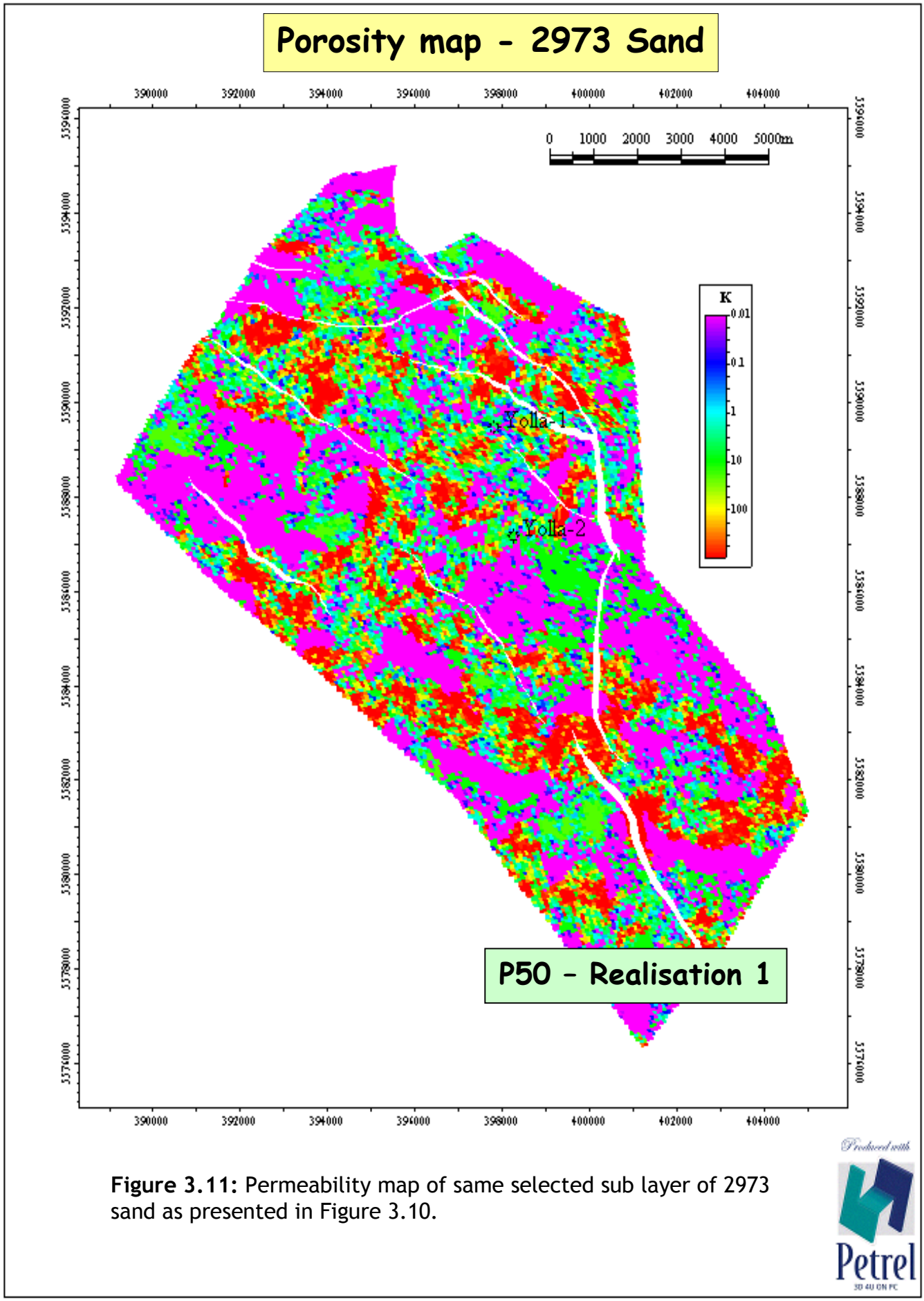

Figure 3.11: Permeability map of same selected sub layer of 2973 sand as presented in Figure 3.10.

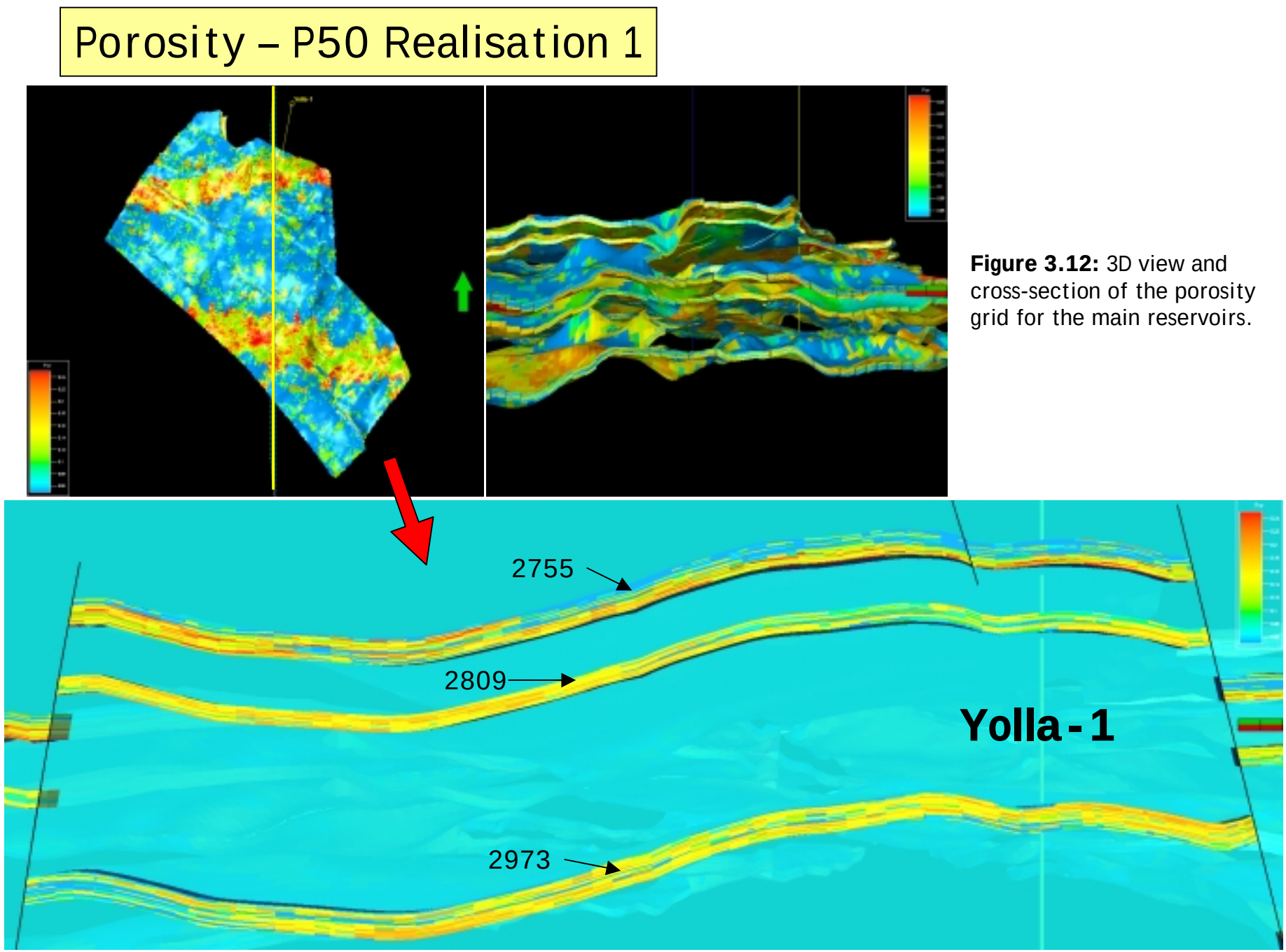

Figure 3.12: 3D view and cross-section of the porosity grid for the main reservoirs.

Porosity map - 2718 Sand

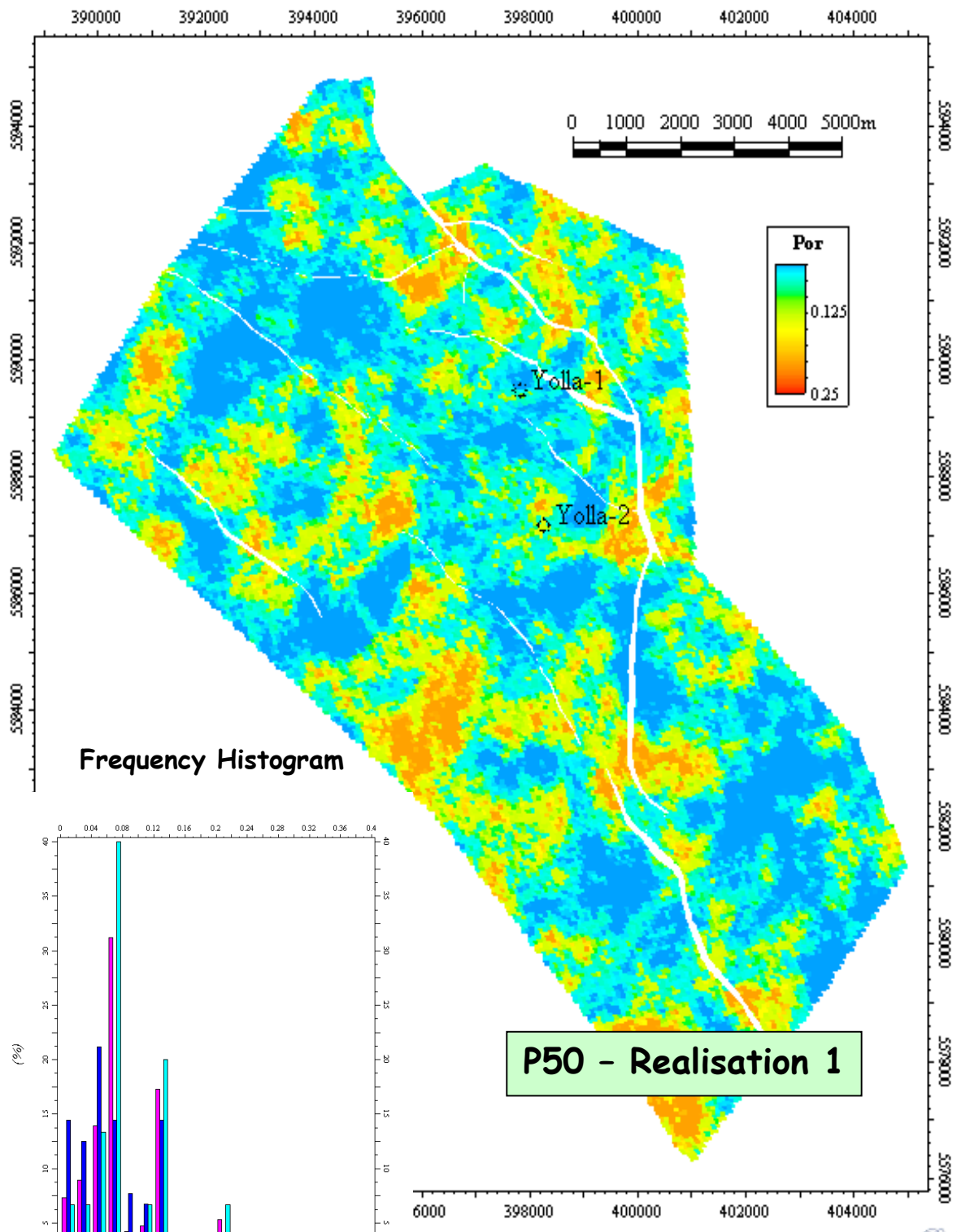

Frequency Histogram

P50 – Realisation 1

Figure 3.13: Porosity map of selected sub layer in 2718 sand for P50 realisation 1 model. Histogram shows comparison of porosity distribution at wells with the total grid distribution.

Produced with Petrel 3D at ON PC

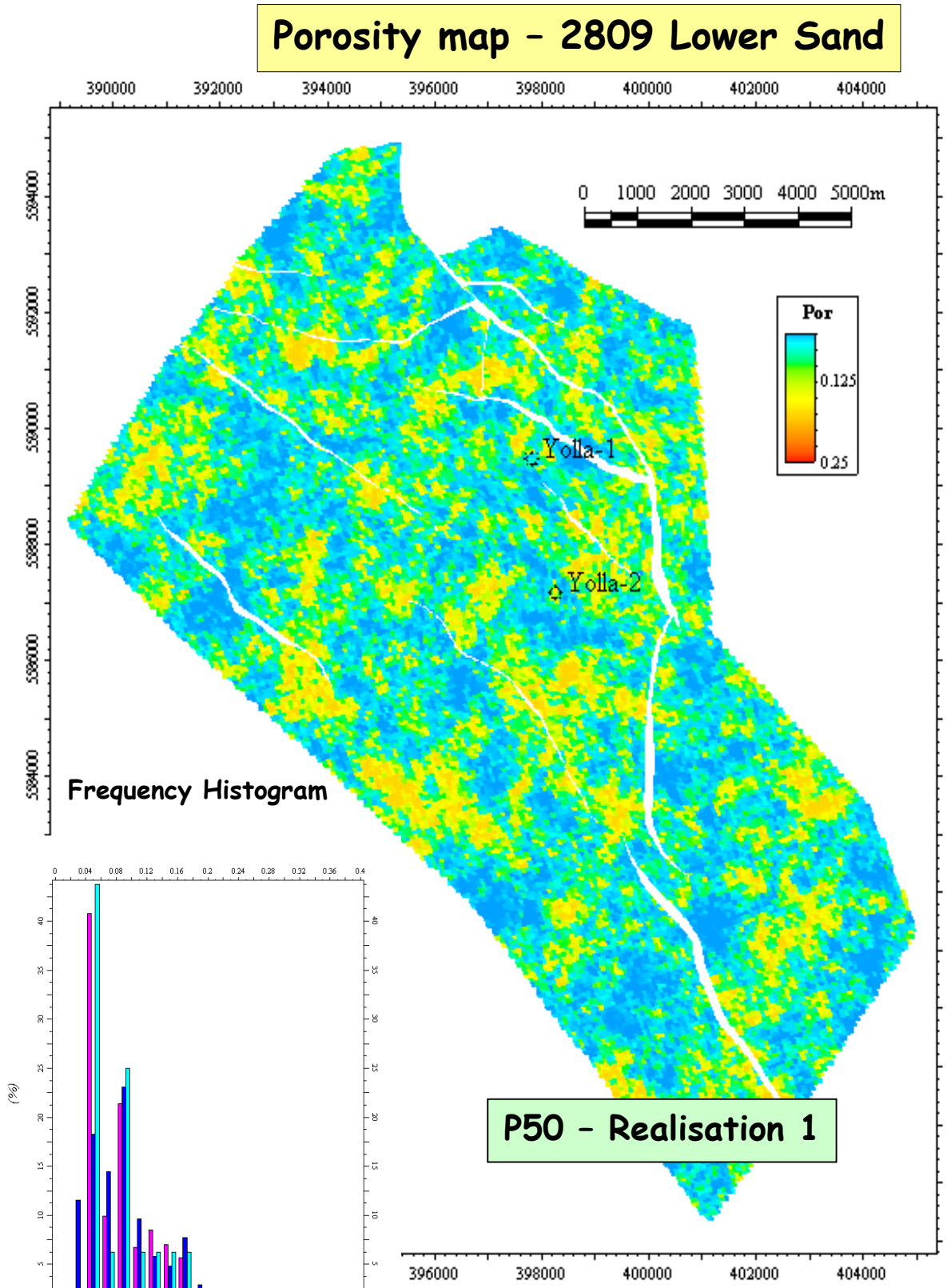

Figure 3.14: Porosity map of selected sub layer in lower 2809 sand for P50 realisation 1 model. Histogram shows comparison of porosity distribution at wells with the total grid distribution.

Produced with Petrel

Porosity map - 2952 Sand

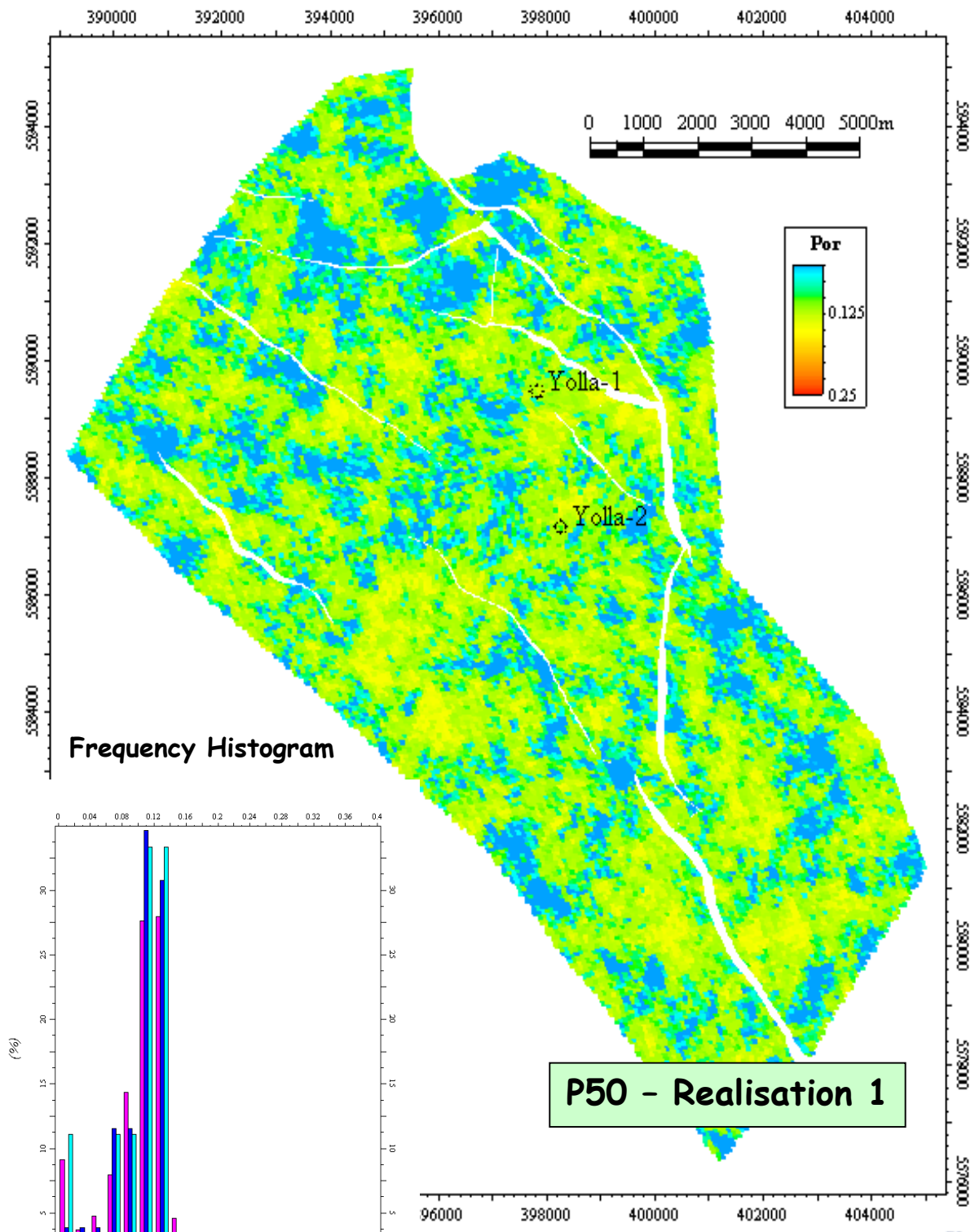

Figure 3.15: Porosity map of selected sub layer in 2952 sand for P50 realisation 1 model. Histogram shows comparison of porosity distribution at wells with the total grid distribution.

Produced with Petrel
3D at its ON PC

3.9 Realisation Descriptions

Several models were constructed for reservoir simulation. Brief descriptions of the parameters used for each model are outlined below. As much as possible the volume of hydrocarbons in place for each of the respective realizations was matched with the equivalent estimate from the probabilistic calculations e.g. the OGIP calculated for the P50 models was matched with the mean OGIP of 500 bcf. The comparison of the OGIP calculated for the simulation realizations and the probabilistic estimates is shown in Table 3.7. Only the reservoir parameters for the 2755, upper 2809 and 2973 units were altered for the different realisations. The changes in the proportion of facies and channel numbers are shown in Table 3.8. Selected porosity maps for the 2755, upper 2809 and 2973 sands for each realization are presented in Appendix 1.

Model	Realisation	OGIP (bcf) from Petrel Realisation	Probabilistic OGIP Estimate (bcf)
P90	1	350.7	393
	2	399.1	
P50	1	483	500
	2	413.2	
	3	511.5	
P10	1	575	621

Table 3.7: Comparison of OGIP calculated from simulation model grids with probabilistic estimate. Note: an 11.5% porosity cutoff was applied to the grid for the purposes of calculating OGIP.

Model	Realisation	Sand	Facies (%)				Max No. Channels
			Channel	Levee	Crevasse	Background	
P50	1	2755	47.3	0	12.6	40.1	50
		2809	56.2	14.00	11.0	18.8	50
		2973	43.5	13.4	10.3	32.8	40
	2	2755	46.9	0	13.3	39.9	40
		2809	29.0	14.3	12.4	44.3	40
		2973	25.7	7.9	8.7	57.7	40
	3	2755	45.16	0	12.7	42.12	40
		2809	53.2	15.25	11.25	20.3	50
		2973	47.8	10.6	9.4	32.2	50
P90	1	2755	17.0	0	6.5	76.5	45
		2809	26.6	15.4	10.9	47.1	35
		2973	29.5	10.0	7.9	52.6	40
	2	2755	38.6	0	11.6	49.8	45
		2809	56.0	15.6	11.4	17.0	35
		2973	50.9	11.9	8.9	28.3	40
P10	1	2755	49.8	0	9.3	40.9	50
		2809	59.8	17.2	9.8	13.1	60
		2973	47.6	11.0	6.8	34.6	40

Table 3.8: Percentage of facies and number of channels within different realisations

P50 Models

Realisation 1

Realisation 1 was built as a "best guess" model and uses the most likely structure map (see Figs. 2.9 & 2.10), based on interval velocity depth conversion methodology. In addition, the sand distribution in each zone is considered to be the most likely and is based on observations at the Yolla-1 and Yolla-2 locations. The reservoir parameters for the facies are shown in Tables 3.4, 3.5 and 3.6. The resultant porosity distribution approximately matched the porosity distribution intersected at the wells. OGIP approximately matches the Mean and P50 OGIP of 504 and 500 bcf respectively. OGIP was scaled within Eclipse (see below) to match the mean OGIP of 504 bcf, but with a lower average field permeability than the base case.

Realisation 2

Realisation 2 uses the same structural model as Realisation 1 but the proportion of finer-grained facies within the fluvial reservoirs has been increased. This has the effect of reducing the porosity/permeability across the model in the 2755, 2809 and 2973 units. OGIP was scaled within Eclipse (see below) to match the mean OGIP of 504 bcf.

Realisation 3

Realisation 3 uses the same structural model as the other P50 realisations but the proportion of higher porosity facies (i.e. channel facies) has been increased, effectively increasing the porosity and permeability of the 2755, 2809 and 2973 units. OGIP has been scaled to match the Mean probabilistic OGIP of 504 bcf.

P90 Models

Realisation 1

This realisation uses the P50 structural model but applied a pessimistic sand distribution to the zones to give a P90 case. The parameters for the sand trends are outlined in Tables 3.4, 3.5 and 3.6. The proportion of good quality reservoir facies (channel facies) was lowered. Channel geometries were also changed to reflect more ribbon-like sand distribution. OGIP was scaled to match the P90 probabilistic estimate of 393 bcf.

Realisation 2

This realisation used a P90 structural model (see section 2.3 & Fig. 2.14) but the sand distribution parameters were modeled as in the P50 case. This allowed the sensitivity of the Field to a pessimistic structural model to be assessed. OGIP was scaled to match the P90 estimate of 393 bcf.

P10 Model

This model applied the high side (P10) or optimistic structural case (see section 2.3 & Fig. 2.13) with the P50 sand distribution. OGIP was scaled to match the P10 probabilistic estimate of 621 bcf.

3.10 Upscaling

All geological realizations were upscaled for reservoir simulation within Eclipse reservoir simulation software. Upscaling is required to decrease the number of grid cells within the model to increase time efficiency of the modeling runs. The areal grid size of the model was increased from 80 x 80m to 200 x 200m dimensions (Fig. 3.16). Fault planes were converted from listric to a linear zig-zag geometry to accommodate the orthogonal and linear grid lines. These changes are required prior to importing the model into Eclipse.

The number of layers within zones was also decreased. The geological model contained an approximately 1m vertical resolution for sub-layers within zones. Table 3.9 shows the subsequent reduction in zones as a result of the upscaling process.

Reservoir unit	Number of layers within Geological model	Upscaled Model
2718	8	1
2755	22	3
2809	23	4
2952	4	1
2973	23	3

Table 3.9: Layer number comparison between geological and upscaled model.

Porosity and permeability were upscaled using arithmetic averaging of the grid cell centrepoints. Each cell in the upscaled grid was assigned a discrete value defining its porosity category (Fig. 3.16). This category was used in the subsequent modeling of water saturation within the reservoir simulation where each category was assigned an initial Sw (see section 4.). These categories are outlined in Table 3.10.

Porosity Category	Porosity range
1	< 8%
2	8 – 10 %
3	10 – 14 %
4	14 – 16 %
5	26 – 18 %
6	> 18%

Table 3.10: Definition of porosity categories for upscaled model. Used in water saturation modeling within Eclipse

The resultant grid, well data and properties (porosity, permeability and porosity category data) were exported from Petrel in an Eclipse ASCI format.

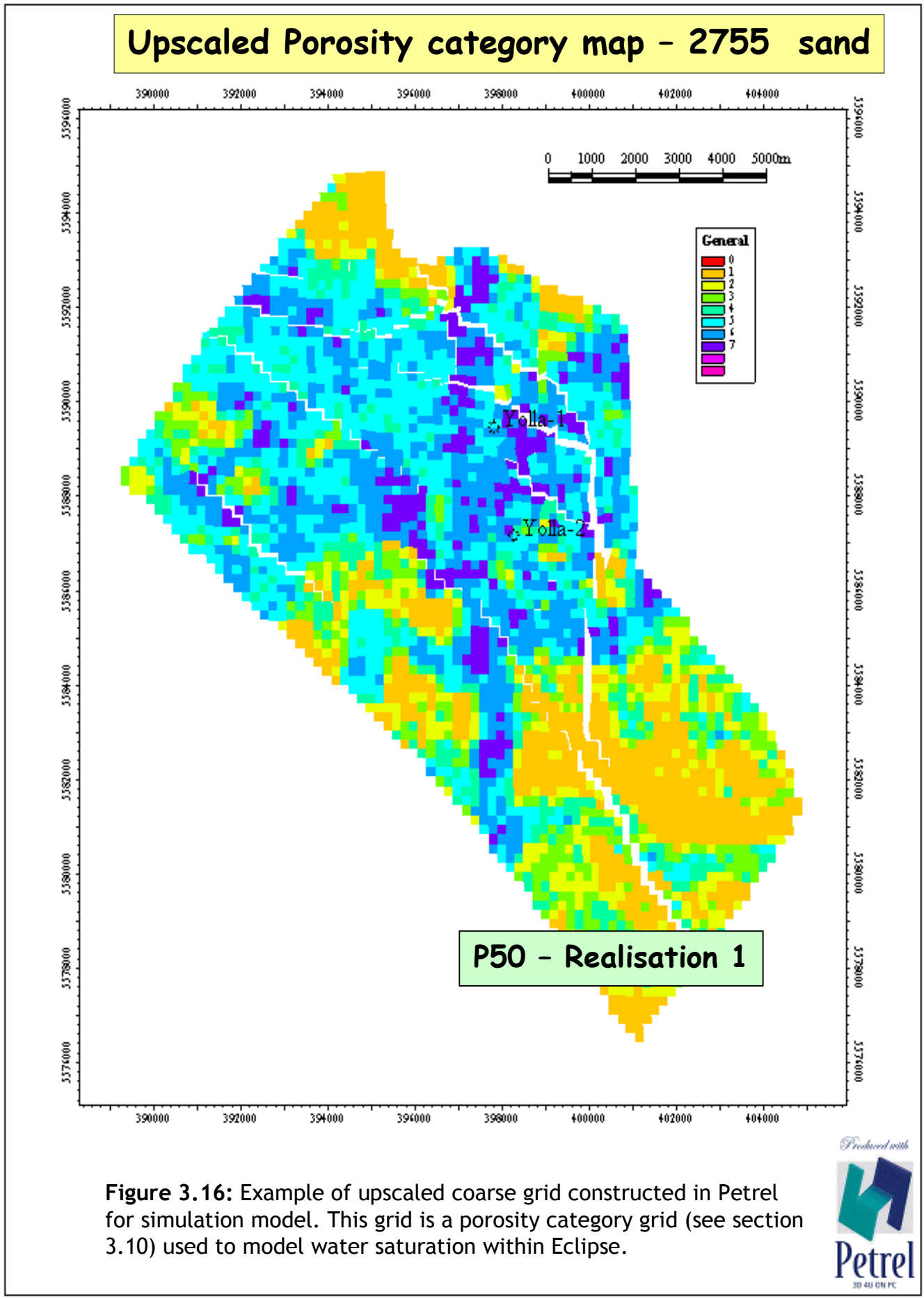

Figure 3.16: Example of upscaled coarse grid constructed in Petrel for simulation model. This grid is a porosity category grid (see section 3.10) used to model water saturation within Eclipse.

4 SUBSURFACE DEVELOPMENT PLAN

Production from the Yolla gas-condensate field has been modelled with the Eclipse 100 Reservoir Simulator (Eclipse 100). The underlying geological model was imported directly from a 3D Yolla geological model constructed using the Petrel package, based on data from Yolla 1 and 2 and the 3D seismic interpretation of May 2001.

The aim of this simulation study is to

- Identify the optimal Intra EVCM reservoir development plan,
- Confirm the ultimate recoverable reserves determined by Malkewicz, Hueni and Associates (MHA) in 2000, and
- Investigate the potential impact of reservoir, sand deposition and other variables on the recoverable reserves

The basic development principle is:

- Dry wellheads with a tubing size of 5-1/2"
- 2 production wells initially at a minimum THP of 1200 psi
- 2 additional wells added 5 to 8 years after production start to maintain deliverability and optimise recovery
- Production maintained at 72 MMscfd of raw gas
- Compression added when required to maintain deliverability (THP can be reduced to 725 psi)
- Wells produce from all Intra EVCM sands initially separately and later commingled to maintain deliverability
- Sands that produce formation water would be isolated (maximum well WGR is 10 bbl/MMscf, equivalent to around 200 bpd of formation water)

The optimal tubing size is determined to be 5-1/2" through a detailed well performance evaluation. The F.A.S.T. VirtuWell from Fekete was chosen as the wellbore simulator to carry out the nodal analysis.

Based on the above development principle, the sand rotation sequence of the well completion design base case examined was as outlined in Table 4.1

Sand	1-Jan-04	1-Aug-06	1-Aug-07	1-Jan-11	1-Apr-11
2718 & 2755	Yolla 3		Yolla 4	Yolla 3	All 4 wells
2809	Yolla 4	Yolla 3		Yolla 3 & 4	All 4 wells
2952 & 2973		Yolla 4	Yolla 3	Yolla 4	All 4 wells

Table 4.1: Well rotation scheme for well completion design base case.

Such a sequence will allow performance of individual reservoir layers to be monitored during early years. This will enable estimates of ultimate recovery by layer to be made to confirm total reserves and to determine whether eastern areas of the field are connected. Later in field life, layers will need to be commingled to maintain the offtake rate plateau required. This is the case to be used in well completion design.

The results of the design base case production using the above sand rotation scheme is summarised below in Table 4.2.

Well Schedule & Compression Timing	
Yolla 3 & 4 (Stage I wells)	1/01/2004
Yolla 5 & 6 (Stage II wells)	1/4/2011
Compression	1/08/2013
Cumulative Production to 31/12/2019 (bcf)	
Yolla 3	124.6
Yolla 4	131.8
Yolla 5	35.7
Yolla 6	45.3
SUM	337.4
OGIP (bcf)	503.4
Recovery	67.0%
Plateau Duration (year)	11.7

Table 4.2: Design base case production results.

The total raw gas recovery agrees very well with that modeled by MHA, which also predicted mean recovery of 337 bcf using a 4 well development scenario.

Further to the above, a number of sensitivity cases have also been performed to investigate the potential impact of reservoir, sand deposition and other variables on the recoverable reserves. The sensitivity scenario description and the corresponding recoveries are summarised in Table 4.3.

It is found that the commingled scheme has no impact on gas recovery compared with the single sand scheme in the design base case. For reservoir management reasons, the single sand case, where individual reservoir units are produced sequentially in early years, is the case used for well completion design. As the two cases are essentially identical in recovery performance, for simplicity in the modelling, all the reservoir sensitivities have been run and compared against the commingled case.

Scenario Description	Cum Prod, 2004 to 2019 (bcf)	Plateau Duration (Year)	OGIP (bcf)	Recovery Factor
Commingled Sand (P50)	339.2	11.6	503.4	67.4%
Dyke Transmissibility (P50)				
- Fully sealed (0% trans)	301.0	10.0	503.4	59.8%
- High trans (40% trans)	339.1	11.5	503.4	67.4%
Poor Sand Trend (P50)	280.9	8.8	503.4	55.8%
Reservoir Permeability (P50)				
- Low permeability	341.2	11.5	503.4	67.8%
- High Permeability	361.6	12.4	503.4	71.8%
Aquifer Strength (P50)				
- Widening fault opening to SW	337.8	11.5	503.4	67.1%
- Closing fault opening to SW	339.3	11.6	503.4	67.4%
- Halving end point Krw to 0.15	338.7	11.5	503.4	67.3%
- Doubling end point Krw to 0.60	336.9	11.4	503.4	66.9%
Upside Potential (P10)	419.4	13.9	621.0	67.5%
Down side Potential (P90)				
- Down side structure	257.2	8.4	393.0	65.4%
- Down side sand trend	226.5	6.9	392.4	57.7%

Table 4.3: Sensitivity scenario description and corresponding recoveries.

The results from the sensitivity studies indicate:

- There is little or no effect on recoverable reserves for the single sand scheme, commingled sand scheme, average reservoir permeability, or aquifer strength sensitivities.
- Upside structure would increase the recoverable reserves while the down side structure would reduce the recoverable reserves. However the recovery factors from both cases are comparable with that from the P50 base model.
- The recoverable reserves are found to be the most sensitive to sand trend and sealing dykes.
- Unfavourable sand trends could have a very profound effect on both recoverable reserves and recovery factor.
- Lack of dyke transmissibility could significantly affect the recoverable reserves.

The oil potential from the Top EVCM reservoir will be evaluated in a separate report.

4.1 Tubing Size Optimisation

In order to examine the effect of the tubing size on the Yolla well flow performance, nodal analysis was performed on various wellbore configurations at a range of flowing conditions. Nodal analysis involves creating the vertical flow performance (VFP) curves and overlaying them on the sandface inflow performance (IPR) curves. The point of the intersection of a particular set of VFP and IPR curves gives the well performance (i.e. the production rate and flowing bottomhole pressure) of a particular wellbore configuration and flow condition. Therefore, the optimal tubing size can

quickly be found through investigating the well performance under various wellbore configuration and flow conditions.

The F.A.S.T. VirtuWell from Fekete was chosen as the wellbore simulator to carry out this Yolla tubing size optimisation study. The Beggs and Brill correlations were selected to generate the VFP curves of the single and multi-phase flow, in vertical and deviated wellbores in the VirtuWell program.

The wellbore configurations investigated were:

- Wellbore trajectory: Vertical 3000 m long, Deviated 6000 m long about 5 Km stepout)
- Tubing size (OD): 4.0", 4.5", 5.0" and 5.5"

The operating and flow conditions are:

- Reservoir pressure: 4169, 3500, 3000 and 2500 psia
- CGR: fixed at 40 bbl/MMscf
- WGR: 0, 5, and 10 bbl/MMscf
- THP: 700 and 1000 psia

The detailed results of the tubing performance evaluation under various wellbore configurations and flow conditions are given in Table 4.4 and Figures 4.1 to 4.12.

The trend observed from Figures 4.1 to 4.12 is that there is a significant increase in maximum gas rate with the increase in tubing size from 4.0" to 5.0". After this, there is a smaller increase in production for 5.5" tubing. In addition, well performance in 5.5" tubing appears to be unstable at high WGR of 5 to 10 bbl/MMscf when the reservoir pressure is below 3,000 psia (see Figures 4.6 and 4.12).

It is obvious that the bigger the tubing size is, the higher the maximum possible gas rate when the reservoir pressure is high with no water production. However, this has to be balanced against the ability to handle liquids production when the reservoir pressure falls below 3,000 psia and the well produces water.

Based on the results of the nodal analysis, the optimal tubing size appears to be either 5.0" or 5.5" for the Yolla gas production.

Other factors affecting the tubing size selection for a gas well are the maximum and minimum gas rates. The gas rate in the tubing should not exceed the maximum rate in order to avoid erosion problems. Also the gas rate must be above the minimum rate to continuously remove the liquids in the wellbore. Otherwise the well will gradually load up and the liquid accumulation will kill the well.

Beggs suggested an equation to determine the maximum gas rate as

F.A.S.T. VirtuWell
Vertical Gas AOF/TPC

Correlation: Beggs & Brill

Absolute Open Flow:

	Reservoir Pressure	n	C	AOF
	psi(a)		MMcfd/(psi^2)^n	MMcfd
A	4169.0	0.800	1.45275e-04	90.000
B	3500.0	0.800	1.45270e-04	68.028
C	3000.0	0.800	1.45270e-04	53.158
D	2500.0	0.800	1.45270e-04	39.708

Tubing Performance Curve:

	Tubing ID	Tubing OD	Tubing Depth	Wellhead Pressure	OGR/CGR	WGR	Rec. Gas Gravity	Rec. Rate Factor	Flow Path
	in	in	ft	psi(a)	bbl/MMcf	bbl/MMcf			
1	3.548	4.000	9843	700.0	40.000	0.000	0.975	1.036	Tubing
2	3.957	4.500	9843	700.0	40.000	0.000	0.975	1.036	Tubing
3	4.494	5.000	9843	700.0	40.000	0.000	0.975	1.036	Tubing
4	4.950	5.000	9843	700.0	40.000	0.000	0.975	1.036	Tubing

Turner Rate:

Gas Rate	Flowin Pres
MMcfd	psi(a)
2.664	
3.276	
4.212	
5.112	

Operating Points:

	Gas Rate MMcfd					Flowing(SF) Pressure psi(a)			
	A	B	C	D		A	B	C	D
1	45.301	35.943	29.045	22.252	1	3164.1	2594.5	2184.2	1794.3
2	53.805	42.212	33.768	25.535	2	2870.8	2345.6	1973.7	1627.9
3	63.239	48.933	38.657	28.796	3	2489.6	2033.4	1719.1	1437.7
4	69.436	53.191	41.657	30.711	4	2193.5	1800.5	1537.3	1310.1

Casing ID	7.025 in	Roughness	0.00060 in	Gas Gravity	0.858
PBTD	9865 ft	Corr. Adj	100.000 %	N_2	0.20 %
MPP	9843 ft			CO_2	18.86 %
		Temp. Wellhead	80 °F	H_2S	0.00 %
		Temp. Sandface	292 °F	Cond API G	51.2 API°
				Sep Temp	100.0 °F
				Sep Pres	100 psi
				Water Gravity	1.000

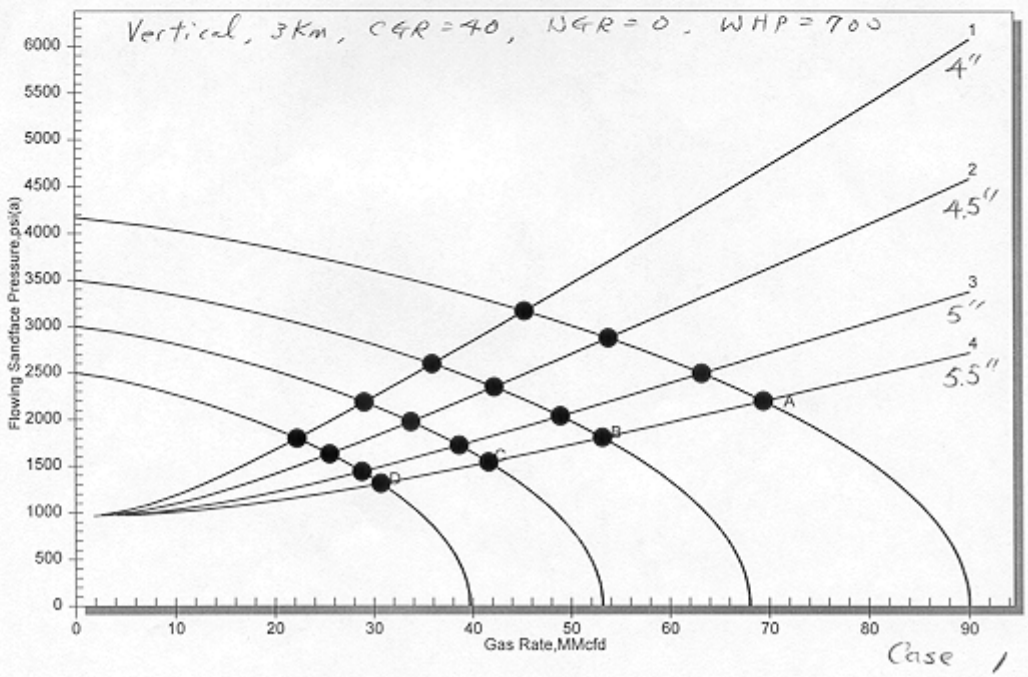

Fast Virtuwell™ Ver 1.541
Ver3km 22-Mar-01

Figure 4.1: Yolla Vertical Well Tubing Performance Curves – Case 1

F.A.S.T. VirtuWell
Vertical Gas AOF/TPC

Correlation: Beggs & Brill

Absolute Open Flow:

	Reservoir Pressure	n	C	AOF
	psi(a)		MMcfd/(psi^{2n})	MMcfd
A	4169.0	0.800	1.45275e-04	90.000
B	3500.0	0.800	1.45270e-04	68.028
C	3000.0	0.800	1.45270e-04	53.158
D	2500.0	0.800	1.45270e-04	39.708

Tubing Performance Curve:

	Tubing ID	Tubing OD	Tubing Depth	Wellhead Pressure	OGR/CGR	WGR	Rec. Gas Gravity	Rec. Rate Factor	Flow Path
	in	in	ft	psi(a)	bbl/MMcf	bbl/MMcf			
1	3.548	4.000	9843	700.0	40.000	5.000	0.975	1.036	Tubing
2	3.957	4.500	9843	700.0	40.000	5.000	0.975	1.036	Tubing
3	4.494	5.000	9843	700.0	40.000	5.000	0.975	1.036	Tubing
4	4.950	5.000	9843	700.0	40.000	5.000	0.975	1.036	Tubing

Turner Rate:

Gas Rate	Flowin Pres
MMcfd	psi(a)
3.024	12
3.744	12
4.860	12
5.904	12

Operating Points:

	Gas Rate MMcfd					Flowing(SF) Pressure psi(a)			
	A	B	C	D		A	B	C	D
1	38.154	30.452	24.735	19.146	1	3381.1	2786.3	2353.8	1933.4
2	46.371	36.644	29.493	22.533	2	3129.1	2568.2	2165.6	1780.7
3	56.192	43.821	34.961	26.262	3	2780.7	2275.7	1915.5	1588.0
4	63.195	48.893	38.509	28.570	4	2491.6	2035.4	1727.5	1452.0

Casing ID	7.025 in	**Roughness**	0.00060 in	**Gas Gravity**	0.858
PBTD	9865 ft	**Corr. Adj**	100.000 %	N_2	0.20 %
MPP	9843 ft			CO_2	18.86 %
		Temp. Wellhead	80 °F	H_2S	0.00 %
		Temp. Sandface	292 °F	**Cond API G**	51.2 API°
				Sep Temp	100.0 °F
				Sep Pres	100 psi
				Water Gravity	1.000

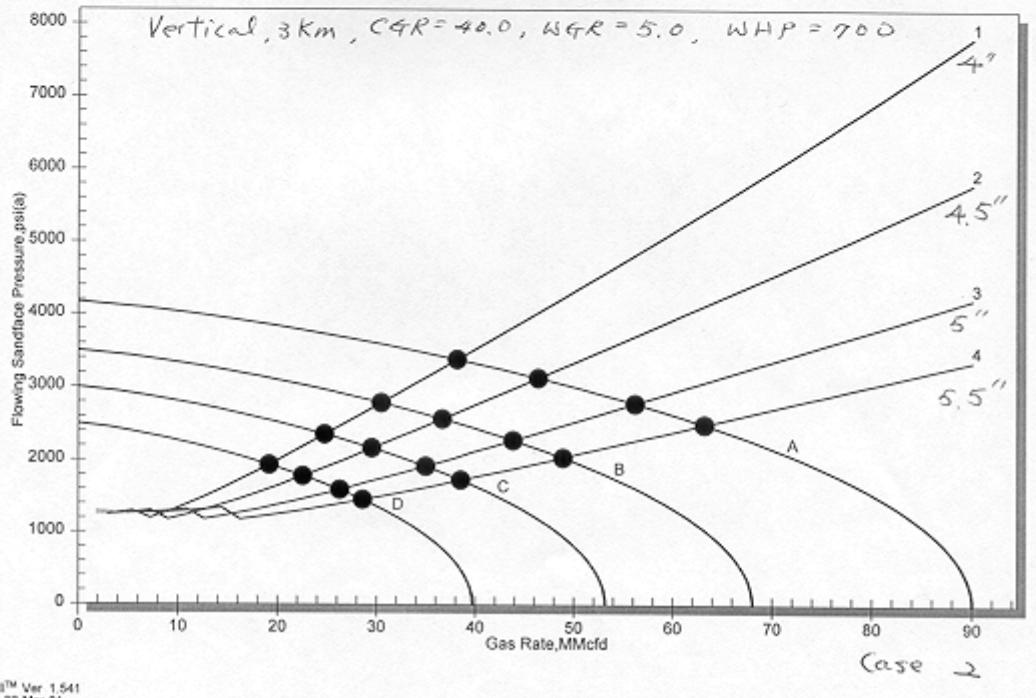

Fast Virtuwell™ Ver 1.541
Ver3km 22-Mar-01

Figure 4.2: Yolla Vertical Well Tubing Performance Curves – Case 2

F.A.S.T. VirtuWell
Vertical Gas AOF/TPC

Correlation: Beggs & Brill

Absolute Open Flow:

	Reservoir Pressure	n	C	AOF
	psi(a)		MMcfd/(psi^2)^n	MMcfd
A	4169.0	0.800	1.45275e-04	90.000
B	3500.0	0.800	1.45270e-04	68.028
C	3000.0	0.800	1.45270e-04	53.158
D	2500.0	0.800	1.45270e-04	39.708

Tubing Performance Curve:

	Tubing ID	Tubing OD	Tubing Depth	Wellhead Pressure	OGR/CGR	WGR	Rec. Gas Gravity	Rec. Rate Factor	Flow Path
	in	in	ft	psi(a)	bbl/MMcf	bbl/MMcf			
1	3.548	4.000	9843	700.0	40.000	10.000	0.975	1.036	Tubing
2	3.957	4.500	9843	700.0	40.000	10.000	0.975	1.036	Tubing
3	4.494	5.000	9843	700.0	40.000	10.000	0.975	1.036	Tubing
4	4.950	5.000	9843	700.0	40.000	10.000	0.975	1.036	Tubing

Turner Rate:

Gas Rate	Flowin Pres
MMcfd	psi(a)
3.276	1
4.068	1
5.256	1
6.408	1

Operating Points:

	Gas Rate MMcfd					Flowing(SF) Pressure psi(a)			
	A	B	C	D		A	B	C	D
1	34.481	27.554	22.390	17.234	1	3484.2	2879.3	2438.2	2011.8
2	42.362	33.541	27.025	20.563	2	3256.3	2680.9	2266.2	1871.8
3	52.114	40.746	32.447	24.316	3	2932.6	2407.0	2035.7	1692.3
4	59.349	45.925	36.222	26.822	4	2655.4	2180.1	1851.4	1556.4

Casing ID	7.025 in	**Roughness**	0.00060 in	**Gas Gravity**	0.858
PBTD	9865 ft	**Corr. Adj**	100.000 %	N_2	0.20 %
MPP	9843 ft			CO_2	18.86 %
		Temp. Wellhead	80 °F	H_2S	0.00 %
		Temp. Sandface	292 °F	**Cond API G**	51.2 API°
				Sep Temp	100.0 °F
				Sep Pres	100 psi
				Water Gravity	1.000

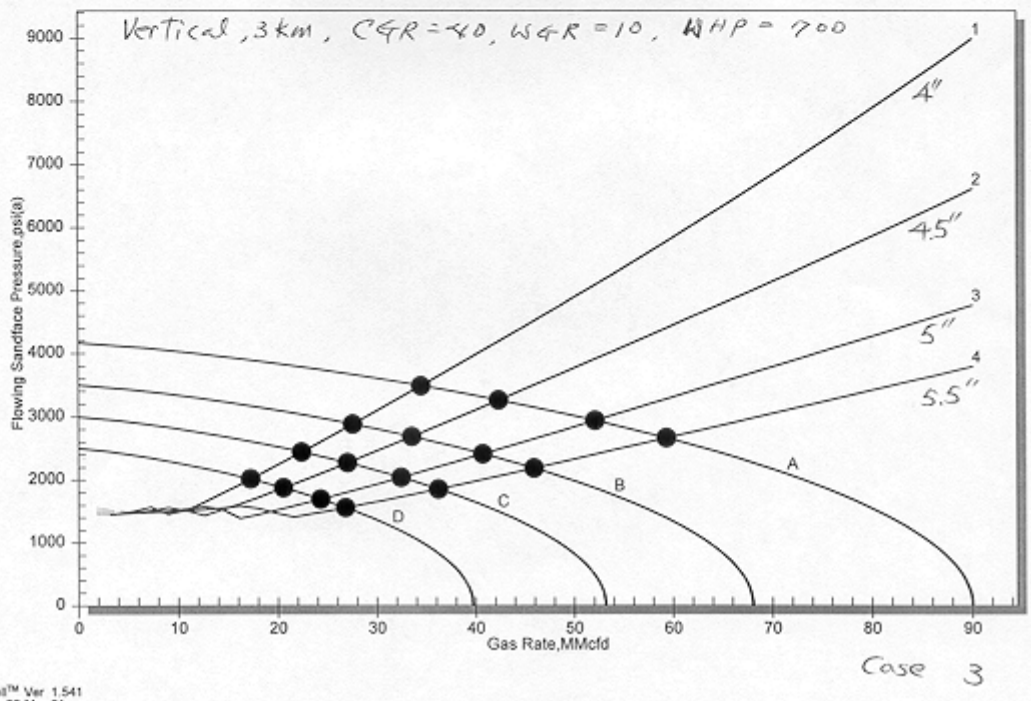

Fast Virtuwell™ Ver 1.541
Ver3km 22-Mar-01

Figure 4.3: Yolla Vertical Well Tubing Performance Curves – Case 3

F.A.S.T. VirtuWell
Vertical Gas AOF/TPC

Correlation: Beggs & Brill

Absolute Open Flow:

	Reservoir Pressure	n	C	AOF
	psi(a)		MMcfd/(psi^{2n})	MMcfd
A	4169.0	0.800	1.45275e-04	90.000
B	3500.0	0.800	1.45270e-04	68.028
C	3000.0	0.800	1.45270e-04	53.158
D	2500.0	0.800	1.45270e-04	39.708

Tubing Performance Curve:

	Tubing ID	Tubing OD	Tubing Depth	Wellhead Pressure	OGR/CGR	WGR	Rec. Gas Gravity	Rec. Rate Factor	Flow Path
	in	in	ft	psi(a)	bbl/MMcf	bbl/MMcf			
1	3.548	4.000	9843	1000.0	40.000	0.000	0.975	1.036	Tubing
2	3.957	4.500	9843	1000.0	40.000	0.000	0.975	1.036	Tubing
3	4.494	5.000	9843	1000.0	40.000	0.000	0.975	1.036	Tubing
4	4.950	5.000	9843	1000.0	40.000	0.000	0.975	1.036	Tubing

Turner Rate:

Gas Rate	Flowin Pres
MMcfd	psi(a)
3.204	1
3.996	1
5.148	1
6.228	1

Operating Points:

	Gas Rate MMcfd					Flowing(SF) Pressure psi(a)			
	A	B	C	D		A	B	C	D
1	43.731	34.046	26.796	19.480	1	3213.5	2663.3	2275.3	1919.1
2	51.834	39.852	30.996	22.180	2	2942.5	2443.6	2101.0	1797.7
3	60.746	45.993	35.265	24.780	3	2597.4	2177.0	1900.1	1668.1
4	66.551	49.832	37.837	26.268	4	2337.1	1986.7	1764.9	1587.7

Casing ID	7.025 in	**Roughness**	0.00060 in	**Gas Gravity**	0.858
PBTD	9865 ft	**Corr. Adj**	100.000 %	N_2	0.20 %
MPP	9843 ft			CO_2	18.86 %
		Temp. Wellhead	80 °F	H_2S	0.00 %
		Temp. Sandface	292 °F	**Cond API G**	51.2 API°
				Sep Temp	100.0 °F
				Sep Pres	100 psi
				Water Gravity	1.000

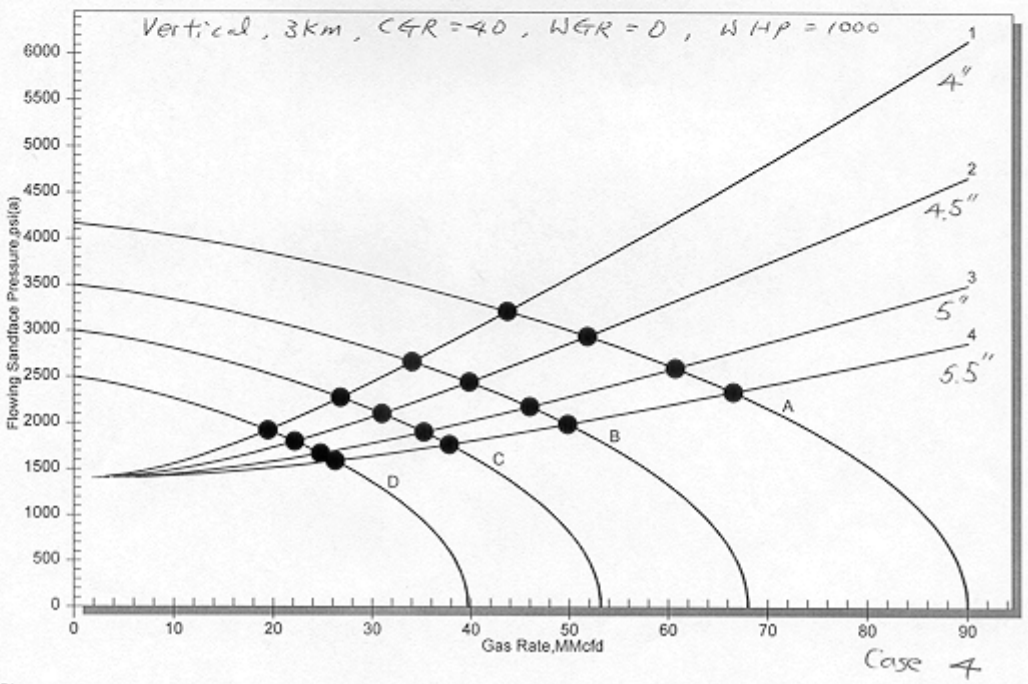

Fast Virtuwell™ Ver 1.541
Ver3km 22-Mar-01

Figure 4.4: Yolla Vertical Well Tubing Performance Curves – Case 4

F.A.S.T. VirtuWell
Vertical Gas AOF/TPC

Correlation: Beggs & Brill

Absolute Open Flow:

	Reservoir Pressure	n	C	AOF
	psi(a)		MMcfd/(psi^2)^n	MMcfd
A	4169.0	0.800	1.45275e-04	90.000
B	3500.0	0.800	1.45270e-04	68.028
C	3000.0	0.800	1.45270e-04	53.158
D	2500.0	0.800	1.45270e-04	39.708

Tubing Performance Curve:

	Tubing ID	Tubing OD	Tubing Depth	Wellhead Pressure	OGR/CGR	WGR	Rec. Gas Gravity	Rec. Rate Factor	Flow Path
	in	in	ft	psi(a)	bbl/MMcf	bbl/MMcf			
1	3.548	4.000	9843	1000.0	40.000	5.000	0.975	1.036	Tubing
2	3.957	4.500	9843	1000.0	40.000	5.000	0.975	1.036	Tubing
3	4.494	5.000	9843	1000.0	40.000	5.000	0.975	1.036	Tubing
4	4.950	5.000	9843	1000.0	40.000	5.000	0.975	1.036	Tubing

Turner Rate:

Gas Rate	Flowin Pres
MMcfd	psi(a)
3.600	1
4.500	1
5.832	1
7.092	1

Operating Points:

	Gas Rate MMcfd					Flowing(SF) Pressure psi(a)			
	A	B	C	D		A	B	C	D
1	36.758	28.728	22.654	16.504	1	3421.3	2842.1	2428.9	2040.5
2	44.578	34.453	26.874	19.265	2	3186.9	2648.6	2272.2	1928.3
3	53.852	41.004	31.571	22.134	3	2869.1	2396.4	2075.2	1799.9
4	60.401	45.453	34.647	20.188	4	2611.7	2201.9	1931.0	1888.4

Casing ID	7.025 in	**Roughness**	0.00060 in	**Gas Gravity**	0.858
PBTD	9865 ft	**Corr. Adj**	100.000 %	**N_2**	0.20 %
MPP	9843 ft			**CO_2**	18.86 %
		Temp. Wellhead	80 °F	**H_2S**	0.00 %
		Temp. Sandface	292 °F	**Cond API G**	51.2 API°
				Sep Temp	100.0 °F
				Sep Pres	100 psi
				Water Gravity	1.000

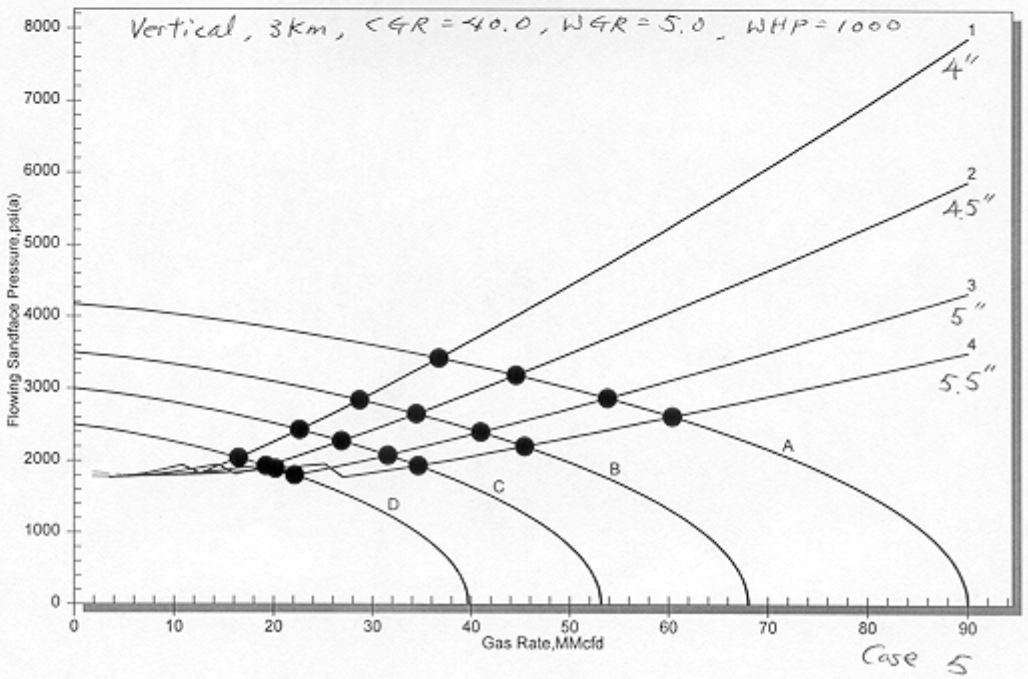

Fast Virtuwell™ Ver 1.541
Ver3km 22-Mar-01

Figure 4.5: Yolla Vertical Well Tubing Performance Curves – Case 5

F.A.S.T. VirtuWell
Vertical Gas AOF/TPC

Correlation: Beggs & Brill

Absolute Open Flow:

	Reservoir Pressure	n	C	AOF
	psi(a)		MMcfd/(psi^{2n})	MMcfd
A	4169.0	0.800	1.45275e-04	90.000
B	3500.0	0.800	1.45270e-04	68.028
C	3000.0	0.800	1.45270e-04	53.158
D	2500.0	0.800	1.45270e-04	39.708

Tubing Performance Curve:

	Tubing ID	Tubing OD	Tubing Depth	Wellhead Pressure	OGR/CGR	WGR	Rec. Gas Gravity	Rec. Rate Factor	Flow Path
	in	in	ft	psi(a)	bbl/MMcf	bbl/MMcf			
1	3.548	4.000	9843	1000.0	40.000	10.000	0.975	1.036	Tubing
2	3.957	4.500	9843	1000.0	40.000	10.000	0.975	1.036	Tubing
3	4.494	5.000	9843	1000.0	40.000	10.000	0.975	1.036	Tubing
4	4.950	5.000	9843	1000.0	40.000	10.000	0.975	1.036	Tubing

Turner Rate:

Gas Rate	Flowin Pres
MMcfd	psi(a)
3.852	1
4.788	2
6.192	2
7.560	2

Operating Points:

	Gas Rate MMcfd					Flowing(SF) Pressure psi(a)			
	A	B	C	D		A	B	C	D
1	33.162	25.914	20.394	11.686	1	3519.7	2929.6	2506.3	2212.3
2	40.655	31.437	24.480	13.232	2	3307.8	2753.3	2363.1	2160.2
3	49.864	38.005	29.172	14.898	3	3011.9	2516.5	2179.0	2101.1
4	56.628	42.648	27.460	15.706	4	2764.0	2327.1	2248.8	2070.9

Casing ID	7.025 in	**Roughness**	0.00060 in	**Gas Gravity**	0.858
PBTD	9865 ft	**Corr. Adj**	100.000 %	N_2	0.20 %
MPP	9843 ft			CO_2	18.86 %
		Temp. Wellhead	80 °F	H_2S	0.00 %
		Temp. Sandface	292 °F	**Cond API G**	51.2 API°
				Sep Temp	100.0 °F
				Sep Pres	100 psi
				Water Gravity	1.000

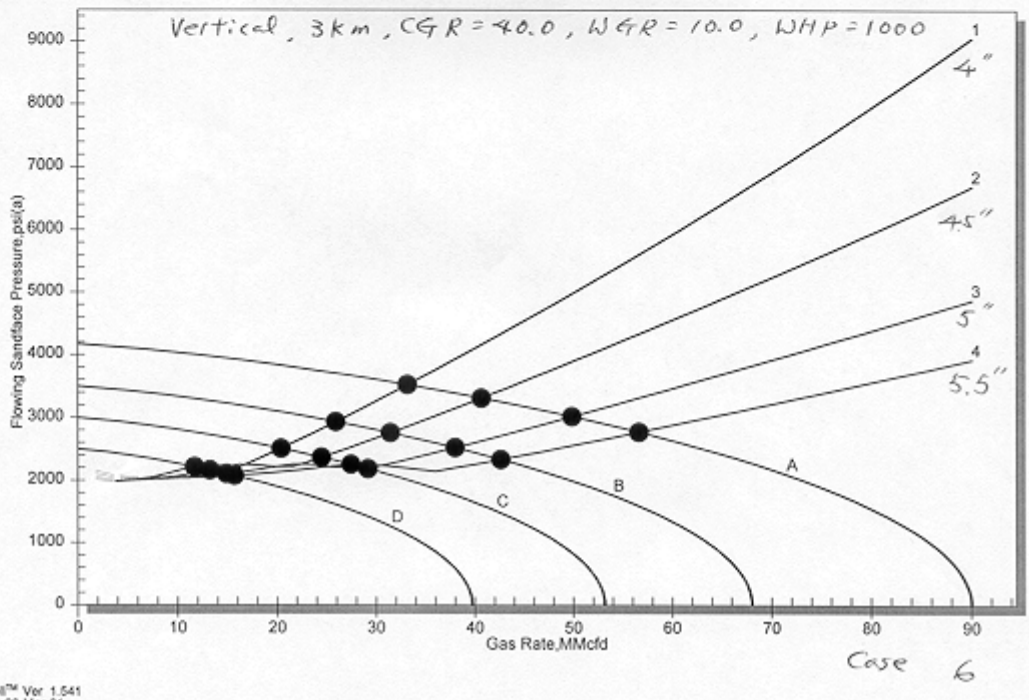

Fast Virtuwell™ Ver 1.541
VerSkm 22-Mar-01

Figure 4.6: Yolla Vertical Well Tubing Performance Curves – Case 6

F.A.S.T. VirtuWell
Horizontal Gas AOF/TPC

Correlation: Beggs & Brill

Absolute Open Flow:

	Reservoir Pressure	n	C	AOF
	psi(a)		MMcfd/(psi^2)^n	MMcfd
A	4169.0	0.800	1.45270e-04	89.997
B	3500.0	0.800	1.45270e-04	68.028
C	3000.0	0.800	1.45270e-04	53.158
D	2500.0	0.800	1.45270e-04	39.708

Tubing Performance Curve:

	Tubing ID	Tubing OD	Tubing Depth	Wellhead Pressure	OGR/CGR	WGR	Rec. Gas Gravity	Rec. Rate Factor	Flow Path
	in	in	ft	psi(a)	bbl/MMcf	bbl/MMcf			
1	3.548	4.000	19685	700.0	40.000	0.000	0.975	1.036	Tubing
2	3.957	4.500	19685	700.0	40.000	0.000	0.975	1.036	Tubing
3	4.494	5.000	19685	700.0	40.000	0.000	0.975	1.036	Tubing
4	4.950	5.500	19685	700.0	40.000	0.000	0.975	1.036	Tubing

Turner Rate:

Gas Rate	Flowir Pres
MMcfd	psi(a)
2.628	
3.240	
4.176	
5.040	

Operating Points:

	Gas Rate MMcfd					Flowing(SF) Pressure psi(a)			
	A	B	C	D		A	B	C	D
1	33.406	26.983	22.180	17.373	1	3513.3	2896.8	2445.6	2006.4
2	41.287	33.050	26.938	20.855	2	3288.7	2698.0	2269.6	1858.3
3	51.219	40.480	32.603	24.877	3	2964.2	2417.9	2028.4	1663.1
4	58.728	45.916	36.617	27.607	4	2680.6	2180.6	1830.6	1510.5

Vertical Casing ID	6.538 in	Roughness	0.00060 in	Gas Gravity	0.858
KOP(MD)	263 ft	Corr. Adj.	100.000 %	N_2	0.20 %
				CO_2	18.86 %
Deviated Casing ID	6.538 in	Temp. Wellhead	80 °F	H_2S	0.00 %
Heel(MD)	19685 ft	Temp. Sandface	292 °F		
Heel(TVD)	9843 ft			Cond API G	51.2 API°
				Sep Temp	100.0 °F
Horizontal Casing ID	6.538 in			Sep Pres	100 psi
Toe(MD)	19686 ft			Water Gravity	1.000
Datum(MD)	19685 ft				

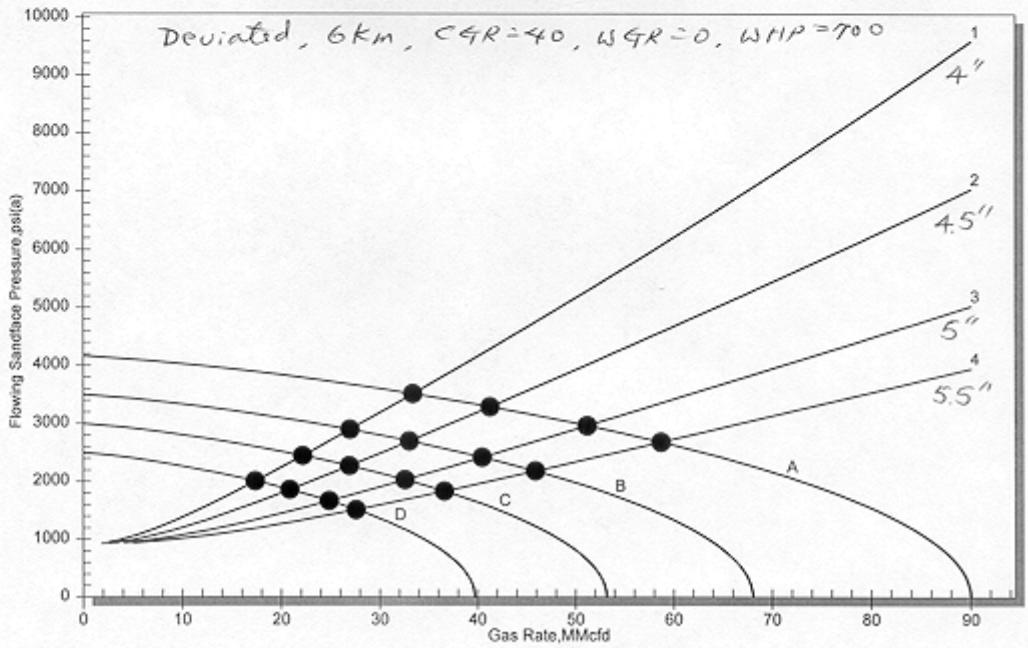

Fast Virtuwell™ Ver 1.541
DevGkm 22-Mar-01

Case 7

Figure 4.7: Yolla Deviated Well Tubing Performance Curves – Case 7

F.A.S.T. VirtuWell
Horizontal Gas AOF/TPC

Correlation: Beggs & Brill

Absolute Open Flow:

	Reservoir Pressure	n	C	AOF
	psi(a)		MMcfd/(psi^{2n})	MMcfd
A	4169.0	0.800	1.45270e-04	89.997
B	3500.0	0.800	1.45270e-04	68.028
C	3000.0	0.800	1.45270e-04	53.158
D	2500.0	0.800	1.45270e-04	39.708

Tubing Performance Curve:

	Tubing ID	Tubing OD	Tubing Depth	Wellhead Pressure	OGR/CGR	WGR	Rec. Gas Gravity	Rec. Rate Factor	Flow Path
	in	in	ft	psi(a)	bbl/MMcf	bbl/MMcf			
1	3.548	4.000	19685	700.0	40.000	5.000	0.975	1.036	Tubing
2	3.957	4.500	19685	700.0	40.000	5.000	0.975	1.036	Tubing
3	4.494	5.000	19685	700.0	40.000	5.000	0.975	1.036	Tubing
4	4.950	5.500	19685	700.0	40.000	5.000	0.975	1.036	Tubing

Turner Rate:

Gas Rate	Flowin Pres
MMcfd	psi(a)
2.880	1
3.600	1
4.644	1
5.616	1

Operating Points:

	Gas Rate MMcfd					Flowing(SF) Pressure psi(a)			
	A	B	C	D		A	B	C	D
1	30.315	24.526	20.354	15.963	1	3594.3	2970.7	2507.6	2061.2
2	37.788	30.359	24.951	19.357	2	3391.7	2789.4	2345.8	1924.0
3	47.480	37.895	30.596	23.415	3	3092.7	2520.8	2118.2	1737.7
4	55.166	43.440	34.744	26.381	4	2820.0	2292.6	1926.3	1581.3

Vertical Casing ID	6.538 in	Roughness	0.00060 in	Gas Gravity	0.858
KOP(MD)	263 ft	Corr. Adj.	100.000 %	N_2	0.20 %
				CO_2	18.86 %
Deviated Casing ID	6.538 in	Temp. Wellhead	80 °F	H_2S	0.00 %
Heel(MD)	19685 ft	Temp. Sandface	292 °F	Cond API G	51.2 API°
Heel(TVD)	9843 ft			Sep Temp	100.0 °F
				Sep Pres	100 psi
Horizontal Casing ID	6.538 in			Water Gravity	1.000
Toe(MD)	19686 ft				
Datum(MD)	19685 ft				

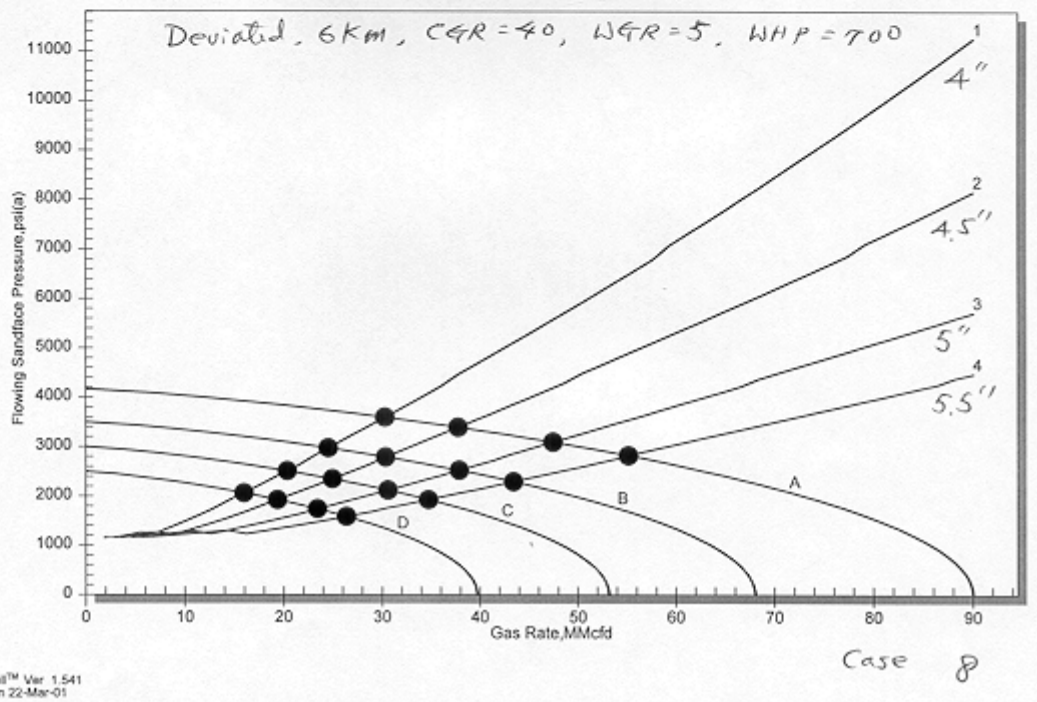

Fast Virtuwell™ Ver 1.541
Dev6km 22-Mar-01

Figure 4.8: Yolla Deviated Well Tubing Performance Curves – Case 8

F.A.S.T. VirtuWell
Horizontal Gas AOF/TPC

Correlation: Beggs & Brill

Absolute Open Flow:

	Reservoir Pressure	n	C	AOF
	psi(a)		MMcfd/(psi^{2n})	MMcfd
A	4169.0	0.800	1.45270e-04	89.997
B	3500.0	0.800	1.45270e-04	68.028
C	3000.0	0.800	1.45270e-04	53.158
D	2500.0	0.800	1.45270e-04	39.708

Tubing Performance Curve:

	Tubing ID	Tubing OD	Tubing Depth	Wellhead Pressure	OGR/CGR	WGR	Rec. Gas Gravity	Rec. Rate Factor	Flow Path
	in	in	ft	psi(a)	bbl/MMcf	bbl/MMcf			
1	3.548	4.000	19685	700.0	40.000	10.000	0.975	1.036	Tubing
2	3.957	4.500	19685	700.0	40.000	10.000	0.975	1.036	Tubing
3	4.494	5.000	19685	700.0	40.000	10.000	0.975	1.036	Tubing
4	4.950	5.500	19685	700.0	40.000	10.000	0.975	1.036	Tubing

Turner Rate:

Gas Rate	Flowin Pres
MMcfd	psi(a)
3.096	1
3.852	1
5.004	1
6.084	1

Operating Points:

	Gas Rate MMcfd					Flowing(SF) Pressure psi(a)			
	A	B	C	D		A	B	C	D
1	27.331	22.312	18.484	14.662	1	3669.1	3034.3	2568.2	2109.6
2	34.347	27.948	22.872	17.983	2	3487.9	2867.1	2421.2	1981.7
3	43.690	35.103	28.479	22.009	3	3214.8	2625.0	2207.7	1805.7
4	51.674	40.705	32.913	24.952	4	2948.1	2408.7	2013.9	1659.2

Vertical Casing ID	6.538 in	**Roughness**	0.00060 in	**Gas Gravity**	0.858
KOP(MD)	263 ft	**Corr. Adj.**	100.000 %	N_2	0.20 %
				CO_2	18.86 %
Deviated Casing ID	6.538 in	**Temp. Wellhead**	80 °F	H_2S	0.00 %
Heel(MD)	19685 ft	**Temp. Sandface**	292 °F	**Cond API G**	51.2 API°
Heel(TVD)	9843 ft			**Sep Temp**	100.0 °F
				Sep Pres	100 psi
Horizontal Casing ID	6.538 in			**Water Gravity**	1.000
Toe(MD)	19686 ft				
Datum(MD)	19685 ft				

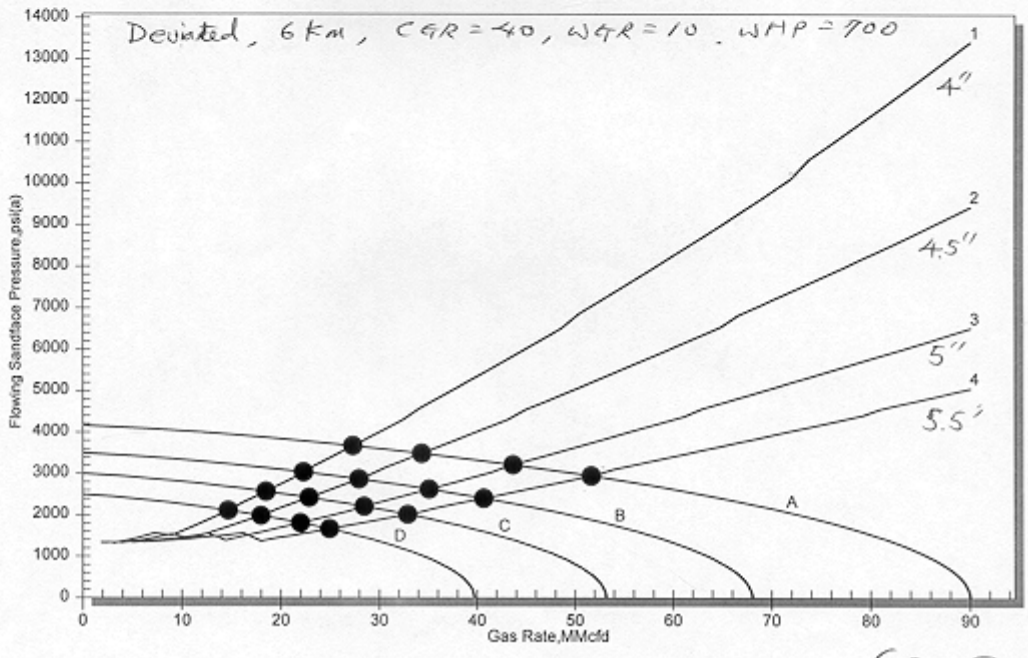

Fast Virtuwell™ Ver 1.541
Dev6km 22-Mar-01

Figure 4.9: Yolla Deviated Well Tubing Performance Curves – Case 9

F.A.S.T. VirtuWell
Horizontal Gas AOF/TPC

Correlation: Beggs & Brill

Absolute Open Flow:

	Reservoir Pressure	n	C	AOF
	psi(a)		MMcfd/(psi^{2n})	MMcfd
A	4169.0	0.800	1.45270e-04	89.997
B	3500.0	0.800	1.45270e-04	68.028
C	3000.0	0.800	1.45270e-04	53.158
D	2500.0	0.800	1.45270e-04	39.708

Tubing Performance Curve:

	Tubing ID	Tubing OD	Tubing Depth	Wellhead Pressure	OGR/CGR	WGR	Rec. Gas Gravity	Rec. Rate Factor	Flow Path
	in	in	ft	psi(a)	bbl/MMcf	bbl/MMcf			
1	3.548	4.000	19685	1000.0	40.000	0.000	0.975	1.036	Tubing
2	3.957	4.500	19685	1000.0	40.000	0.000	0.975	1.036	Tubing
3	4.494	5.000	19685	1000.0	40.000	0.000	0.975	1.036	Tubing
4	4.950	5.500	19685	1000.0	40.000	0.000	0.975	1.036	Tubing

Turner Rate:

Gas Rate	Flowi Pres
MMcfd	psi(a)
3.168	1
3.924	1
5.040	1
6.084	1

Operating Points:

	Gas Rate MMcfd					Flowing(SF) Pressure psi(a)			
	A	B	C	D		A	B	C	D
1	32.454	25.819	20.782	15.631	1	3538.4	2932.6	2493.2	2073.7
2	40.058	31.552	25.158	18.669	2	3325.7	2749.5	2338.2	1953.6
3	49.589	38.519	30.298	22.088	3	3021.2	2496.3	2131.1	1802.1
4	56.753	43.568	33.895	24.361	4	2759.1	2287.0	1967.5	1689.9

Vertical Casing ID	6.538 in	Roughness	0.00060 in	Gas Gravity	0.858
KOP(MD)	263 ft	Corr. Adj.	100.000 %	N_2	0.20 %
				CO_2	18.86 %
Deviated Casing ID	6.538 in	Temp. Wellhead	80 °F	H_2S	0.00 %
Heel(MD)	19685 ft	Temp. Sandface	292 °F		
Heel(TVD)	9843 ft			Cond API G	51.2 API°
				Sep Temp	100.0 °F
Horizontal Casing ID	6.538 in			Sep Pres	100 psi
Toe(MD)	19686 ft			Water Gravity	1.000
Datum(MD)	19685 ft				

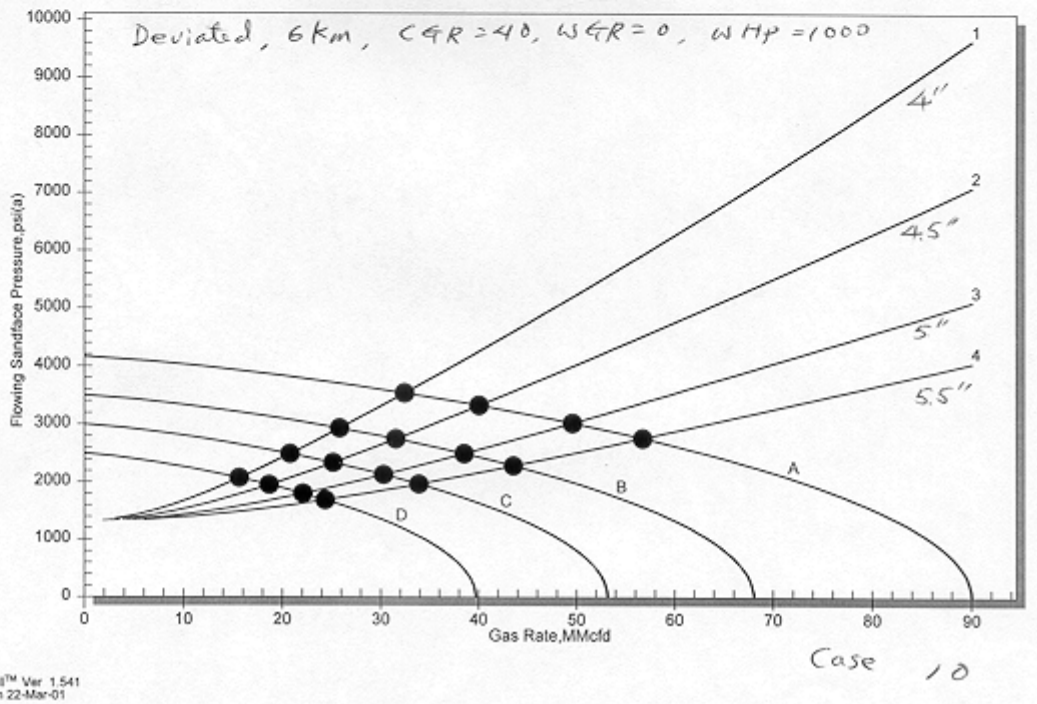

Fast Virtuwell™ Ver 1.541
DevGkm 22-Mar-01

Figure 4.10: Yolla Deviated Well Tubing Performance Curves – Case 10

F.A.S.T. VirtuWell
Horizontal Gas AOF/TPC

Correlation: Beggs & Brill

Absolute Open Flow:

	Reservoir Pressure	n	C	AOF
	psi(a)		MMcfd/(psi^2)^n	MMcfd
A	4169.0	0.800	1.45270e-04	89.997
B	3500.0	0.800	1.45270e-04	68.028
C	3000.0	0.800	1.45270e-04	53.158
D	2500.0	0.800	1.45270e-04	39.708

Tubing Performance Curve:

	Tubing ID	Tubing OD	Tubing Depth	Wellhead Pressure	OGR/CGR	WGR	Rec. Gas Gravity	Rec. Rate Factor	Flow Path
	in	in	ft	psi(a)	bbl/MMcf	bbl/MMcf			
1	3.548	4.000	19685	1000.0	40.000	5.000	0.975	1.036	Tubing
2	3.957	4.500	19685	1000.0	40.000	5.000	0.975	1.036	Tubing
3	4.494	5.000	19685	1000.0	40.000	5.000	0.975	1.036	Tubing
4	4.950	5.500	19685	1000.0	40.000	5.000	0.975	1.036	Tubing

Turner Rate:

Gas Rate	Flowin Pres
MMcfd	psi(a)
3.455	1
4.284	1
5.544	1
6.732	1

Operating Points:

	Gas Rate MMcfd					Flowing(SF) Pressure psi(a)			
	A	B	C	D		A	B	C	D
1	29.422	23.432	19.017	14.285	1	3616.7	3002.8	2551.1	2123.1
2	36.631	28.908	23.236	17.226	2	3424.8	2836.4	2408.4	2012.1
3	45.928	36.003	28.352	20.615	3	3143.5	2592.3	2213.0	1869.4
4	53.157	41.149	32.055	20.862	4	2894.6	2390.5	2053.5	1858.5

Vertical Casing ID	6.538 in	**Roughness**	0.00060 in	**Gas Gravity**	0.858
KOP(MD)	263 ft	**Corr. Adj.**	100.000 %	N_2	0.20 %
				CO_2	18.86 %
Deviated Casing ID	6.538 in	**Temp. Wellhead**	80 °F	H_2S	0.00 %
Heel(MD)	19685 ft	**Temp. Sandface**	292 °F	**Cond API G**	51.2 API°
Heel(TVD)	9843 ft			**Sep Temp**	100.0 °F
				Sep Pres	100 psi
Horizontal Casing ID	6.538 in			**Water Gravity**	1.000
Toe(MD)	19686 ft				
Datum(MD)	19685 ft				

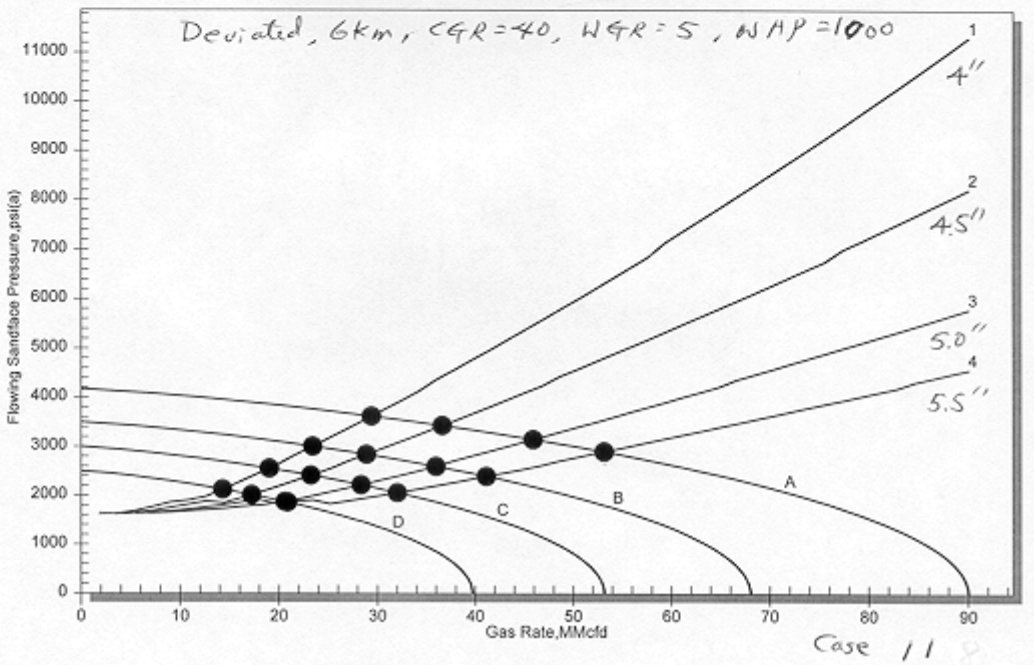

Fast Virtuwell™ Ver. 1.541
Dev6km 22-Mar-01

Figure 4.11: Yolla Deviated Well Tubing Performance Curves – Case 11

F.A.S.T. VirtuWell
Horizontal Gas AOF/TPC

Correlation: Beggs & Brill

Absolute Open Flow:

	Reservoir Pressure	n	C	AOF
	psi(a)		MMcfd/(psi^{2n})	MMcfd
A	4169.0	0.800	1.45270e-04	89.997
B	3500.0	0.800	1.45270e-04	68.028
C	3000.0	0.800	1.45270e-04	53.158
D	2500.0	0.800	1.45270e-04	39.708

Tubing Performance Curve:

	Tubing ID	Tubing OD	Tubing Depth	Wellhead Pressure	OGR/CGR	WGR	Rec. Gas Gravity	Rec. Rate Factor	Flow Path
	in	in	ft	psi(a)	bbl/MMcf	bbl/MMcf			
1	3.548	4.000	19685	1000.0	40.000	10.000	0.975	1.036	Tubing
2	3.957	4.500	19685	1000.0	40.000	10.000	0.975	1.036	Tubing
3	4.494	5.000	19685	1000.0	40.000	10.000	0.975	1.036	Tubing
4	4.950	5.500	19685	1000.0	40.000	10.000	0.975	1.036	Tubing

Turner Rate:

Gas Rate	Flowing Pres
MMcfd	psi(a)
3.672	18
4.572	18
5.904	18
7.200	18

Operating Points:

	Gas Rate MMcfd					Flowing(SF) Pressure psi(a)			
	A	B	C	D		A	B	C	D
1	26.499	21.187	17.222	12.928	1	3688.8	3065.6	2607.3	2170.6
2	33.263	26.597	21.245	13.058	2	3517.1	2908.7	2477.6	2166.2
3	42.232	33.301	26.281	15.537	3	3260.2	2689.3	2295.2	2077.2
4	49.613	38.500	30.063	17.050	4	3020.4	2497.1	2141.3	2019.0

Vertical Casing ID	6.538 in	**Roughness**	0.00060 in	**Gas Gravity**	0.858
KOP(MD)	263 ft	**Corr. Adj.**	100.000 %	N_2	0.20 %
				CO_2	18.86 %
Deviated Casing ID	6.538 in	**Temp. Wellhead**	80 °F	H_2S	0.00 %
Heel(MD)	19685 ft	**Temp. Sandface**	292 °F	**Cond API G**	51.2 API°
Heel(TVD)	9843 ft			**Sep Temp**	100.0 °F
				Sep Pres	100 psi
Horizontal Casing ID	6.538 in			**Water Gravity**	1.000
Toe(MD)	19686 ft				
Datum(MD)	19685 ft				

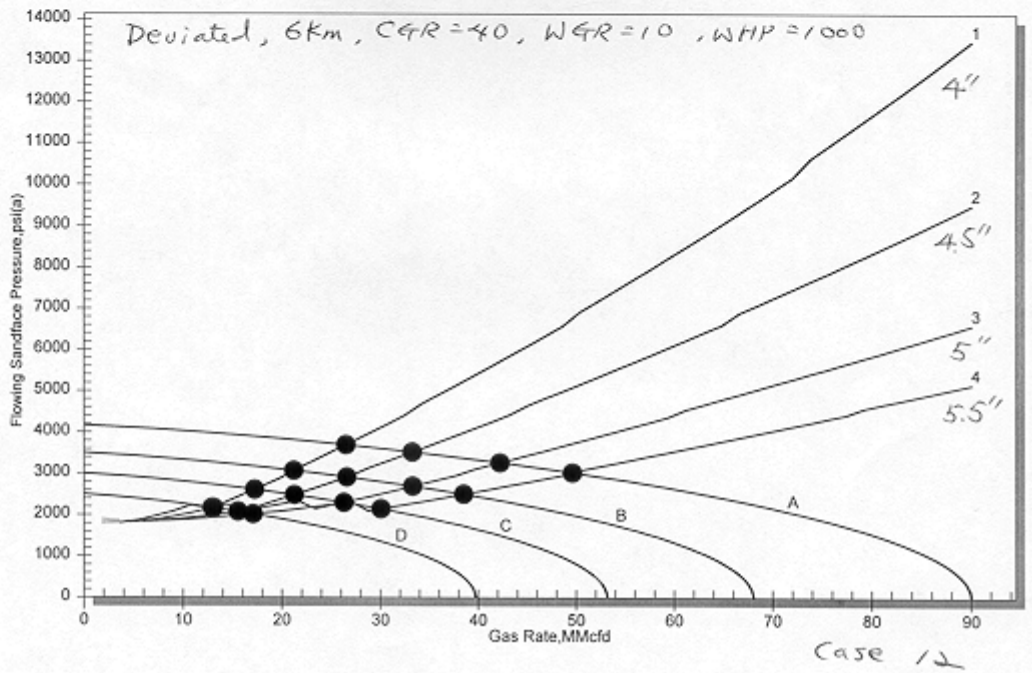

Fast VirtuWell™ Ver 1.541
DevGkm 22-Mar-01

Figure 4.12: Yolla Deviated Well Tubing Performance Curves – Case 12

$$Qe = 186 * A * \left(\frac{P}{Z * T * G} \right)^{0.50}$$

Where

Qe is the maximum gas rate (MMscfd)
A is the cross-sectional area of flow (ft^2)
P is the effective average pressure (psia)
Z is the effective average gas compressibility
T is the effective average temperature (^oR)
G is the gas gravity

Turner proposed the following equations for calculating the minimum gas rate to lift water as

$$Vg\ (water) = 5.62 * \frac{(67 - K * P)^{0.25}}{(K * P)^{0.50}}$$

$$K = 2.693 * \frac{G}{Z * T}$$

$$Qg = \frac{3.06 * P * Vg * A}{Z * T}$$

Where

Vg (water) is the minimum gas velocity required to lift water (ft/s)
Qg is the minimum gas rate to lift liquid (MMscfd)

Case	Wellbore		CGR	WGR	WHP	Res Pres	Gas Rate (MMscfd)			
	Config	Length (m)	(bbl/MMcf)	(bbl/MMcf)	(psia)	(psia)	4" Tbg	4.5" Tbg	5" Tbg	5.5" Tbg
1	Vertical	3000	40	0	700	4169	45.30	53.81	62.24	69.44
						3500	35.94	42.21	48.93	53.19
						3000	29.05	33.77	38.66	41.66
						2500	22.25	25.54	28.80	30.71
2	Vertical	3000	40	5	700	4169	38.15	46.37	56.19	63.20
						3500	30.45	36.64	43.82	48.89
						3000	24.74	29.49	34.96	38.51
						2500	19.15	22.53	26.26	28.57
3	Vertical	3000	40	10	700	4169	34.48	42.36	52.11	59.35
						3500	27.55	33.54	40.75	45.93
						3000	22.39	27.03	32.45	36.22
						2500	17.23	20.56	24.32	26.82
4	Vertical	3000	40	0	1000	4169	43.73	51.83	60.75	66.55
						3500	34.05	39.85	45.99	49.83
						3000	26.80	31.00	35.27	37.84
						2500	19.48	22.18	24.78	26.27
5	Vertical	3000	40	5	1000	4169	36.76	44.58	53.85	60.40
						3500	28.73	34.45	41.00	45.45
						3000	22.65	26.87	31.57	34.65
						2500	16.50	19.27	21.13	20.19
6	Vertical	3000	40	10	1000	4169	33.16	40.66	49.86	56.63
						3500	25.91	31.44	38.01	42.65
						3000	20.39	24.48	29.17	27.46
						2500	11.69	13.23	14.90	15.71
7	Deviated	6000	40	0	700	4169	33.41	41.29	51.22	58.73
						3500	26.98	33.05	40.48	45.92
						3000	22.18	26.94	32.60	36.62
						2500	17.37	20.87	24.88	27.61
8	Deviated	6000	40	5	700	4169	30.32	37.79	47.48	55.17
						3500	24.53	30.36	37.90	43.44
						3000	20.35	24.95	30.60	34.74
						2500	15.96	19.37	23.42	26.38
9	Deviated	6000	40	10	700	4169	27.33	34.35	43.69	51.67
						3500	22.31	27.95	35.10	40.71
						3000	18.48	22.87	28.48	32.91
						2500	14.66	17.98	22.01	24.95
10	Deviated	6000	40	0	1000	4169	32.45	40.06	49.59	56.75
						3500	25.16	31.55	38.52	43.57
						3000	20.78	25.16	30.30	33.90
						2500	15.63	18.67	22.09	24.36
11	Deviated	6000	40	5	1000	4169	29.42	36.63	45.93	53.16
						3500	23.43	28.91	36.00	41.15
						3000	19.02	23.24	28.35	32.06
						2500	14.29	17.23	20.62	20.86
12	Deviated	6000	40	10	1000	4169	26.50	33.26	42.23	49.61
						3500	21.19	26.60	33.30	38.50
						3000	17.22	21.25	26.28	30.06
						2500	12.93	13.06	15.54	17.05

Table 4.4: Yolla Gas Well Tubing Size Performance Evaluation

The Turner correlation incorporates separate equations for water and condensate. The liquid lift rate will be calculated for water if the flow through the wellbore includes gas, condensate and water.

The calculated maximum and minimum gas rates for 5" and 5.5" tubing are shown in Figures 4.13 and 4.14, and summarised in Table 4.5.

Average Wellbore Pressure	Maximum Gas Rate (MMscfd)		Minimum Gas Rate (MMscfd)	
(psia)	5" Tubing	5-1/2" Tubing	5" Tubing	5-1/2" Tubing
1000	27.7	33.7	4.4	5.3
1250	31.4	38.1	5.0	6.0
1500	34.8	42.3	5.5	6.6
1750	38.0	46.1	5.9	7.2
2000	40.9	49.6	6.3	7.7
2250	43.6	52.9	6.7	8.2
2500	46.0	55.8	7.1	8.6
2750	48.3	58.5	7.4	8.9
3000	50.3	61.0	7.6	9.3
3250	52.0	63.1	7.9	9.5
3500	53.6	65.0	8.1	9.8
3750	54.9	66.6	8.2	10.0
4000	56.0	68.0	8.4	10.1

Table 4.5: Maximum and minimum gas rates for tubing sizes.

Based on the calculations, 5.5" tubing is found to be able to flow at a higher maximum rate than 5.0" tubing. However 5.5" tubing requires a higher minimum rate to lift the wellbore liquids. This finding is consistent with the results from Nodal analysis.

While the average production rate is 72 MMscfd (55 Tj/d), the contract envisages rates up to 84 MMscfd (64 Tj/d) to account for downtime. In order to maintain this kind of peak field deliverability, particularly in early years when there are likely to be just 2 producers, the better choice is use 5.5" tubing to avoid the risk of erosion if one well is used to provide the majority of the gas demand.

The minimum rate in 5.5" tubing to ensure continuous liquids lifting is less than 10 MMscfd at initial conditions and falls to 8 MMscfd as reservoir and well flowing pressures decline later in the field life. This is adequate to cater for tail production from the four wells expected to be on production at that time.

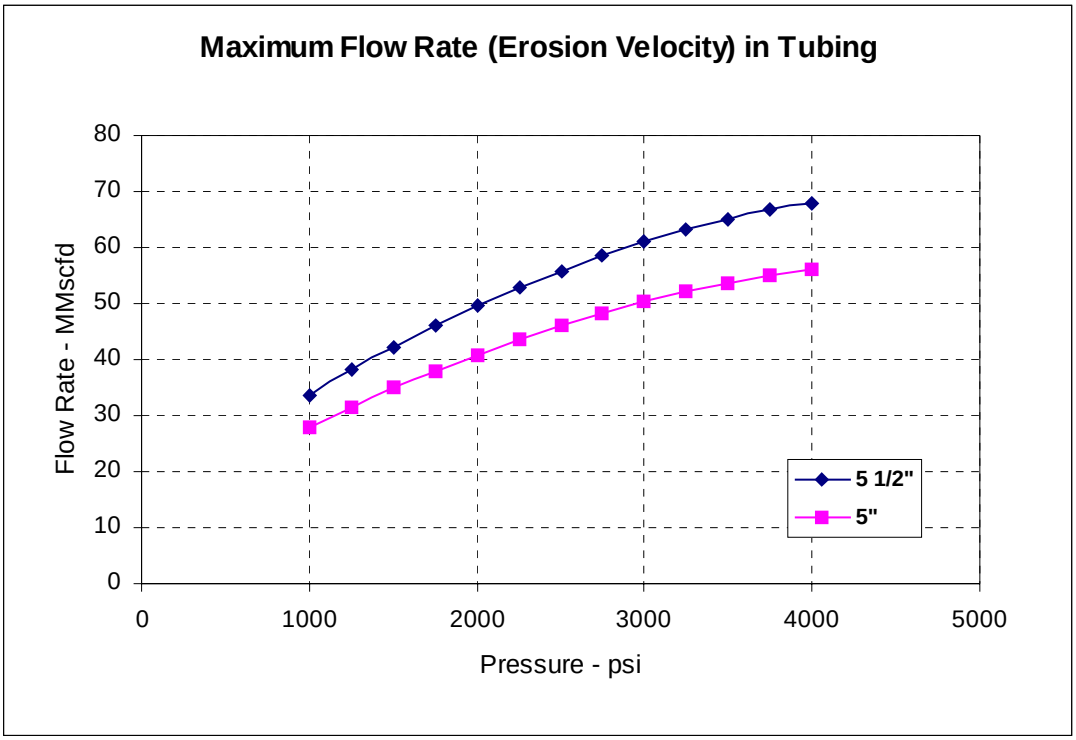

Figure 4.13: Yolla Maximum Gas rate Calculation

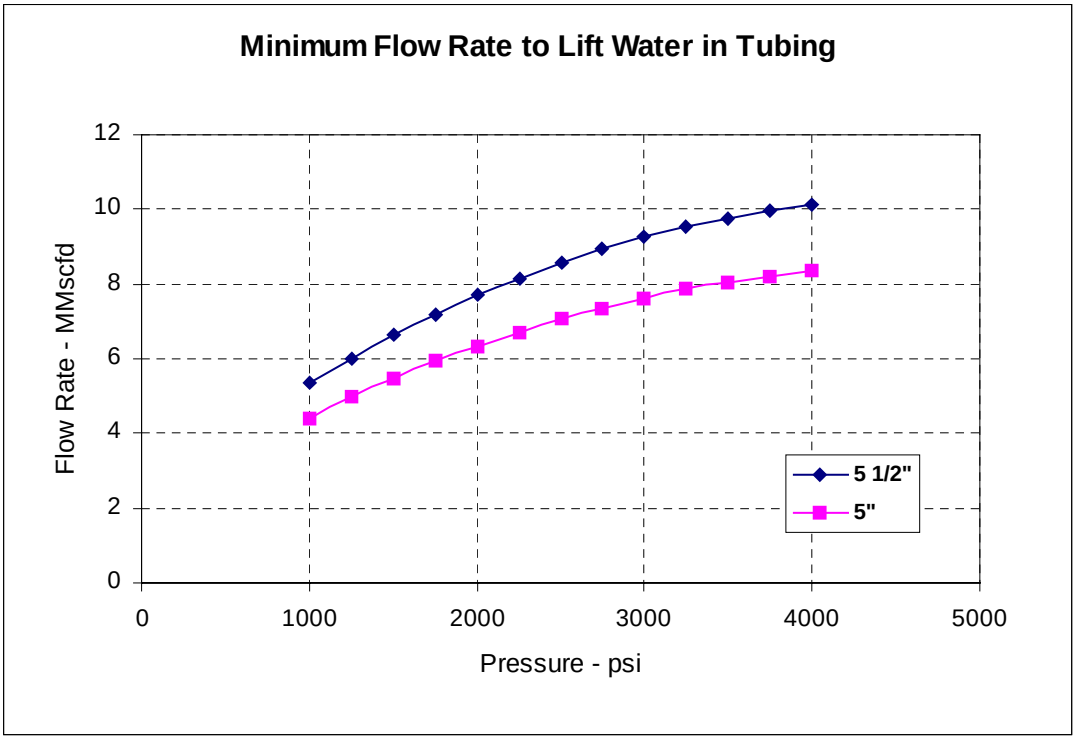

Figure 4.14: Yolla Minimum Gas rate Calculation

Combining the results of nodal analysis and the maximum and minimum rate calculations, the optimal tubing size appears to be 5.5" for the Yolla gas production.

Consequently, the Yolla production forecast was performed assuming 5.5" tubing.

4.2 Yolla Simulation Model Description

4.2.1 Model Construction

A 3D geological modelling package, Petrel from Technoguide, Norway was utilised to build a 3D geological model of the Yolla field. This geological model was constructed incorporating the petrophysical data from Yolla 1 and 2 well logs, and the 3D seismic interpretation of May 2001. The fine grid cell dimension of the geological model was 80 metres by 80 metres by 1 metre.

The base case P50 fine grid geological model constructed using the Petrel package was upscaled to produce a 20-layer coarse grid model with an areal grid cell dimension of approximately 200 metres by 200 metres. Permeability and porosity was upscaled using the arithmetic averaging technique.

This upscaled coarse grid geological model was then transferred to the Eclipse 100 reservoir simulator. The petrophysical and geological parameters transferred directly to each grid block of the simulation model are:

- Areal grid and vertical layering system
- Structure depth
- Net thickness
- Porosity
- Porosity category
- Horizontal permeability
- Fault and dyke locations

The other parameters used in the model are discussed below.

4.2.2 Areal Grid and Vertical Layering System

The grid system of the Yolla simulation model was imported directly from a 3D coarse grid geological model constructed using Petrel. The areal grid dimension is 78-column by 92-row with a grid cell size of approximately 200 metres by 200 metres.

The number of layers was then reduced from 20 to 16 layers by deactivating the shale layers between the sands. The final vertical layering system is summarised as follows:

- Layer 1: 2718 Sand
- Layer 2: Dummy / Inactive
- Layer 3 to 5: 2755 Sand

- Layer 6: Dummy / Inactive
- Layer 7 to 10: 2809 Sand
- Layer 11 to 15: Dummy / Inactive
- Layer 16: 2952 Sand
- Layer 17: Dummy / Inactive
- Layer 18 to 20: 2973 Sand

The total number of active grid cells is approximately 40,000. The areal grid system of Layer 5 (bottom of 2755 sand) of the model is presented in Figure 4.15.

4.2.3 Initial Gas and Water Saturation

At the beginning, the initial gas and water saturations were directly imported from the geological model. However, the operation of such a model was extremely unstable and slow. Further investigation discovered that the run instability was due to the un-equalised gas and water potentials in the model. Therefore, it was decided to initialise the gas and water saturations inside the Eclipse model using the equilibration option.

The modified scheme to initialise the water and gas saturations in the model involved creating a porosity category table with seven porosity groups. The mean porosity and initial gas and water saturation for each porosity category were calculated in Petrel. Then seven sets of the relative permeability curves were generated using the end points from each porosity group, by Corey's correlation. The porosity category table was subsequently imported into the model as the saturation region table. The initial gas and water saturations were calculated for each saturation region using its corresponding set of the relative permeability curves.

The porosity categories and their corresponding mean porosity and initial gas saturation are presented in Table 4.6.

Category	Porosity			Mean Porosity	Mean Sgi
1		<	8%	6%	0.20
2	8%	to	10%	9%	0.47
3	10%	to	12%	11%	0.56
4	12%	to	14%	13%	0.63
5	14%	to	16%	15%	0.68
6	16%	to	18%	17%	0.72
7		>	20%	20%	0.76

Table 4.6: Porosity categories with corresponding mean porosity and mean gas saturation.

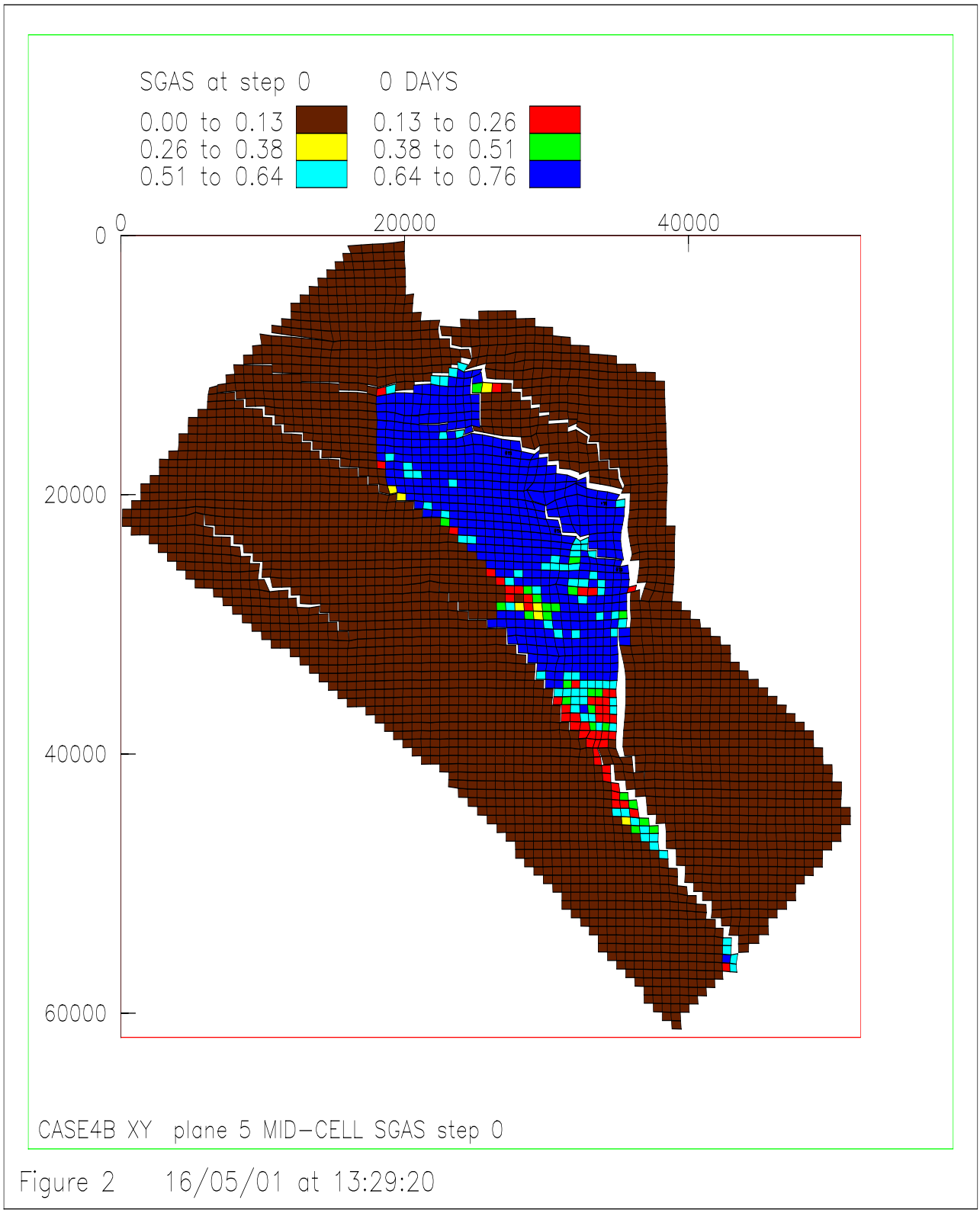

Figure 4.15: Yolla Model Areal Grid System Layout and Initial Gas Saturation – Layer 5 (2755 Sand)

4.2.4 Relative Permeability

Relative permeability measurements have not been obtained from the Yolla field as there has been no core cut in gas saturated rock. The Corey correlation was applied to calculate the imbibition gas and water relative permeabilities using the end points of each porosity category. The formulae used are given below,

- $$Krw = Krw(Sgrw) * \left(\frac{Sw - Swcr}{Swmax - Swcr - Sgrw} \right)^{Cw}$$

- $$Krg = Krg(Swmin) * \left(\frac{Swmax - Sw - Sgrw}{Swmax - Swcr - Sgrw} \right)^{Cg}$$

Where

Cg	is the Corey gas exponent
Cw	is the Corey water exponent
Swmin	is the minimum water saturation
Swcr	is the critical / connate water saturation
Sgrw	is the residual gas saturation to water
Krw(Sgrw)	is the water relative permeability at residual gas saturation
Krg(Swmin)	is the gas relative permeability at minimum water saturation

The saturation end points and Corey exponent for each porosity category used in the model are shown in Table 4.7.

	Cat 1	Cat 2	Cat 3	Cat 4	Cat 5	Cat 6	Cat 7
Cg	2.5	2.5	2.5	2.5	2.5	2.5	2.5
Cw	3.5	3.5	3.5	3.5	3.5	3.5	3.5
Swmin	0.0	0.0	0.0	0.0	0.0	0.0	0.0
Swcr	0.8	0.53	0.44	0.37	0.32	0.28	0.24
Sgrw	0.25	0.25	0.25	0.25	0.25	0.25	0.25
Krw(Sgrw)	0.0	0.3	0.3	0.3	0.3	0.3	0.3
Krg(Swmin)	0.0	1.0	1.0	1.0	1.0	1.0	1.0

Table 4.7: Saturation end points and corey exponents for each porosity category.

Water and gas relative permeability curves were generated using the above parameters and applied to the model in order to account for the relative permeability effect. It is assumed that there is no water or gas flow in the porosity category 1, due

to the tight formation. The relative permeabilities of porosity category 7 are presented in Figure 4.16 and tabulated in Table 4.8 to demonstrate the calculations.

Sw	Krg	Krw
1.00	0.0000	1.0000
0.85	0.0000	0.5800
0.80	0.0000	0.4400
0.75	0.0000	0.3000
0.70	0.0030	0.2091
0.65	0.0170	0.1398
0.60	0.0469	0.0887
0.55	0.0963	0.0525
0.50	0.1682	0.0284
0.45	0.2654	0.0134
0.40	0.3902	0.0052
0.35	0.5448	0.0014
0.30	0.7313	0.0002
0.24	1.0000	0.0000

Table 4.8: Relative permeabilities for porosity category 7.

Capillary pressures for each porosity category were assumed to be zero in the model. This is a reasonable assumption, as the sand is thin with the edge water drive in the field and the effect of the initial gas-water transition zone on gas recovery is expected to be insignificant.

4.2.5 Rock Properties

The porosity, net-to-gross and permeability were imported from the coarse grid geological model. The rock compressibility, the vertical to horizontal permeability ratio and the fault and dyke transmissibility data are not available. They are assumed to be 3.0×10^{-6} psi^{-1}, 0.1, 0.0 and 0.2 in the model, respectively.

The faults are believed to be fully sealed to trap the gas in the formation. It is expected that only dyke transmissibility may affect gas recovery and this variable was further investigated in the sensitivity study.

4.2.6 Gas & Condensate PVT Properties

The gas and condensate properties used in the simulation are based on the reservoir fluid PVT study of Yolla 1, DST 1. The Intra EVCM fluid properties are summarised in Table 4.9.

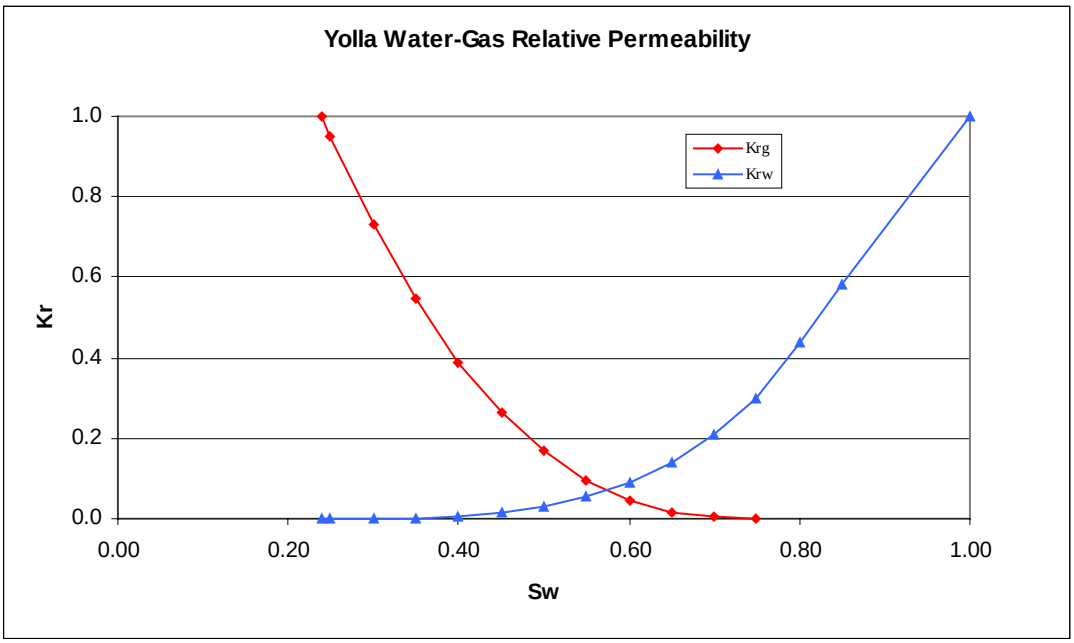

Figure 4.16: Yolla Gas-Water Relative Permeability – Category 7

Pressure (psia)	Gas PVT Properties			Condensate PVT Properties		
	Rv (stb/Mcf)	Bg (rb/Mscf)	Vg (cp)	Rs (Mcf/stb)	Bo (rb/stb)	Vo (cp)
515	0.0426	7.146	0.0142	0.153	1.020	0.191
1015	0.0387	3.525	0.0153	0.360	1.032	0.171
1515	0.0352	2.307	0.0167	0.581	0.040	0.156
2115	0.0360	1.622	0.0188	0.862	1.051	0.142
2715	0.0381	1.250	0.0214	1.162	1.063	0.132
3215	0.0430	1.058	0.0240	1.427	1.073	0.125
3698 (D.P.)	0.0467	0.929	0.0269	1.695	1.084	0.118
3815	0.0467	0.905	0.0276	1.695	1.083	0.120
4015	0.0467	0.868	0.0289	1.695	1.081	0.123
4215	0.0467	0.836	0.0302	1.695	1.080	0.125
4515	0.0467	0.794	0.0324	1.695	1.078	0.129
5015	0.0467	0.738	0.0362	1.695	1.075	0.136

Table 4.9: Fluid properties for Intra EVCM.

The wet gas and condensate properties were used in a single well radial model to estimate the extent of the permeability impairment around the wellbore due to the condensate dropout. The dry gas properties (Bg and Vg) were applied to the full field model for the production forecast.

4.2.7 Initial Gas-Water Contact and Reservoir Pressure and Temperature

The initial gas-water contact and the reservoir pressure were taken from MHA's Yolla 1 RFT and Yolla 2 MDT data interpretation. The detailed interpretation results can be found in the report of "Yolla Gas Field Reserves Review" of August 2000. The initial fluid contact and reservoir pressure were calculated as:

- 2727 m ss for 2718 Sand with a datum pressure of 4130.9 psia
- 2834 m ss for 2755 & 2809 Sands with a datum pressure of 4179.5 psia
- 2997 m ss for 2952 & 2973 Sands with a datum pressure of 4401.3 psia

The reservoir temperature was taken as 292 ^{o}F, from Yolla 1 DST 1 Reservoir fluid study report.

The aquifer pressure was calculated assuming it is in equilibrium with the reservoir.

4.2.8 Aquifer Modelling

Water is handled in the model by using aquifer grid blocks. The initial water in-place is 6480 MMbbl. This equates to a water/gas volume ratio of 15,000 rb/rb, to represent an extensive regional aquifer. No other numerical or analytical aquifer was incorporated in the model.

4.2.9 Vertical Flow Performance Curves

Vertical flow performance (VFP) curves were generated for the model using VFPi in the Eclipse Suite software package. The curves assume 5.5" tubing with the following flow conditions:

- Gas Rate: 0.1 to 40 MMscfd
- THP: 600 to 3600 psi
- WGR: 0 to 100 Bbl/MMscf
- OGR: 0 to 50 Bbl/MMscf

Four sets of curves are generated with the following wellbore configuration (Table 4.10).

VFP Set No	1 (Yolla 6)	2 (Yolla 4)	3 (Yolla 3)	4 (Yolla 5)
Length (m/ft)	3095/10154	3211/10535	3460/11352	3680/12074
Step out (m/ft)	751/2464	1130/3707	1702/5585	2106/6908

Table 4.10: Well bore configuration.

4.2.10 Original Gas In-Place

After the entry of the required data into the P50 Yolla simulation model, the original gas in-place (OGIP) was calculated as 527.8 bcf. This OGIP is slightly higher than the probabilistic mean OGIP of 503.4 bcf. The discrepancy is due to that no porosity cut off has been applied in the data imported in the model. A pore volume multiplier was used to adjust the OGIP in each individual sands of the model to match that from the probabilistic mean OGIP in order that predicted recoveries could be compared with those estimated by MHA. The OGIP in each sand prior to and after the adjustment is shown in Table 4.11.

Sand	Initial E100 OGIP (bcf)	Adjusted E100 OGIP (bcf)	Probabilistic Mean OGIP (bcf)
2718	26.8	41.3	41.3
2755	254.9	236.8	236.8
2809	110.9	97.6	97.6
2952	13.1	9.4	9.4
2973	122.0	118.3	118.3
Sum	527.8	503.4	503.4

Table 4.11: Initial and adjusted OGIP modeled in Eclipse and probabilistic estimate of OGIP for each reservoir unit.

The average multiplier used was 0.954.

The total mean OGIP is only 19 bcf (3%) higher than that calculated by MHA. The distribution of OGIP between sands differs somewhat from MHA, but predicted overall recovery is very similar.

4.3 Model Calibration

4.3.1 Yolla 1 DST 1 Results Matching

In order to verify the model input and to calibrate the wellbore parameters, a radial single well model covering the 2809 Sand with the wet gas and condensate properties was constructed using the Yolla 1 well block properties. The dimensions of the radial model were 40 x 1 x 5. The inner ring radius was 0.40 ft (representing 9.625" open hole wellbore) and outer ring radius 2591.4 ft. The radius expansion ratio is 1.25.

A history matching was conducted to match the Yolla 1 DST 1 results. The control parameter was the DST rates and the matching parameter was bottomhole pressure. Matching was achieved by adjusting skin parameters. The matching result obtained was reasonable as shown in Figure 4.17.

The wellbore parameters derived from the history matching are:

- Darcy skin: 3.0
- Non-Darcy skin: 0.0015 day/Mscf

It is impossible to make a unique comparison of formation properties (such as permeability and skin) between the DST and the model. This is because the DST pressure data were gently decreasing during the main shut-in period making the test results impossible to analyse. History matching is the only way to confirm the model's permeability and completion effectiveness to actual production. However the total skin of around 18 at the DST rate of 10 MMscfd compares well with Amoco's interpretation of 13.5.

4.3.2 Near Wellbore Condensate Dropout

The impact of the near wellbore condensate dropout on well productivity has been studied using the radial single well model. A three-stage approach was taken:

- The radial simulation model was tuned to match Yolla 1 DST 1 data, to provide tuning parameters for Darcy and non-Darcy skin.
- These tuning parameters were then used to provide a long-term production profile allowing for condensate dropout.
- The wellbore parameters of the full field model using the dry gas properties were adjusted to approximate the production profile from the radial model.

The result of the production profile comparison between the radial and full field model is shown in Figure 4.18. It suggests that the effect of the productivity

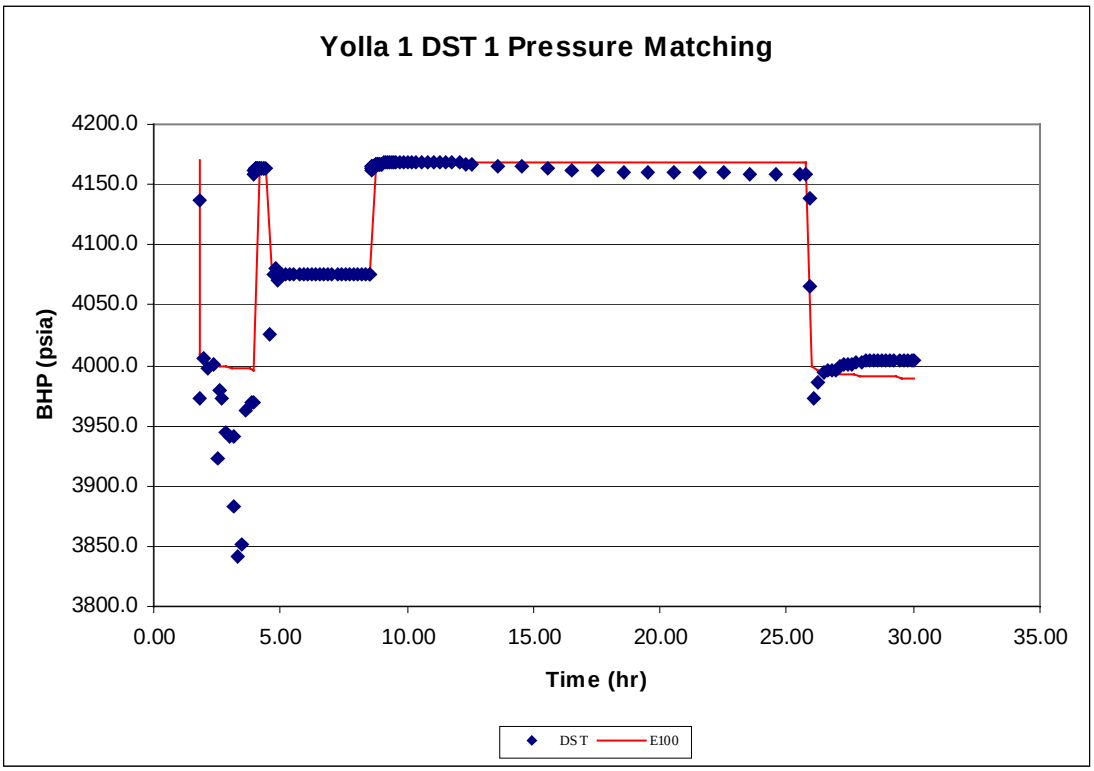

Figure 4.17: Yolla 1 DST 1 Pressure Matching

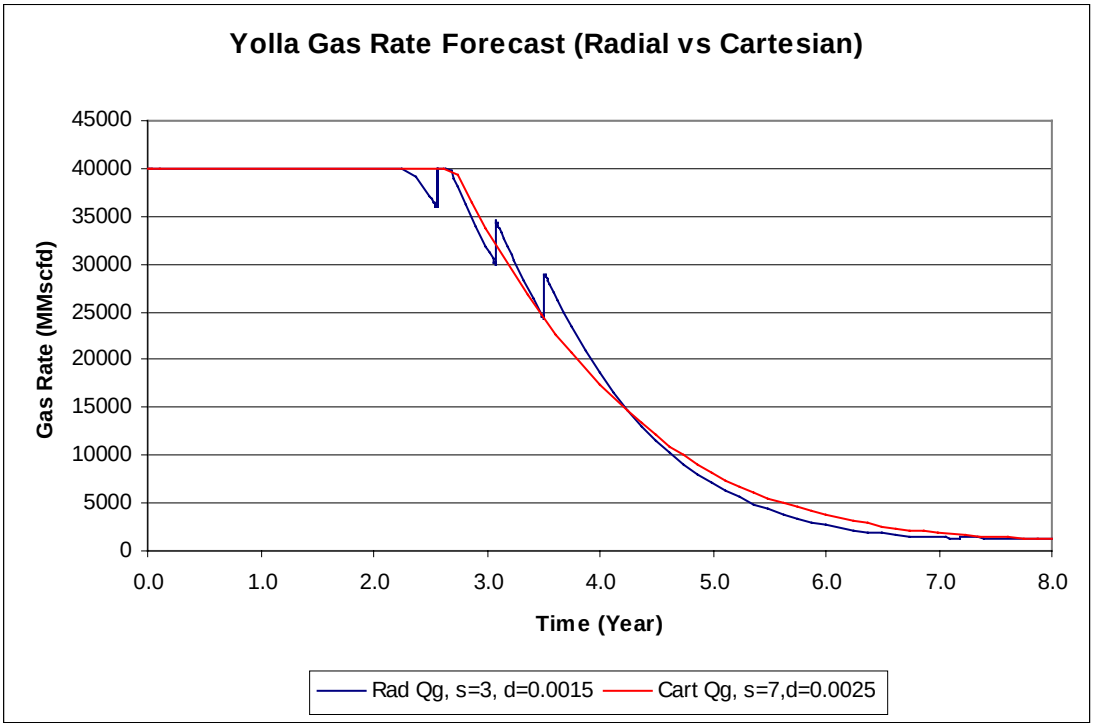

Figure 4.18: Yolla 1 DST 1 Near Wellbore Condensate Dropout Calibration

impairment due to near wellbore condensate dropout for a typical Yolla well is equivalent to a Darcy skin of 7 and a non-Darcy skin of 0.0025, over the life of the well. These values were therefore used as the default wellbore parameters for each of the producers in the full field model, to account for the effect of the near wellbore condensate dropout.

4.4 Well Optimisation and Production Forecast

The production forecast was performed following the completion of the model calibration to the Yolla 1 DST 1 results and the near wellbore condensate dropout effect. The production forecast was carried out in two stages. Stage one considers the well location optimisation, while the well schedule and compression timing is studied in the second stage.

4.4.1 Well Location Optimisation

Case 1 (base case) assumes a four well program of Yolla 3, 4, 5, and 6. These well locations were chosen to effectively deplete the main, central and SE compartments of the field. Yolla 3 is about 500m NW of Yolla 1 aiming to drain the northern flank of the main compartment while Yolla 4 is 1000m up dip of Yolla 2 to cover the southern flank of the main compartment. Yolla 5 and 6 are located in the SE and central compartments, respectively. Yolla 4, 5, and 6 are all close to the bounding faults and cannot be shifted due to the geological risk involved. Therefore Yolla 3 is the only well that can be moved and optimized.

Alternative well locations for Yolla 3 are Yolla 1, 3A and 3B. The well layout is shown in Figure 4.19.

The optimisation was performed assuming all 4 wells commencing production together and running for 12 years with automatic workover. The production constraints were 1200 psi THP and a maximum gas rate of 76 MMscfd.

Case 1 is the base case that involves Yolla 3, 4, 5 and 6. In Cases 2, 3 and 4, Yolla 3 is replaced by Yolla 3B, Yolla 1 and Yolla 3A, respectively. The purpose of varying the Yolla 3 location is to test the benefit to total gas recovery of possibly delaying water break through into Yolla 3 by shifting well away east toward the central block. Case 5 is a 5 well program with Yolla 3, 4 and 5 as the Stage I wells and Yolla 3A and 6 for Stage II. The results of Cases 1 to 5 are summarised in Table 4.12.

The results show that the gas recovery is insensitive to the location of Yolla 3. This is because any production increase in Yolla 3 has been offset by the production decrease in Yolla 4 and 5, due to the production interference.

On balance, the more westerly Yolla 3 location is preferred providing a drainage point closer to the western extremities of the field. This location was examined further in the later cases. The results also indicate a fifth well cannot be justified.

Yolla Gas Field T/RL1

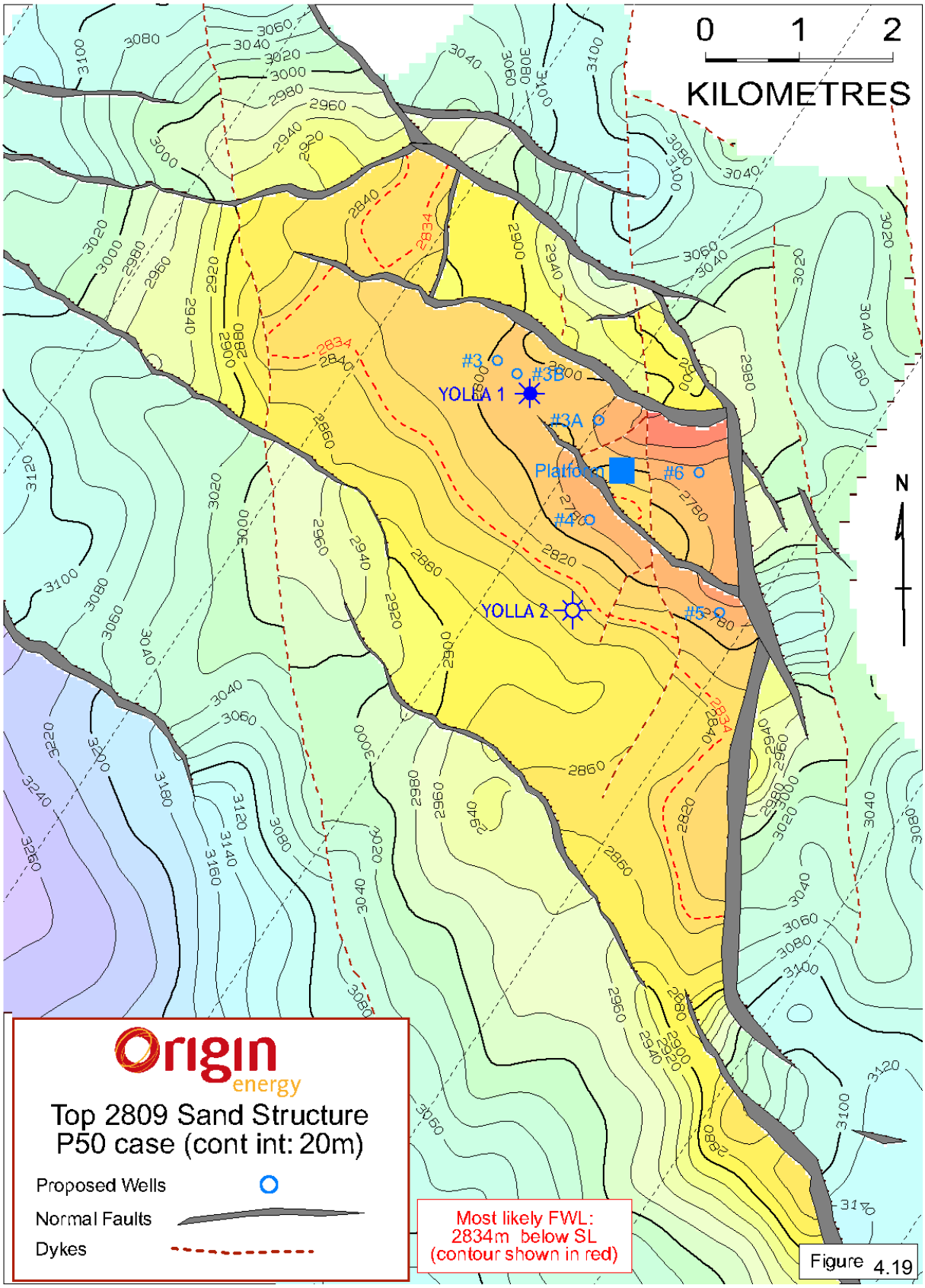

Figure 4.19

Description	Case	Well Cumulative Production (bcf)							Sum
		Y1	Y3A	Y3B	Y3	Y4	Y5	Y6	(bcf)
Base Case	1				86.4	79.4	79.9	33.3	279.1
Shifting Y3 to Y3B	2			84.4		77.1	87.9	33.4	282.7
Shifting Y3 to Y1	3	85.4				76.4	87.3	33.4	282.5
Shifting Y3 to Y3A	4		90.5			73.5	80.9	33.3	278.2
Five well program. Stage I with Y3, Y4 & Y5. Stage II with Y3A & Y6	5		13.0		79.6	75.8	84.2	33.3	285.9

Table 4.12: Summary of cumulative production results from Cases 1 to 5.

4.4.2 Well Schedule and Compression

In this phase of the production forecast, eight cases with various well schedules and compression timing are performed to determine the optimal field development sequence. The basic development guideline adopted in the forecast is:

- 2 production wells initially at a minimum THP of 1200 psi
- 2 additional wells added 5 to 8 years after production start to maintain deliverability and summarise recovery
- Production maintained at 76 MMscfd of raw gas
- Compression added when required to maintain deliverability (THP can be reduced to 725 psi)
- Wells produce from all Intra EVCM sands, commingled
- Sands that produce formation water would be isolated (maximum well WGR is 10 bbl/MMscf, equivalent to around 200 bpd of formation water)

Note commingling was assumed for simplicity in model runs. Production from individual sands via selective completion is the final design case.

The well schedule, compression timing and well production summary for each case is given in Table 4.13.

Case 1 (base case) is a four well program with Yolla 3, 4, 5 and 6. Yolla 3 and 4 will be on line on 1/1/2004 as the Stage I wells, followed by Yolla 5 and 6 (Stage II wells) on 1/7/2009 and compression on 1/1/2013. The production plateau can be maintained up to 10.8 years with a cumulative production (to 31/12/2017) of 329.9 bcf. It is found that about two thirds of production is from the Stage I wells and Stage II wells produce the remainder but are necessary to maintain offtake rate.

Case	Stage I		Stage II		Compression	Well Cum Prod to 31/12/2017 (bcf)					Sum	RF	Plateau
	Well	Timing	Well	Timing	Timing	Y3A	Y3	Y4	Y5	Y6	(bcf)	(%)	(Yr)
1	Y3, Y4	1-Jan-04	Y5, Y6	1-Jul-09	1-Jan-13		118.6	120.6	48.6	42.2	329.9	65.5	10.8
2	Y3, Y5	1-Jan-04	Y4, Y6	1-Jun-09	1-Jan-13		119.0	43.0	125.8	42.2	330.0	65.6	10.7
3	Y4, Y5	1-Jan-04	Y3, Y6	1-Jan-09	1-Sep-12		51.8	115.3	120.4	42.2	329.8	65.5	10.5
4	Y3, Y4, Y5	1-Jan-04	Y6	1-Oct-10	1-Oct-12		93.3	92.9	101.4	42.2	329.8	65.5	10.7
5	Y3, Y4, Y5	1-Jan-04	Y6	1-Jul-10	1-Dec-12		77.8	100.6	109.3	42.2	329.9	65.5	10.6
6	Y3, Y3A	1-Jan-04	Y5, Y6	1-Jul-09	1-Apr-13	134.6	112.4		47.6	42.2	336.8	66.9	10.8
7	Y3, Y4	1-Jan-04	Y3A, Y5, Y6	1-Jul-09	1-Jul-13	41.3	105.6	110.3	38.2	42.2	337.6	67.1	11.3
8	Y3, Y4, Y5	1-Jan-04	Y3A, Y6	1-Oct-10	1-May-13	31.4	82.2	85.3	92.9	42.2	334.1	66.4	11.1

Table 4.13: Summary of well schedule, compression timing and cumulative production for Case 1 to 8.

Aiming to improve gas recovery from Yolla 5 region (SE compartment), Case 2 brings up Yolla 3 and 5 as the Stage I wells. As expected, Yolla 5 recovery has significantly improved, but there is no change in the cumulative field production. The production increase from Yolla 5 has been offset by the production reduction from Yolla 4 due to gas migrating east through the dyke. The case of sealing dykes is examined later.

Case 3 is similar to Case 2 except Yolla 4 and 5 are the Stage I wells. As with Case 2, no improvement in the field production as the production increase from Yolla 5 has been offset by the production reduction from Yolla 3.

The results from Cases 1 to 3 illustrate that the production from the Stage II wells is lower than the Stage I wells. It is obvious that the waterfront would be approaching Stage II wells when Stage I wells are hit by the aquifer water. Therefore, the production life from Stage II wells would be short with lower recoveries, but they are necessary to achieve full drainage and to maintain plateau rate.

Cases 4 and 5 use 3 Stage I wells (Yolla 3, 4, and 5) to try to improve recovery from Yolla 5 region. Case 4 has no rate restrictions on all the producers while Case 5 restricts Yolla 3 production at 15 MMscfd for 5 years. Though the production from Yolla 5 has increased, the production from Yolla 3 and 4 has decreased due to the production interference. Overall, there is no improvement in the field recovery.

Case 6 has similar features to the base case, except Yolla 4 is replaced by Yolla 3A. The purpose of doing so is to delay the water breakthrough to Yolla 4 in order to maximize the gas recovery. Yolla 3A is on the western edge of the central compartment and separated from Yolla 4 by a bounding fault. Field recovery from

Case 6 increases slightly to 336.8 bcf, from 329.9 bcf of the base case. However this scenario leaves the southern area of the main compartment without an offtake point which, in the event of reservoir heterogeneity, could jeopardise recovery in that area.

With the encouraging result from Case 6, a five well program was attempted by adding Yolla 3A into the base case (four well program). Case 7 has three Stage I wells and two Stage II wells while Case 8 has two Stage I wells and three Stage II wells. Similar to the well location optimisation study in the previous section, the field recovery only increases marginally under the five well program. The fifth well cannot be justified.

The results of the production forecast with the various well schedules and compression timing indicate:

- Not much difference in final saturation or recovery for the various well schedules.
- Fifth well cannot be justified.
- On balance, the preferred approach is to go with Case 1 (the base case) for reservoir management reasons:
  - Case 1 involves drilling two safe well locations up front in the main compartment
  - Monitor production performance to see whether other compartments are contributing and before committing to further drilling
  - Add wells later as required to maintain deliverability
  - The timing and capex of the second phase wells should be delayed as long as possible by commencing production in the main compartment of the field

A selective well completion design of the base case to allow sands initially produced separately and sequentially for monitoring individual reservoir performance was further investigated in the sensitivity runs.

4.5 Simulation Results and Sensitivities

Due to the limited well control, there is some risk of variability in the interpreted geological data. The reservoir simulator can be used to assess the sensitivity of field performance to data uncertainties. A number of sensitivity runs were undertaken to investigate the rock properties or reservoir features that may potentially affect gas recovery. Those sensitivities include:

- Single sand production scheme (P50 model) – well completion design base case
- Commingled sand production scheme (P50 model) – sensitivity base case
- Dyke transmissibility (P50 model)
- Poor Sand trend (P50 model)
- Reservoir permeability (P50 model)
- Aquifer strength (P50 model)
- Upside potential – P10 Model with the upside structure
- Down side potential – P90 Model with down side structure or poor sand trend

The development sequence and principle used is the same as that coming from the well schedule and compression timing study, except that production is maintained at 72 MMscfd, instead 76 MMscfd. 72 MMscfd is the raw gas rate required to achieve production of 20 Pj of sales gas per year. 76 MMscfd was a preliminary figure used early in the study before process calculations were completed. Also the cumulative production is determined at 31/12/2019, instead of 31/12/2017 to capture the tail associated with the lower rates.

The base case in the well schedule and compression timing study was further broken into two well completion design scenarios and they are the single and commingled sand completion/production schemes. For the reservoir management purpose, the single sand scheme was chosen as the completion design base case and the commingled sand was used as the sensitivity base case to simplify running the sensitivity cases.

4.5.1 Single Sand Production Scheme Sensitivity

The effect of single sand production scheme on gas recovery is evaluated with the base case model. The scheme involves using selective completions and producing the reservoir sands singly, one by one.

Such a sequence will allow performance of individual reservoir layers to be monitored during early years. This will enable estimates of ultimate recovery by layer to be made to confirm total reserves and to determine whether eastern areas of the field are connected. Later in field life, layers will need to be commingled to maintain the offtake rate plateau required. This is the base case to be used in well completion design.

The employed sand and well rotation sequence is outlined in Table 4.14.

Sand	1-Jan-04	1-Aug-06	1-Aug-07	1-Jan-11	1-Apr-11
2718 & 2755	Yolla 3		Yolla 4	Yolla 3	All 4 wells
2809	Yolla 4	Yolla 3		Yolla 3 & 4	All 4 wells
2952 & 2973		Yolla 4	Yolla 3	Yolla 4	All 4 wells

Table 4.14: Reservoir sand produced and well rotation sequence for single sand production scheme.

Other sequences are possible. The sequence adopted when production commences will be determined after the results of Yolla 3 and Yolla 4 are known.

The results of the single sand production scheme using the above well rotation scheme are summarised in Table 4.15.

	Single Sand
OGIP (bcf)	
Stage I (Y3, Y4) on Line timing	1-Jan-04
Stage II (Y5, Y6) on line timing	1-Apr-11
Compression on line timing	1-Aug-13
Field Cum Prod (bcf) – 31/12/19	337.4
- Yolla 3	124.6
- Yolla 4	131.8
- Yolla 5	35.7
- Yolla 6	45.3
Production Plateau (Year)	11.7
Recovery Factor (%)	67.0

Table 4.15: Results of single zone production scheme.

The field and well production profiles, and tubing head and reservoir pressures of the single sand scenario are presented in Figures 4.20 to 4.24.

4.5.2 Commingled Sand Production Scheme Sensitivity

The commingled sand scheme has the same features as the single sand scheme except all reservoir units will be commingled to maintain the offtake rate from beginning. The performance comparison of the single and commingled sand schemes are shown in Table 4.16.

Sand Production Scheme	Single Sand (Design Base)	Commingled (Sensitivity Base)
OGIP (bcf)	503.4	503.4
Stage I (Y3, Y4) on Line timing	1-Jan-04	1-Jan-04
Stage II (Y5, Y6) on line timing	1-Apr-11	1-Dec-09
Compression on line timing	1-Aug-13	1-Jul-13
Field Cum Prod (bcf) – 31/12/19	337.4	339.2
- Yolla 3	124.6	122.7
- Yolla 4	131.8	127.3
- Yolla 5	35.7	42.9
- Yolla 6	45.3	46.3
Production Plateau (Year)	11.7	11.6
Recovery Factor (%)	67.0	67.4

Table 4.16: Performance comparison of single and commingled sand schemes.

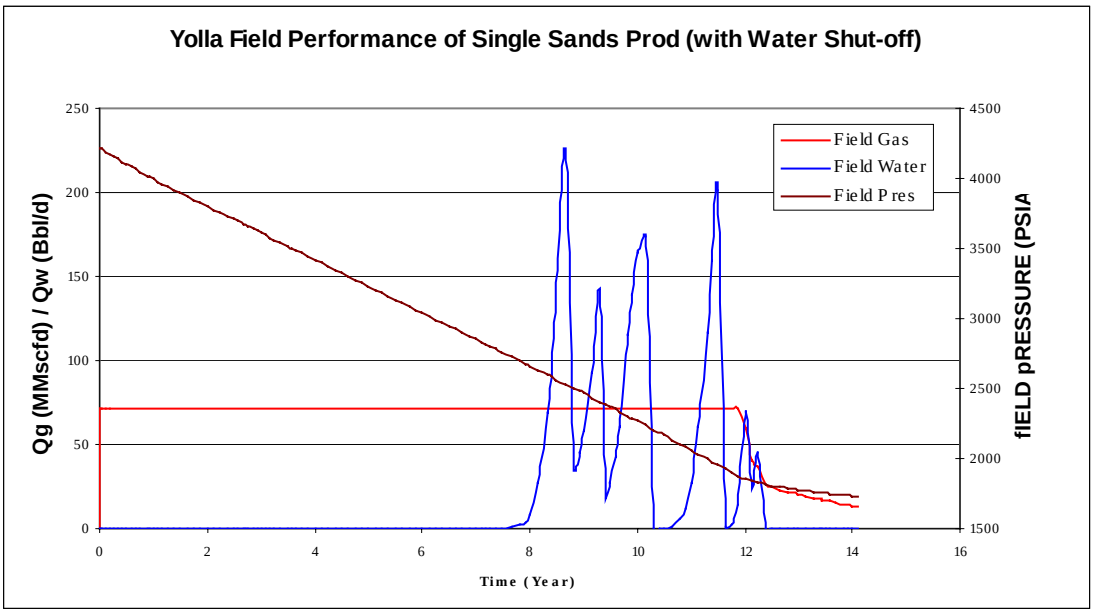

Figure 4.20: Yolla Field Performance of Single Sands Production Scheme

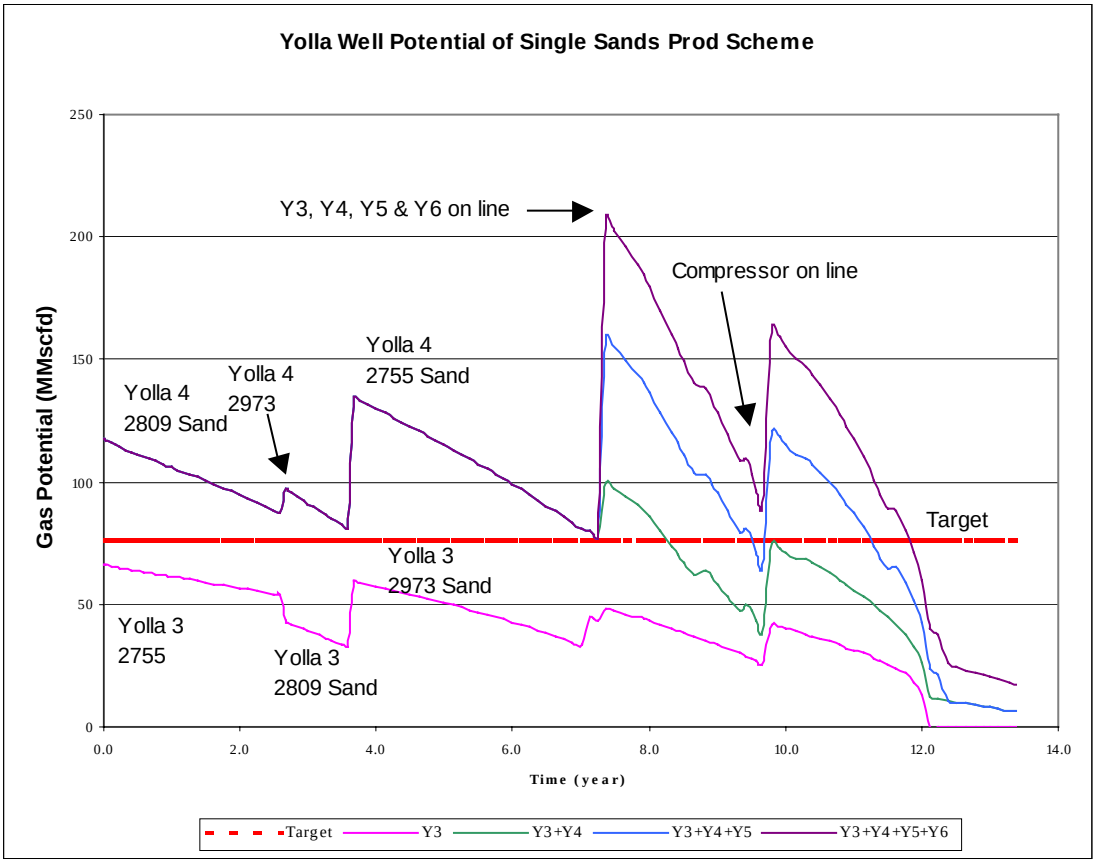

Figure 4.21: Yolla Well Performance of Single Sands Production Scheme

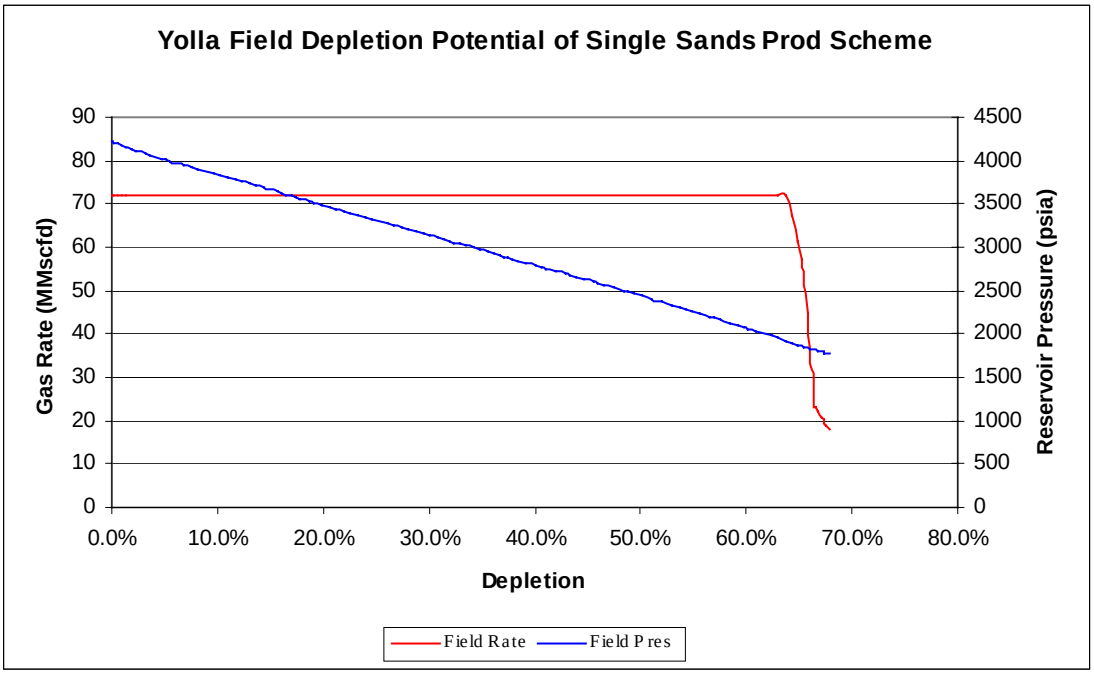

Figure 4.22: Yolla Field Depletion Potential of Single Sands Production Scheme

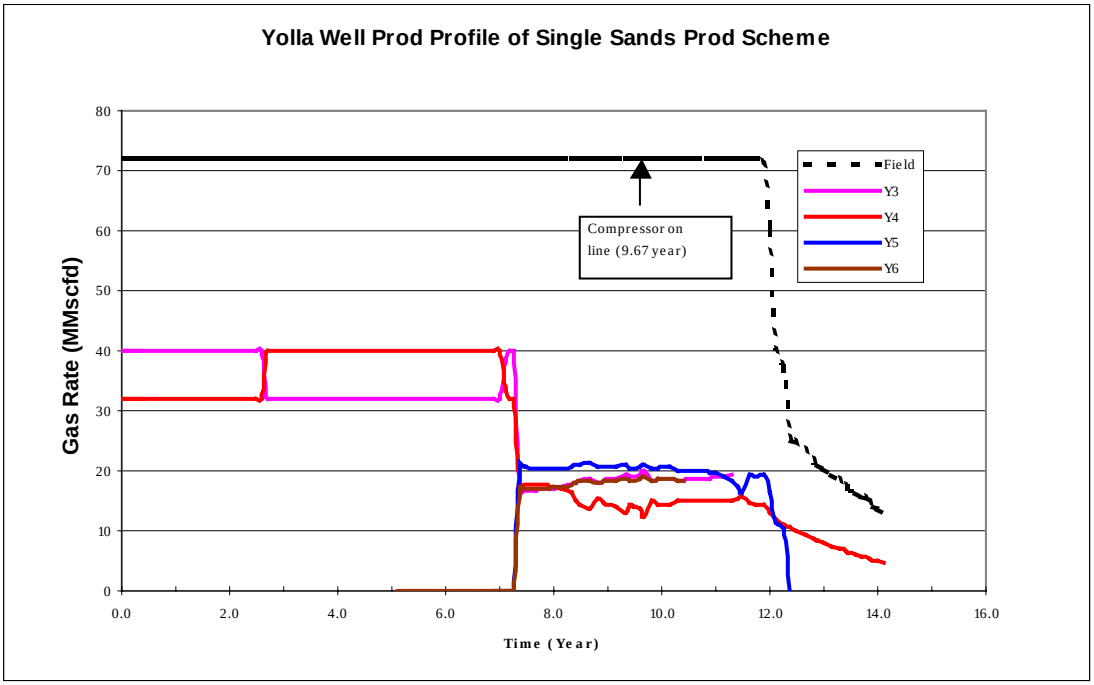

Figure 4.23: Yolla Well Production Profile of Single Sands Production Scheme

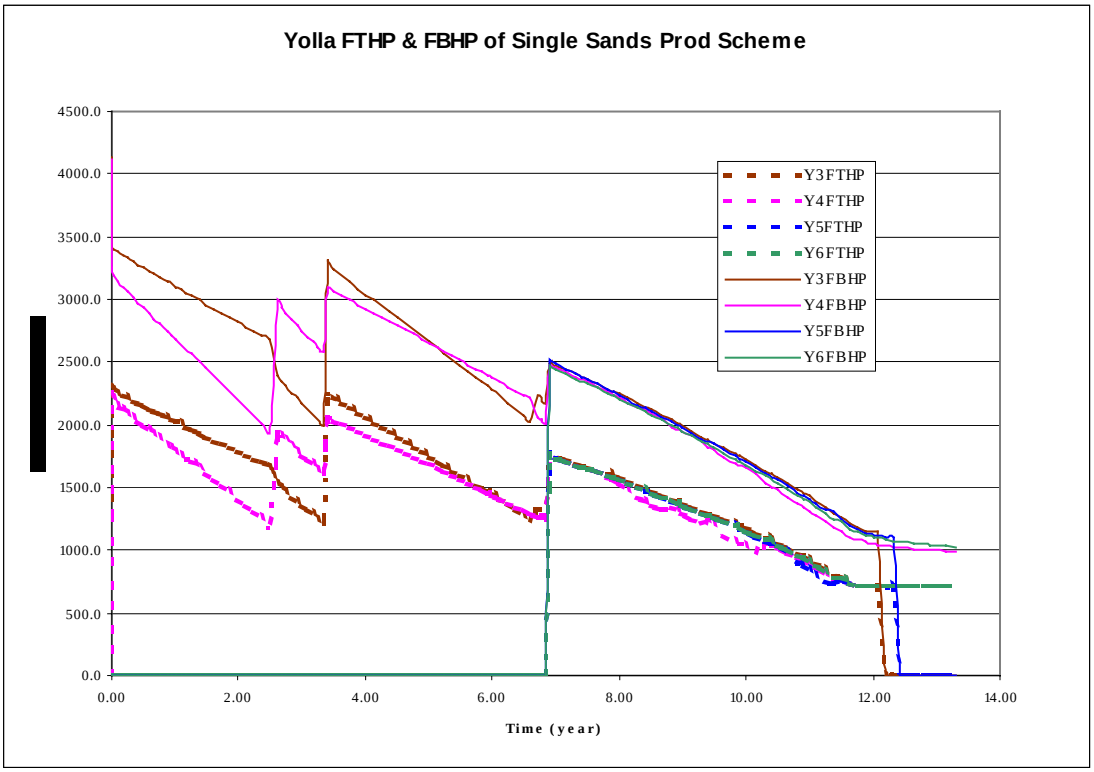

Figure 4.24: Yolla FTHP & FBHP of Single Sands Production Scheme

It is found that the commingled scheme has no impact on gas recovery, compared with the single sand scheme. Therefore, while the selective case is the prime design case, sensitivities were run using commingled schemes for simplicity. The commingled scheme is used as the sensitivity base case for the results comparison purposes.

4.5.3 Dyke Transmissibility Sensitivity

Changes in the reservoir lateral properties such as dyke transmissibility could have an impact on the field recovery. The sensitivities on the dyke transmissibility were undertaken to quantify this impact. The ranges of dyke transmissibility assumed were 0% (fully sealed), 20% (sensitivity base case) or 40% of the rock horizontal transmissibility.

The results of the dyke transmissibility are shown in Table 4.17.

The results show that lack of dyke transmissibility (0% transmissibility case) would affect the gas recovery. If this effect is seen in initial reservoir production performance, Yolla 5 and 6 may need to be brought forward to improve overall recovery.

Dyke Transmissibility	0%	20% (Base)	40%
OGIP (bcf)	503.4	503.4	503.4
Stage I (Y3, Y4) on Line timing	1-Jan-04	1-Jan-04	1-Jan-04
Stage II (Y5, Y6) on line timing	1-Jan-09	1-Dec-09	1-Oct-10
Compression on line timing	1-Jun-12	1-Jul-13	1-Jul-13
Field Cum Prod (bcf) – 31/12/19	301.0	339.2	339.1
- Yolla 3	108.6	122.7	122.5
- Yolla 4	107.9	127.3	127.8
- Yolla 5	52.7	42.9	42.2
- Yolla 6	31.8	46.3	46.6
Production Plateau (Year)	10.0	11.6	11.5
Recovery Factor (%)	59.8	67.4	67.4

Table 4.17: Performance comparison of cases with variable dyke transmissibility sensitivity.

4.5.4 P50 Poor Sand Trend Sensitivity

This is a scenario to capture the impact of a pessimistic sand distribution in the zones on the P50 model. The proportion of good reservoir facies (channel facies) was lowered. Channel geometries were also changed to reflect more ribbon like sand distribution. The OGIP distribution with this poor sand trend realisation is summarized in Table 4.18.

Sand	P50 Base	Poor Sand Trend
2718	41.3	34.4
2755	236.8	213.3
2809	97.6	102.2
2952	9.4	16.8
2973	118.3	136.7
SUM	503.4	503.4

Table 4.18: OGIP distribution for poor sand trend case.

A comparison of field performance of poor sand trend and the sensitivity base case is given in Table 4.19.

As observed from the results, the cumulative gas production of the poor sand trend case is reduced by 58.3 bcf (11.6% RF), to 280.9 bcf. The Phase II wells would be brought forward by about 1.7 years and 2.7 years for the compression. The production plateau is shortened by about 2.8 years.

Sand Trend	Base Case	Poor Sand Trend
OGIP (bcf)	503.4	503.4
Stage I (Y3, Y4) on Line timing	1-Jan-04	1-Jan-04
Stage II (Y5, Y6) on line timing	1-Dec-09	1-Apr-08
Compression on line timing	1-Jul-13	1-Nov-10
Field Cum Prod (bcf) – 31/12/19	339.2	280.9
- Yolla 3	122.7	94.4
- Yolla 4	127.3	104.9
- Yolla 5	42.9	27.2
- Yolla 6	46.3	54.5
Production Plateau (Year)	11.6	8.8
Recovery Factor (%)	67.4	55.8

Table 4.19: Comparison of results from base and poor sand trend cases.

The unfavourable sand trend is found to have a very profound effect on both the recoverable reserves and the recovery factor. This possibility results in recovery similar to the P90 reserves level, and is viewed as one outcome illustrating how the P90 may result.

4.5.5 Reservoir Permeability Sensitivity

The variable with respect to the reservoir permeability is the proportion of higher porosity facies (i.e. channel facies) to the finer-grained facies within the fluvial reservoirs. The higher proportion of the finer-grained facies would reduce the porosity/permeability across the model in the 2755, 2809 and 2973 sands. On the contrary, the porosity and permeability of the 2755, 2809 and 2973 zones would increase if the proportion of higher porosity facies has been increased.

The results of the reservoir connectivity sensitivity are presented in Table 4.20.

Reservoir Permeability	Low permeability	Base Case	High permeability
OGIP (bcf)	503.4	503.4	503.4
Stage I (Y3, Y4) on Line timing	1-Jan-04	1-Jan-04	1-Jan-04
Stage II (Y5, Y6) on line timing	1-Aug-09	1-Dec-09	1-Oct-10
Compression on line timing	1-Jul-13	1-Jul-13	1-Jul-13
Field Cum Prod (bcf) – 31/12/19	341.2	339.2	361.6
- Yolla 3	129.2	122.7	146.8
- Yolla 4	105.7	127.3	135.8
- Yolla 5	49.1	42.9	36.7
- Yolla 6	57.2	46.3	42.3
Production Plateau (Year)	11.5	11.6	12.4
Recovery Factor (%)	67.8	67.4	71.8

Table 4.20: Results from reservoir permeability sensitivity.

The results show that the gas recovery could increase to 361.6 bcf if higher proportions of high porosity facies were presented in the reservoir. However, there is no change in the gas recovery in the low permeability case that is unexpected.

The possible explanation is that there are two effects in lowering formation permeability. It will reduce the well productivity but it would also slow down the water invasion. It is likely that the effect of low well productivity has been offset by the effect of delaying water influx. Consequently, there is no change in gas recovery for the low permeability case.

The results show that there is little effect of sand permeability on gas recovery provided sand connectivity is maintained.

4.5.6 Aquifer Strength Sensitivity

Aquifer support is considered one of the key parameters that could have a major impact on field recovery. The aquifer strength parameters investigated were:

- Fault opening to SW: widened or closed
- End point Krw: halving to 0.15 or doubling to 0.6

Aquifer size is not included in the investigation as it is considered to be sufficiently extensive already. Rather, the case of otherwise with which the aquifer can encroach is the parameter investigated.

The field performance under various aquifer strength are shown in Table 4.21.

Aquifer Strength Parameter	Close fault opening	Widen fault opening	Base	Halving end point Krw	Doubling end point Krw
OGIP (bcf)	503.4	503.4	503.4	503.4	503.4
Stage I (Y3, Y4) on Line timing	1-Jan-04	1-Jan-04	1-Jan-04	1-Jan-04	1-Jan-04

Stage II (Y5, Y6) on line timing	1-Oct-10	1-Oct-10	1-Dec-09	1-Jan-14	1-Oct-10
Compression on line timing	1-May-13	1-Aug-13	1-Jul-13	1-Oct-13	1-Aug-13
Field Cum Prod (bcf) – 31/12/19	337.8	339.3	339.2	338.7	336.9
- Yolla 3	125.0	119.8	122.7	125.6	116.5
- Yolla 4	127.3	132.0	127.3	129.1	130.3
- Yolla 5	41.9	38.5	42.9	40.8	37.4
- Yolla 6	43.7	49.0	46.3	43.1	52.7
Production Plateau (Year)	11.5	11.6	11.6	11.5	11.4
Recovery Factor (%)	67.1	67.4	67.4	67.3	66.9

Table 4.21: Field performance under varying aquifer strength.

The results indicate that there is little effect of aquifer strength on gas recovery. This was unexpected. It was thought that the weaker aquifer would reduce the extent of water influx, resulting in reservoir pressure having a steeper decline, due to the lack of aquifer pressure support. Compression would be required earlier.

Conversely, it was thought that a stronger aquifer would accelerate water influx and wells would be hit harder. However, it would provide extra pressure support and would maintain a better productivity prior to water arrival. It seems the favorable and unfavorable effects offset each other for either stronger or weaker aquifer strength scenarios. The effect can be explained by realising that the reservoir is predominantly depletion drive due to the relatively low permeability resulting in low water mobility. Variations in parameters governing aquifer encroachment only change influx marginally.

4.5.7 Upside Potential – P10 Structure Sensitivity

This upside potential sensitivity evaluates the field performance by using a high side or optimistic structural model. The OGIP of the upside model was adjusted to match the P10 probabilistic estimate of 621 bcf. The OGIP comparison between the base and the upside case is presented in Table 4.22.

Sand	Base Case E100 OGIP (bcf)	P10 Structure E100 OGIP (bcf)
2718	41.3	57.4
2755	236.8	283.6
2809	97.6	127.0
2952	9.4	11.7
2973	118.3	141.3
Sum	503.4	621.0

Table 4.22: OGIP comparison of base case and high side case.

The results of the upside structural case are summarised in Table 4.23.

The field gas production of the upside structural model is significantly higher than the sensitivity base case. This is primarily due to a higher OGIP in the upside structure model. However, a similar recovery factor to the base case could be expected if the sand distribution parameters in the upside case are kept as the same with the base case.

Structure	Base	P10 Structure
OGIP (bcf)	503.4	621.0
Stage I (Y3, Y4) on Line timing	1-Jan-04	1-Jan-04
Stage II (Y5, Y6) on line timing	1-Dec-09	1-Sep-11
Compression on line timing	1-Jul-13	1-Jul-15
Field Cum Prod (bcf) – 31/12/19	339.2	419.4
- Yolla 3	122.7	147.2
- Yolla 4	127.3	140.1
- Yolla 5	42.9	68.1
- Yolla 6	46.3	64.1
Production Plateau (Year)	11.6	13.9
Recovery Factor (%)	67.4	67.5

Table 4.23: Results from upside structural case.

Upside structure is found to increase the recoverable reserves but not the recovery factor.

4.5.8 Down Side Potential – P90 Structure and Poor Sand Trend Sensitivity

Two P90 OGIP geological models were imported into the Yolla simulation model. For the down side structure scenario, it adopts a pessimistic structural model but has the same sand distribution parameters as with the base case. This allows the sensitivity of the lower field structure to be assessed.

The down side sand trend model also uses a pessimistic sand distribution to the zones on the same structural model as the base case. The proportion of good quality reservoir facies was lowered. Channel geometries were also changed to reflect more ribbon-like sand distribution. OGIP matched the P90 probabilistic estimate of 393 bcf.

The OGIP comparison for the base and the down side cases is tabulated in Table 4.24.

Sand	Base Case E100 OGIP (bcf)	Poor Sand Trend E100 OGIP (bcf)	P90 Structure E100 OGIP (bcf)
2718	41.3	26.8	24.5
2755	236.8	166.3	194.2
2809	97.6	79.7	68.1
2952	9.4	13.1	6.7
2973	118.3	106.5	99.6
Sum	503.4	392.4	393.0

Table 4.24: Comparison of OGIP for base, P90 (poor sand trend) and P90 structure case.

The results of the down side cases are summarised in Table 4.25.

The field gas recoveries of the down side models are significantly lower than the base case. The major contributor is that the down side models have a significant lower OGIP than the base case.

Same as with the upside structural case, the down side structural model has a comparable recovery factor to the base case. This is expected, as the sand distribution parameters are not changed between the base case and the P90 structural models.

However, the down side sand trend model has a significant lower recovery factor, in addition to the lower gas recovery. The cumulative gas production of the down side sand trend case has reduced by 112.7 bcf, to 226.5 bcf with a recovery factor of 57.7%. The Phase II wells would be brought forward by about 1.8 years and 4.2 years for the compression. The production plateau is shortened by about 4.7 years.

Down Side Potential	Base Case	Poor Sand Trend	P90 Structure
OGIP (bcf)	503.4	392.4	393.0
Stage I (Y3, Y4) on Line timing	1-Jan-04	1-Jan-04	1-Jan-04
Stage II (Y5, Y6) on line timing	1-Dec-09	1-Mar-08	1-Apr-09
Compression on line timing	1-Jul-13	1-May-09	1-Apr-11
Field Cum Prod (bcf) – 31/12/19	339.2	226.5	257.2
- Yolla 3	122.7	80.5	85.8
- Yolla 4	127.3	87.1	119.9
- Yolla 5	42.9	18.1	18.6
- Yolla 6	46.3	40.7	32.9
Production Plateau (Year)	11.6	6.9	8.4
Recovery Factor (%)	67.4	57.7	65.4

Table 4.25: Results from P90 cases.

Similar to the P50 poor sand trend sensitivity, it is found that the unfavorable sand trend could have a very profound effect on both the recoverable reserves and the recovery factor. This particular case combining a lowside OGIP with a lowside sand distribution is viewed as an unlikely outcome, illustrating a reserves level higher than P90, possibly around P95 level.

5 PROPOSED DRILLING LOCATIONS AND WELL PATHS

On the basis of the above reservoir simulation and geological modeling 4 preliminary well paths have been designed. These wells are deviated from the proposed platform location. All of these locations assume a platform location at:

Easting: 398796
Northing: 5588641

The proposed well path for each of the wells is shown on Figures 5.1 and 5.2. The proposed well paths, potential hazards associated with each, and proposed evaluation are discussed below.

5.1 Yolla 3

Yolla-3 is planned as a development well for the Intra-EVCM and an appraisal well for the Upper EVCM. The well is to be deviated from the platform location in a northwesterly direction (Figs. 5.1 to 5.4). The primary objective for the well is to provide deliverability and produce gas from the intra-EVCM in northern part of the structural closure within the vicinity of Yolla-1. The well will deviate from vertical at a depth of 200m SS and will maintain an angle of deviation of approximately 45 degrees (Fig. 5.4).

A well prognosis is provided as Figure 5.5 and is summarized in Table 5.1. The well path will intersect the Upper EVCM reservoir (TEV4) 90m from Yolla-1 and 2m stratigraphically higher than Yolla-1. The 2809 Sand at intra-EVCM level is prognosed to be intersected at 2798m SS (2m higher than Yolla-1) with a predicted horizontal offset from Yolla-1 of 480m to the northwest. A horizontal tolerance of 100m is acceptable for this target. The total measured depth for the well is predicted to be 3628m.

5.1.1 Potential Hazards

The main hazards/risk associated with Yolla-3 well path concern the potential intersection of volcanic sills within the section. All of these volcanic units have the potential to be hard drilling. Based on seismic mapping an approximately 170m thick unit of tuffaceous Miocene volcanics is predicted in the intermediate section of the hole. A small sill is predicted at 2657m SS, approximately 50m above the intra-EVCM reservoir section based on seismic amplitude. This correlates with a 65m sill that was intersected at approximately 2574m SS in Yolla-1. In addition, a high amplitude seismic response at the 2809 Sand reservoir level (Fig. 5.3) in Yolla-3 may also be indicative of a volcanic sill. This will be a risk for the viability of this location in the development plan and will need to be investigated in more detail prior to drilling with a view to potentially moving this location slightly. Prior to final well design it is proposed that acoustic impedance inversion of the 3D seismic data be done to investigate whether thin sills can be detected (and hence avoided) in the reservoir section. The well is predicted to TD in Palaeocene Basalt.

Yolla Gas Field: Top EVCM (TEV 4 Horizon) DEPTH

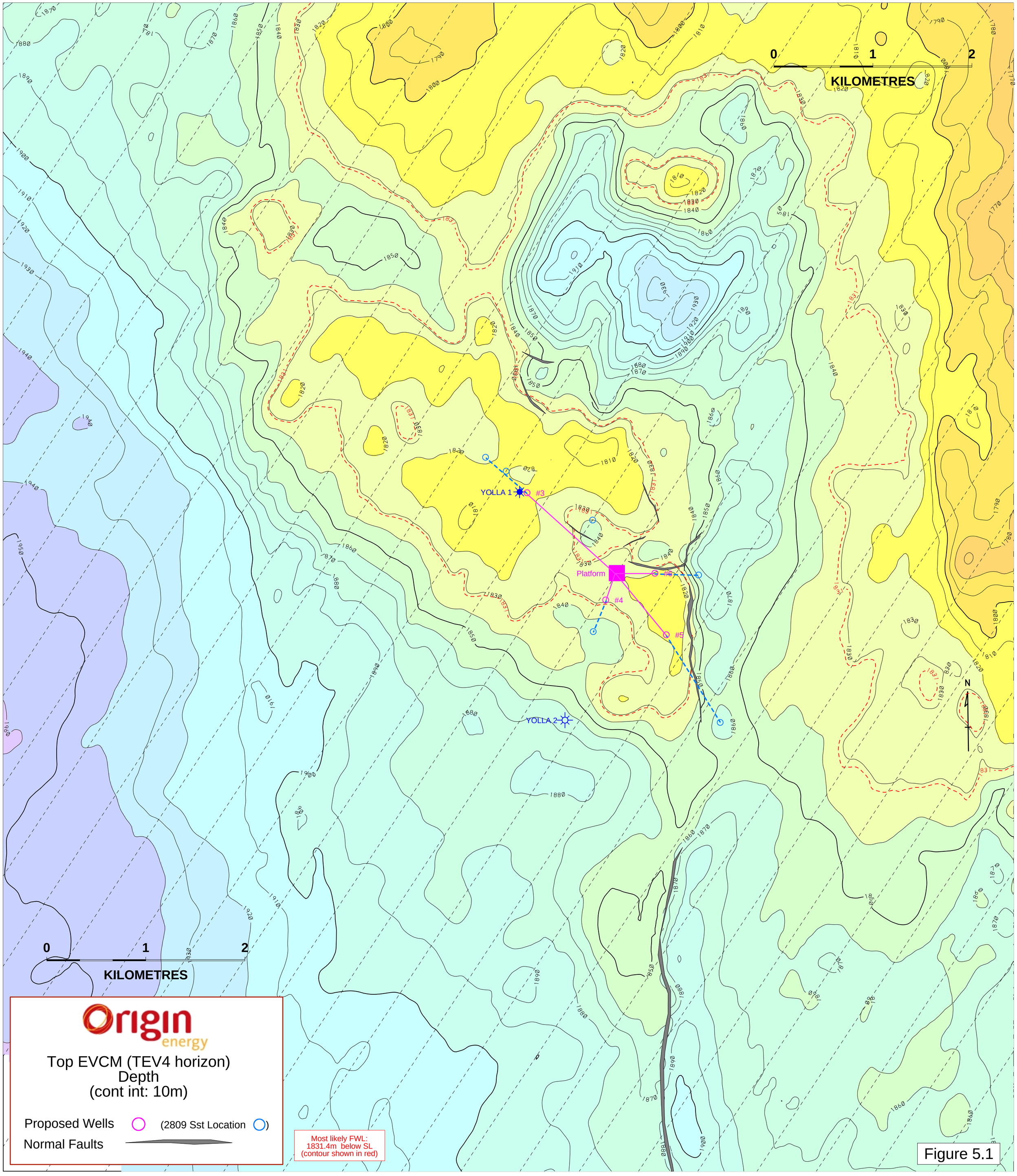

Figure 5.1

Yolla Gas Field: 2809 Sand Depth (P50 case)

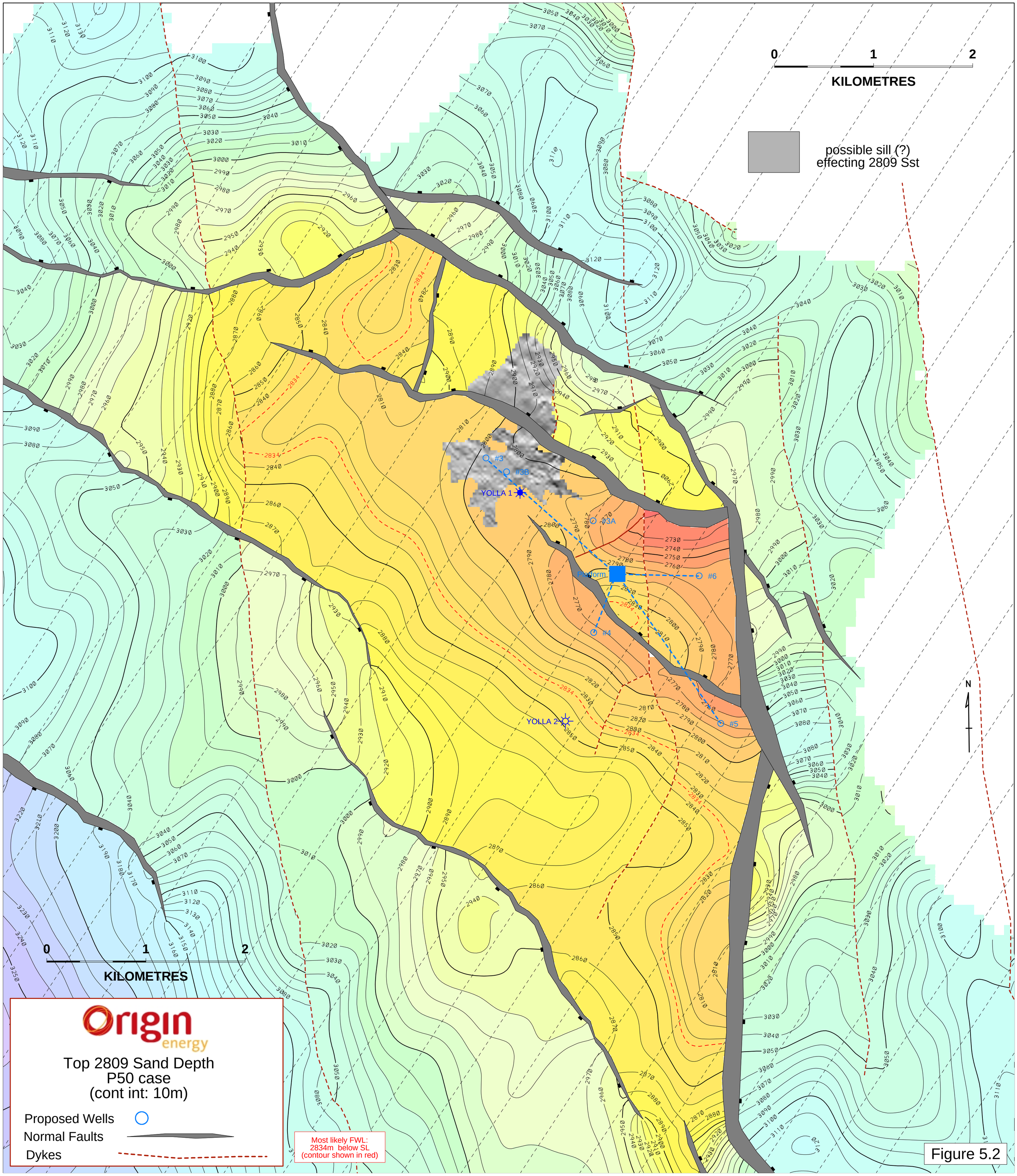

Figure 5.2

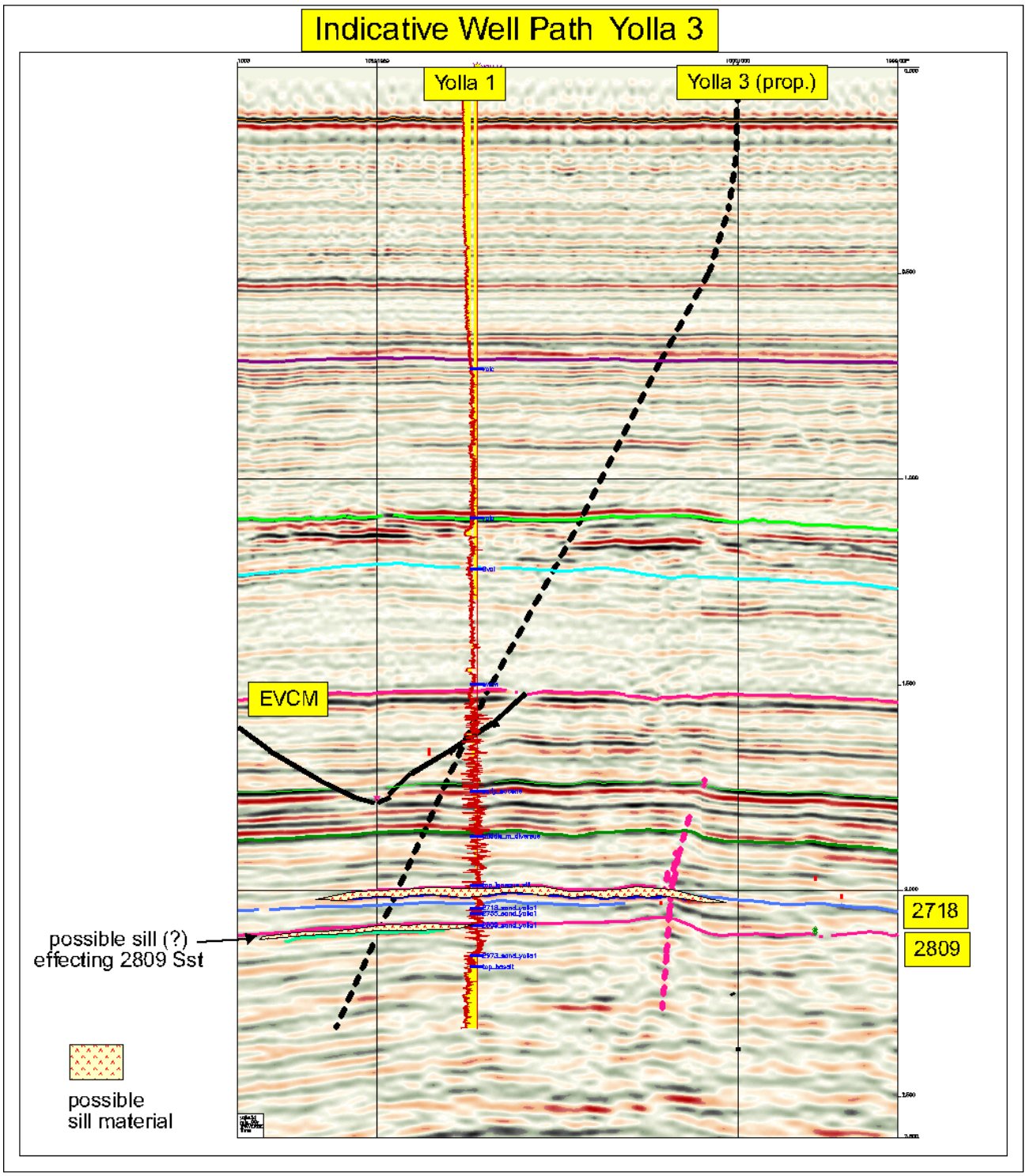

Figure 5.3: Seismic section showing Yolla 3 well path.

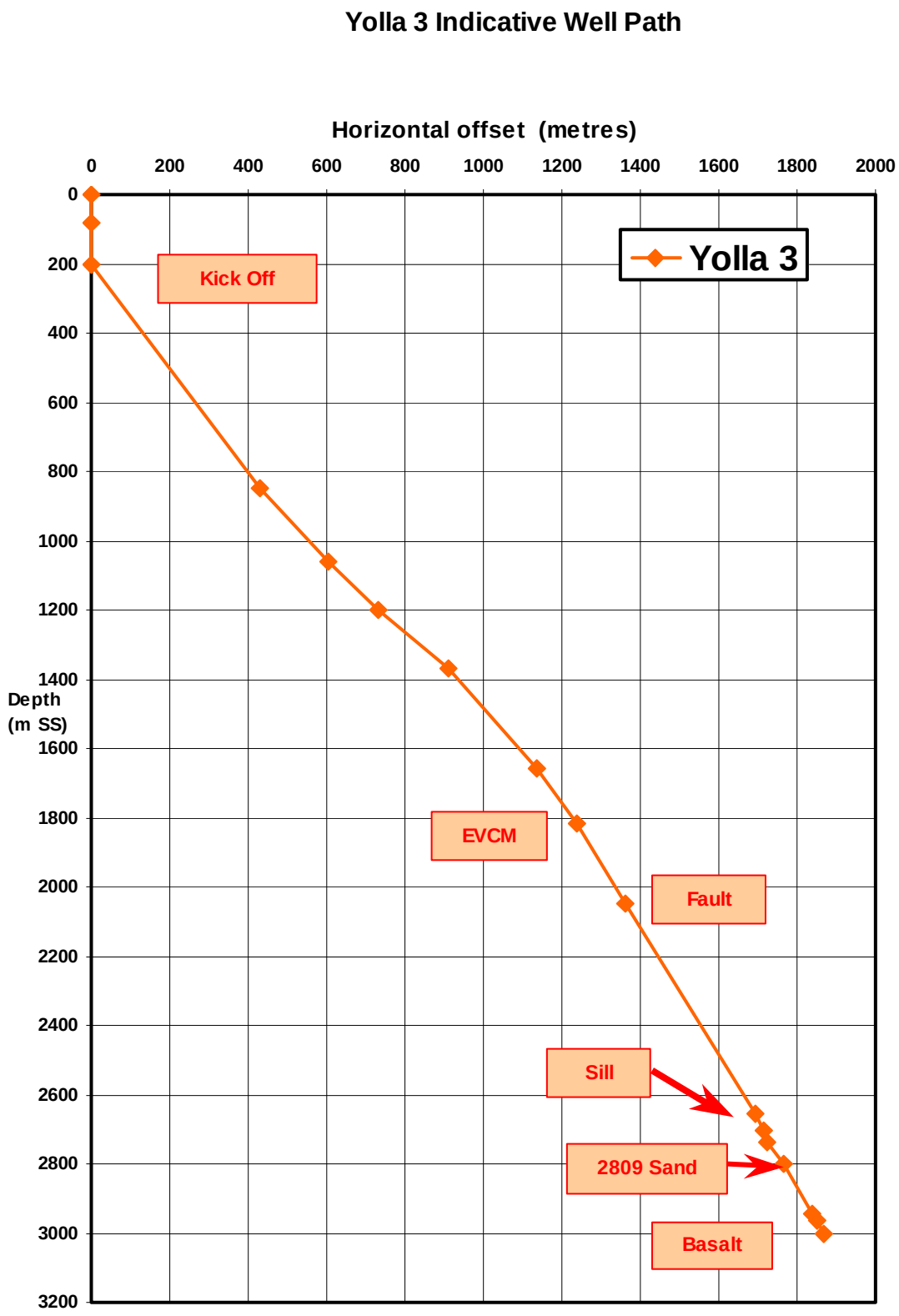

Figure 5.4: Yolla 3 indicative well path.

YOLLA-3

Inline 840 CDP 2665

Platform Location:
Easting: 398 796
Northing: 558 8641
Horizontal Offset at TD: 1869m

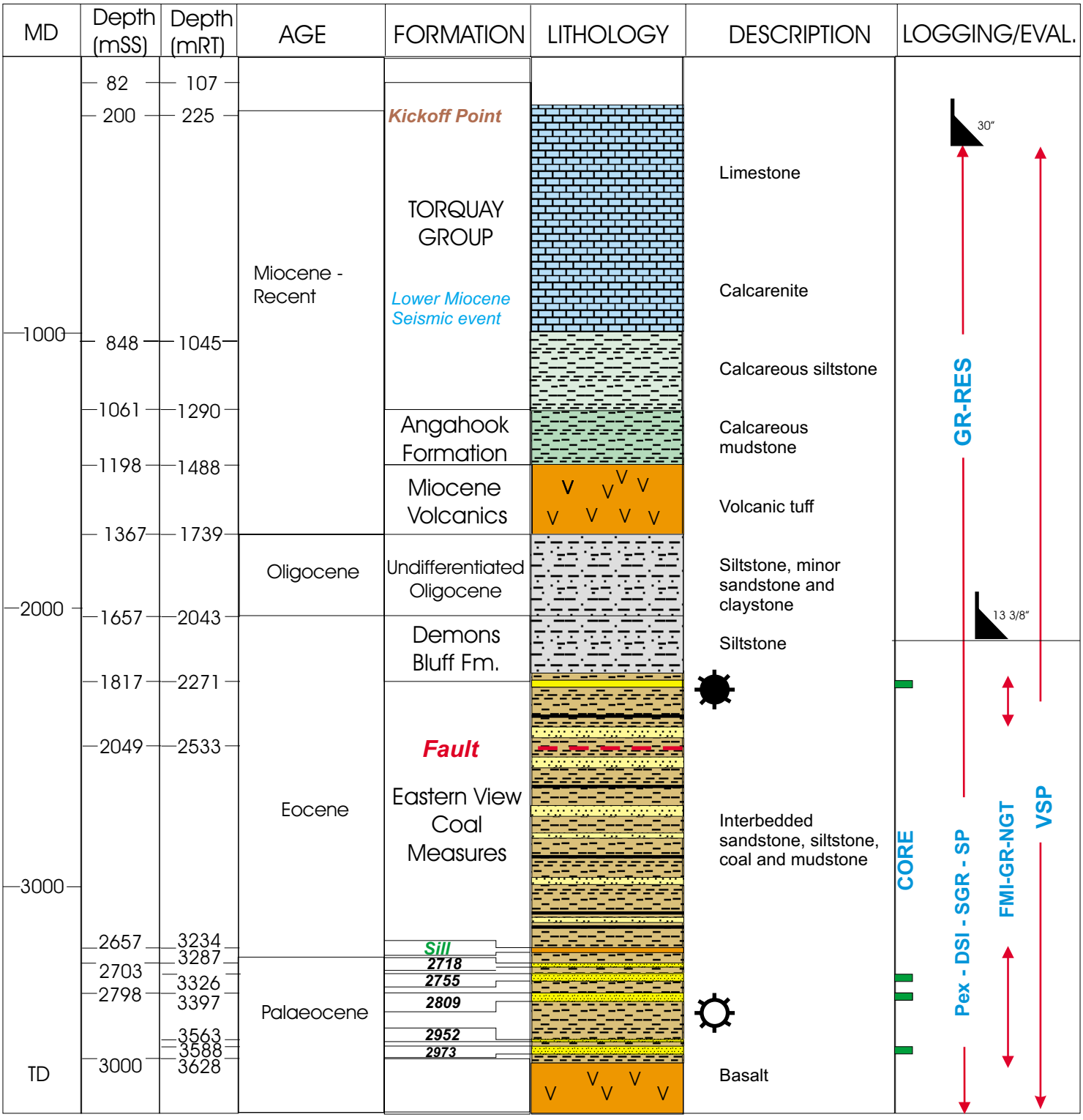

Figure 5.5: Predicted stratigraphy for Yolla 3.

In addition a major fault (Frank) is prognosed to be intersected at 2049m SS (2533m RT) in the upper part of the EVCM.

Horizon	Depth SS	MD	Horizon Offset	Inline	Xline	Target Radius	Easting	Northing
Sea Level	0	25	0	480	1000			
Sea Bed	81.8	106.8	0	480	1000			
Kick Off	200	225	0	480	1000			
Lwr Mid Mio	848	1045	430	497	1005			
Angahook	1061	1290	606	504	1007			
Volcano	1198	1488	732	509	1008			
Base Volc	1367	1739	909	516	1010			
Demons Bluff	1657	2043	1137	525	1013			
EVCM (TEV4)	1817	2271	1237	529	1014	20m	397889	5589453
Fault	2049	2533	1363	534	1015			
Sill	2657	3234	1692	547	1019			
2718 Sand	2703	3287	1717	548	1019			
2755 Sand	2737.4	3326	1725					
2809 Sand	2798	3396.5	1768	550	1020	100m		
2952 Sand	2943.3	3562.5	1840					
2973 Sand	2965.5	3587.5	1850					
Basalt	3000	3628	1869	554	1021			

Table 5.1: Progonsis Summary – Yolla 3.

5.1.2 Evaluation

In order to further appraise and evaluate the Yolla Field the following evaluation programme is proposed (Sclumberger log mnemonics):

- 1 x 27m core to be taken from the Upper EVCM
- 3 X 27m cores to be taken from the Intra-EVCM, 1 from each of the 2755, 2809 and 2973 Sands
- Run1 - Pex-DSI-SGR-SP: Platform express including basic gamma, spontaneous potential, resistivity, neutron-density plus dipole sonic. Gamma-ray only in cased-hole section. Note: the intention is not to run openhole logs in the intermediate section.
- Run 2 - FMI-GR-NGT: Formation microscanner, spectral gamma
- Run 3 - VSP survey

5.2 Yolla 4

Yolla-4 is designed as a development well for the Intra-EVCM reservoir units. The main reservoirs (2755, 2809 and 2973 sands) are designed to be intersected 960m northeast (Fig. 5.2) and prognosed to be 72m structurally higher than Yolla-2 in the main fault

block. A horizontal tolerance of 100m is acceptable for this target. The well will be deviated from the platform and has a total horizontal offset of 716m with a measured depth of 3161m at TD. The well will deviate from vertical at a depth of 900m SS and maintain a vertical angle of deviation of approximately 20 degrees from vertical (Fig 5.6, 5.7). A graphic well prognosis is provided (Fig. 5.8) and is summarized in Table 5.2.

5.2.1 Potential Hazards

Yolla-4 is predicted to intersect an approximately 180m tuffaceous Miocene volcanic unit at 1062m SS (1095m RT; Fig. 5.6) and Palaeocene basalt at 3005m SS (3152m RT) based on seismic interpretation. No volcanic sills are predicted within or close to the reservoir section. A major fault (Fardles) will be intersected at approximately 2540m RT (Fig. 5.6).

Horizon	Depth SS	Depth MD	Horiz Offset	Inline	Xline	Target Radius	Easting	Northing
Sea Level	0	25	0	480	1000			
Sea Bed	81.8	106.8	0	480	1000			
Lmio	849	874	0	480	1000			
Kick Off	900	925	0	480	1000			
Angahook	1062	1095	63	480	995			
Volcano	1201	1241	103	479	992			
Base Volc	1378	1427	177	479	986			
Demons Bluff	1705	1770	280	478	978			
EVCM	1832	1904	334	477	974		398683	5588370
Fault	2453	2540	534	476	958			
2718 Sand	2667	2792.2	601	475	953			
2755 Sand	2702.9	2831	613					
2809 Sand	2775	2905.2	637	475	950	100m	398557	5588050
2952 Sand	2928.2	3070.4	690					
2973 Sand	2950.4	3094	700					
Basalt	3005	3152	716	474	944			

Table 6.1: Prognosis Summary – Yolla 4.

5.2.2 Evaluation

In order to further evaluate the Yolla Field the following evaluation programme is proposed (Sclumberger log mnemonics):

- Run1 - Pex-DSI-SGR-SP: Platform express including basic gamma, spontaneous potential, resistivity, neutron-density plus dipole sonic. Gamma-ray only in cased-hole section. Note: the intention is not to run openhole logs in the intermediate section.
- Run 2 - FMI-GR-NGT: Formation microscanner, spectral gamma
- Run 3 - VSP survey

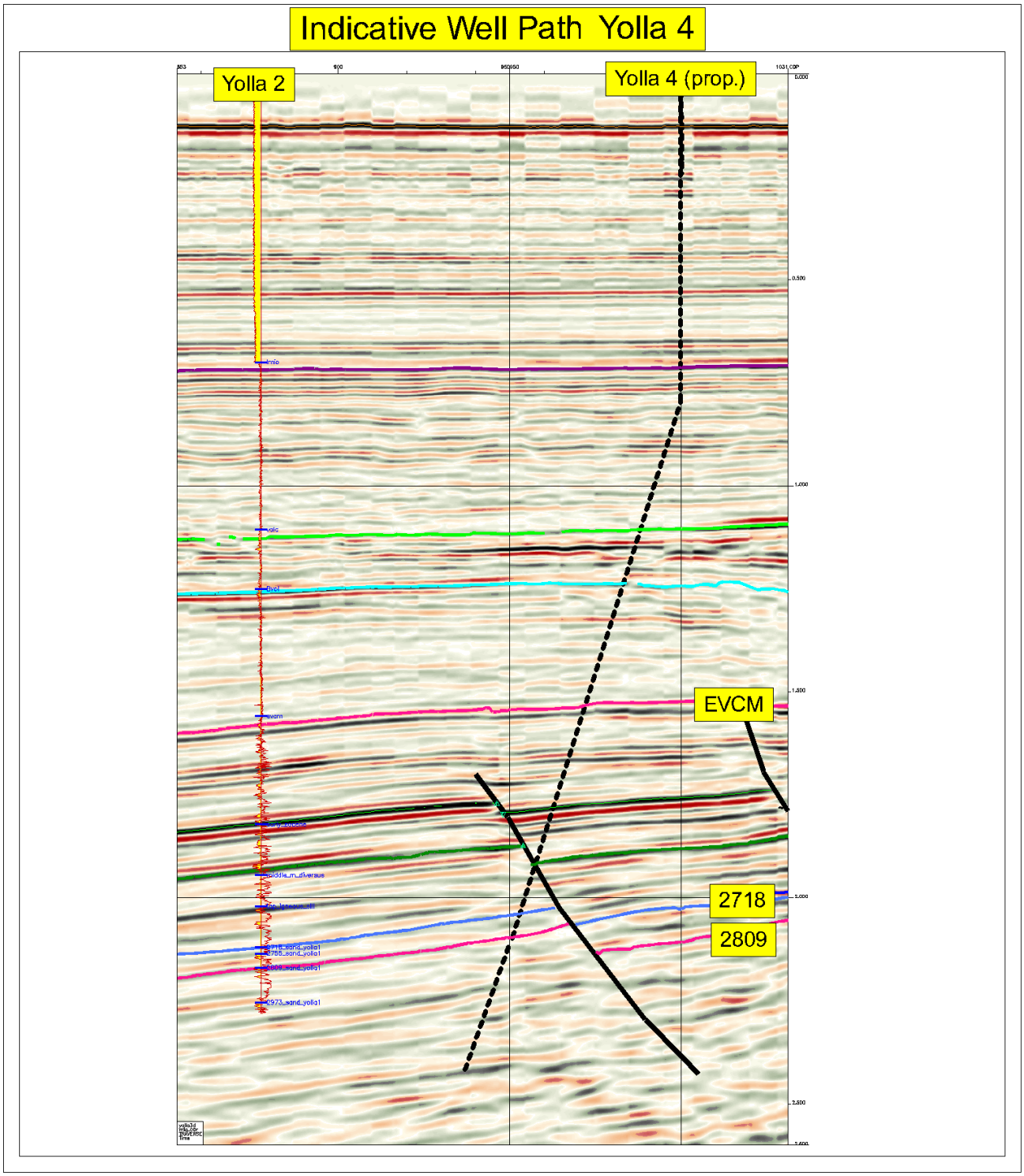

Figure 5.6: Seismic section showing Yolla 4 well path.

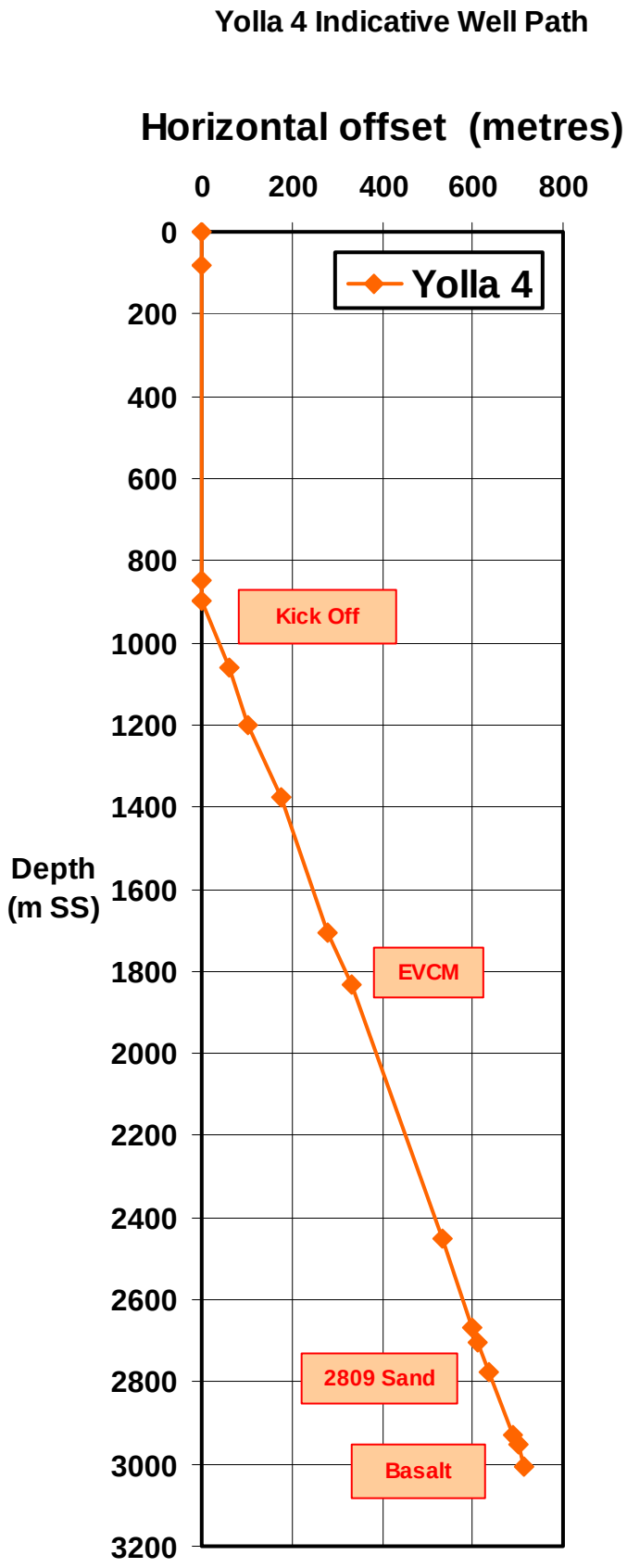

Figure 5.7: Yolla 4 indicative well path.

YOLLA-4

Inline 840 CDP 2665

Platform Location:
Easting: 398 796
Northing: 558 8641
Horizontal Offset at TD: 716m

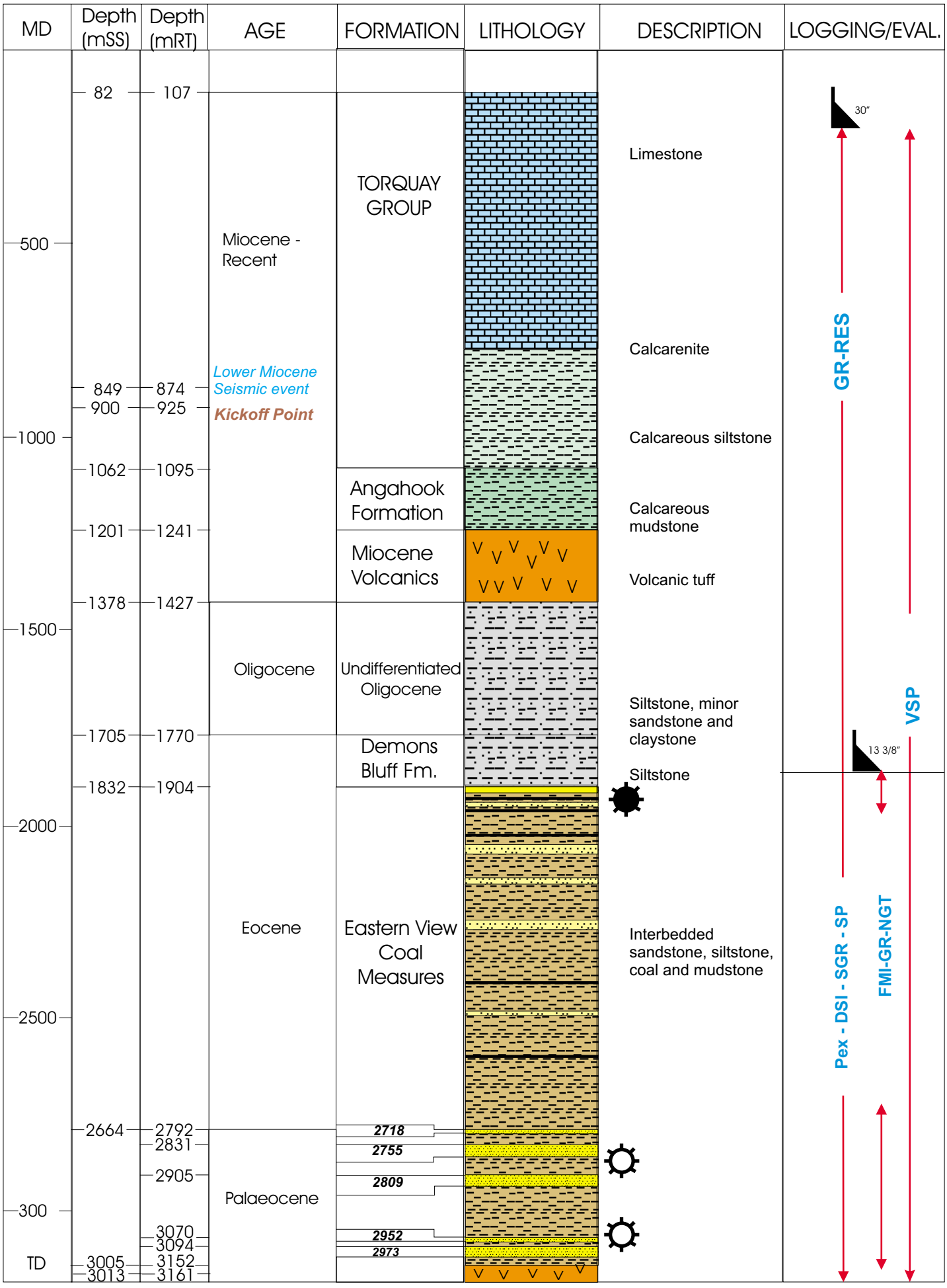

Figure 5.8: Predicted stratigraphy for Yolla 4.

5.3 Yolla 5 and Yolla 6

The drilling of Yolla 5 and Yolla 6 under the preliminary development plan is forecast for approximately 7 years after the drilling of Yolla 3 and Yolla 4. This will be dependant upon reservoir performance in the first two wells. Both of these wells will target areas that have potentially been isolated by dykes (see Fig. 5.1 and 5.2). Preliminary well paths for these wells are presented in Figures 5.9 to 5.12.

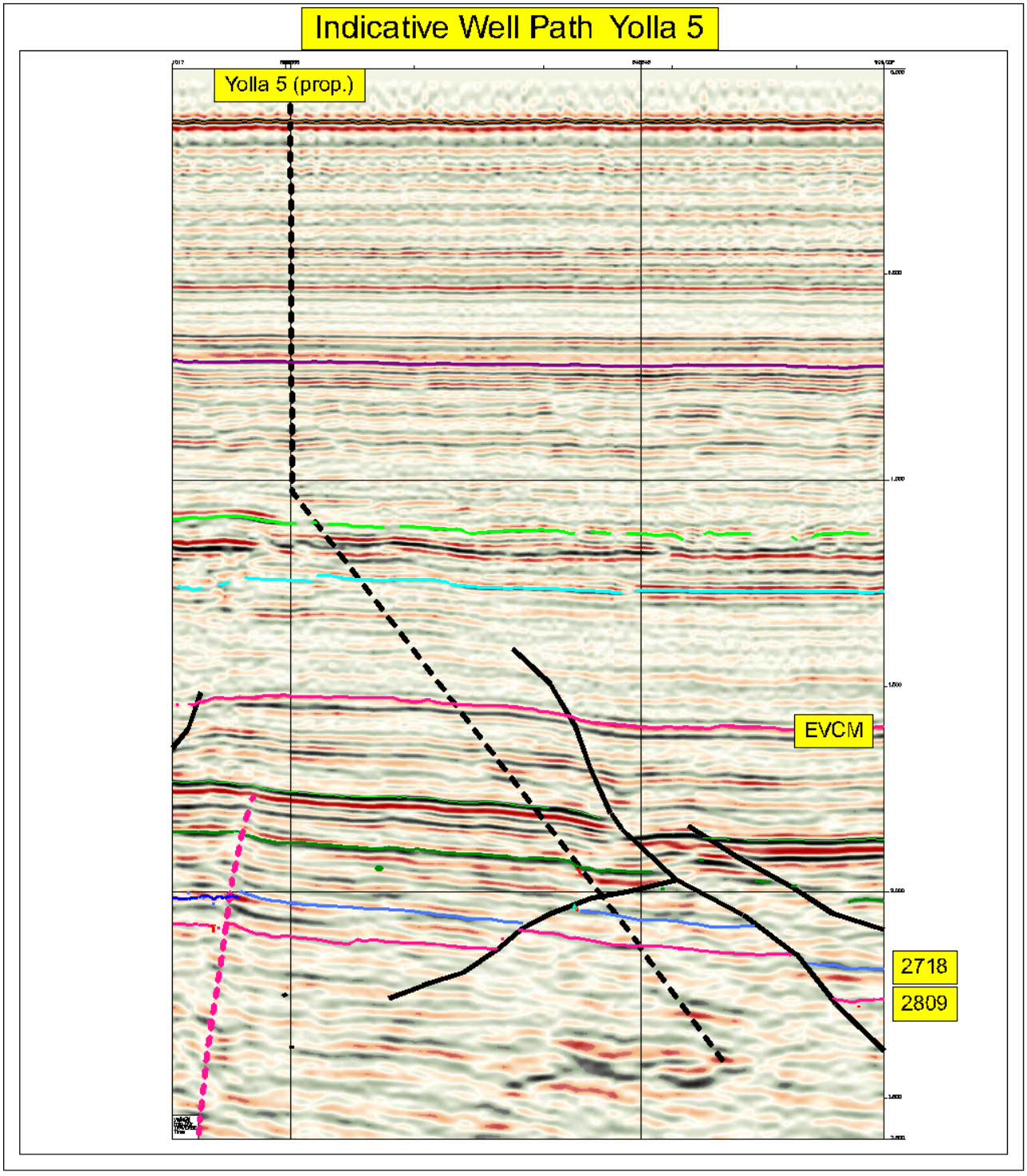

Figure 5.9: Seismic section showing Yolla 5 well path.

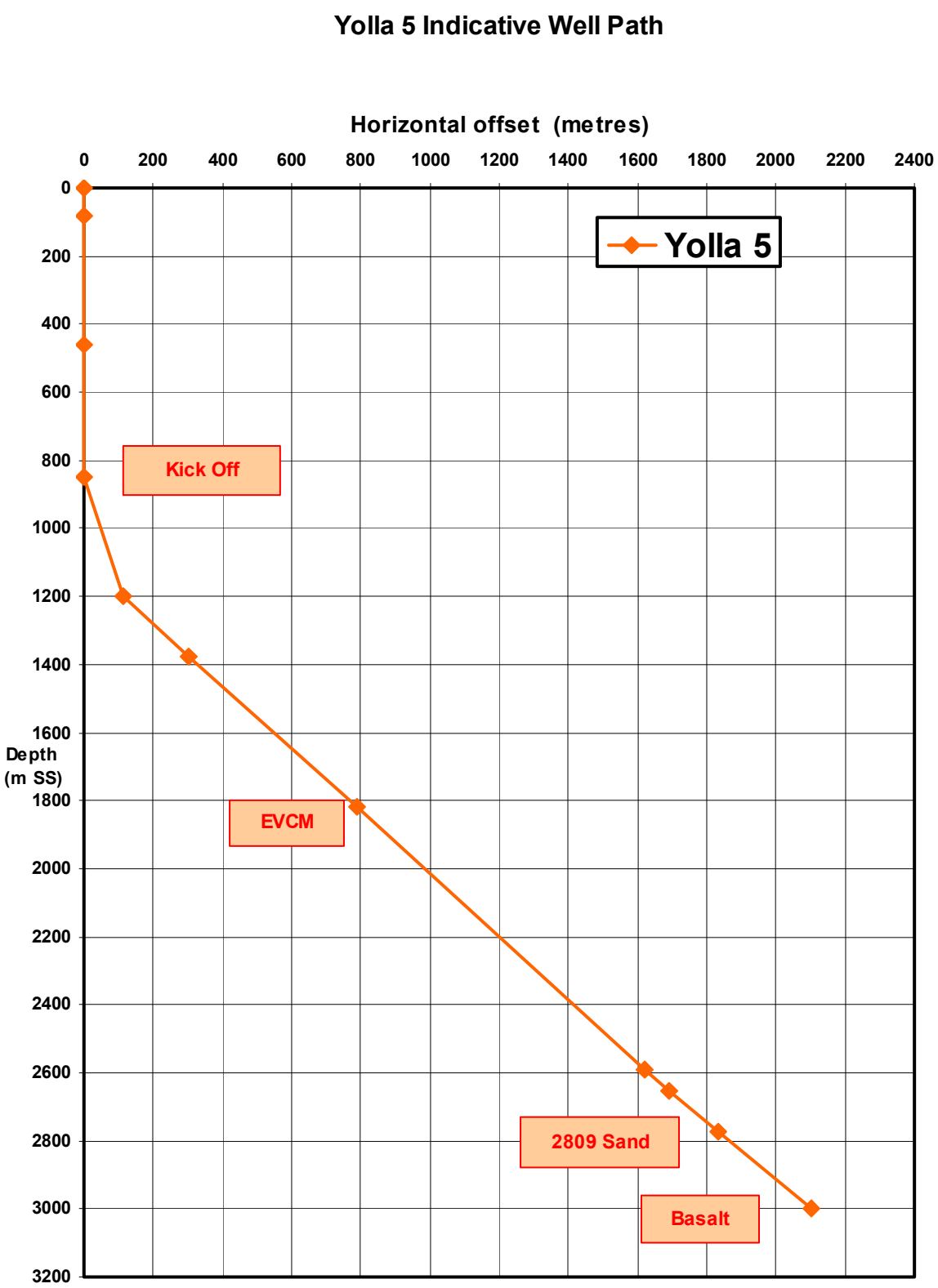

Figure 5.10: Yolla 5 indicative well path.

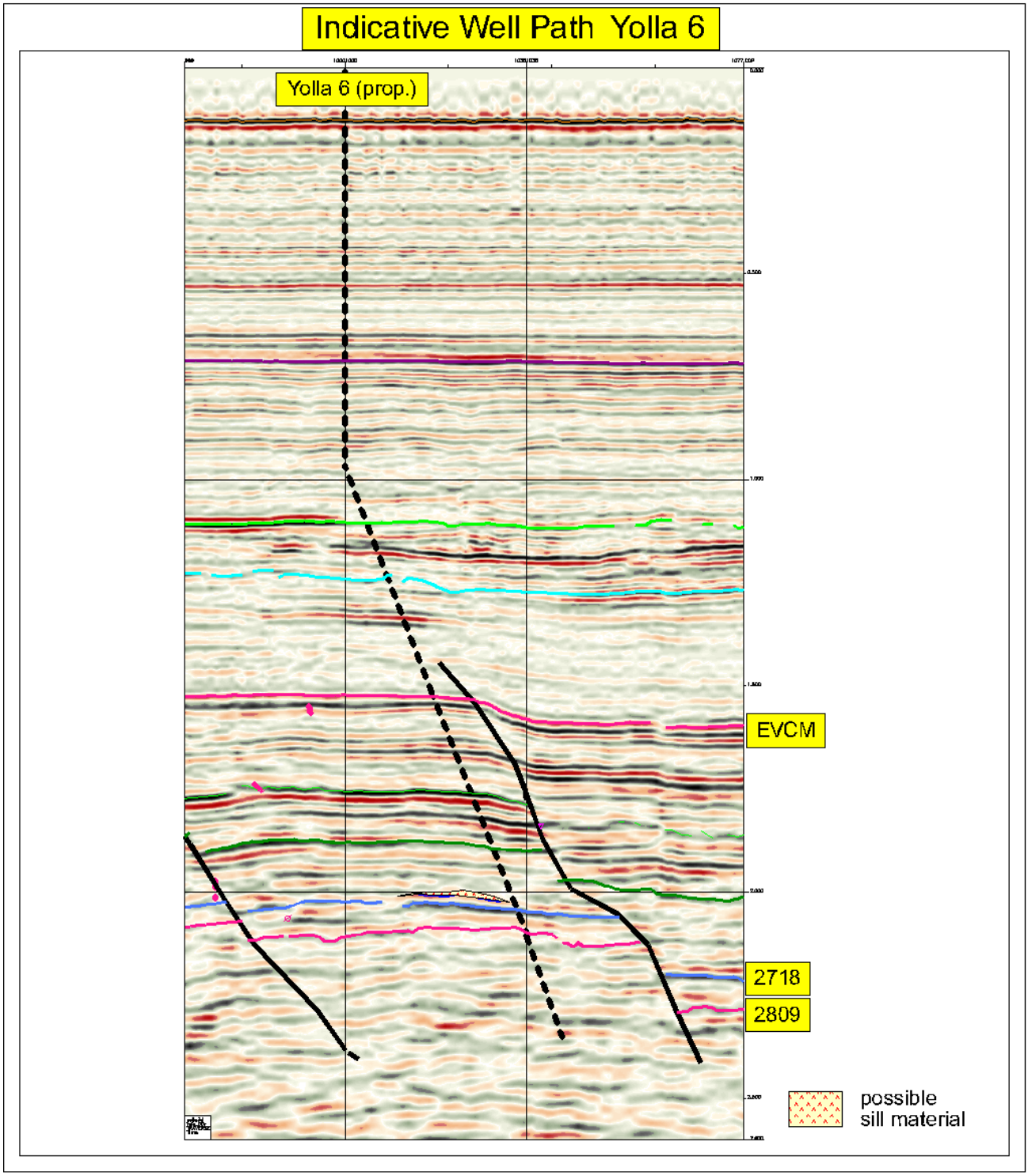

Figure 5.11: Seismic section showing Yolla 6 well path.

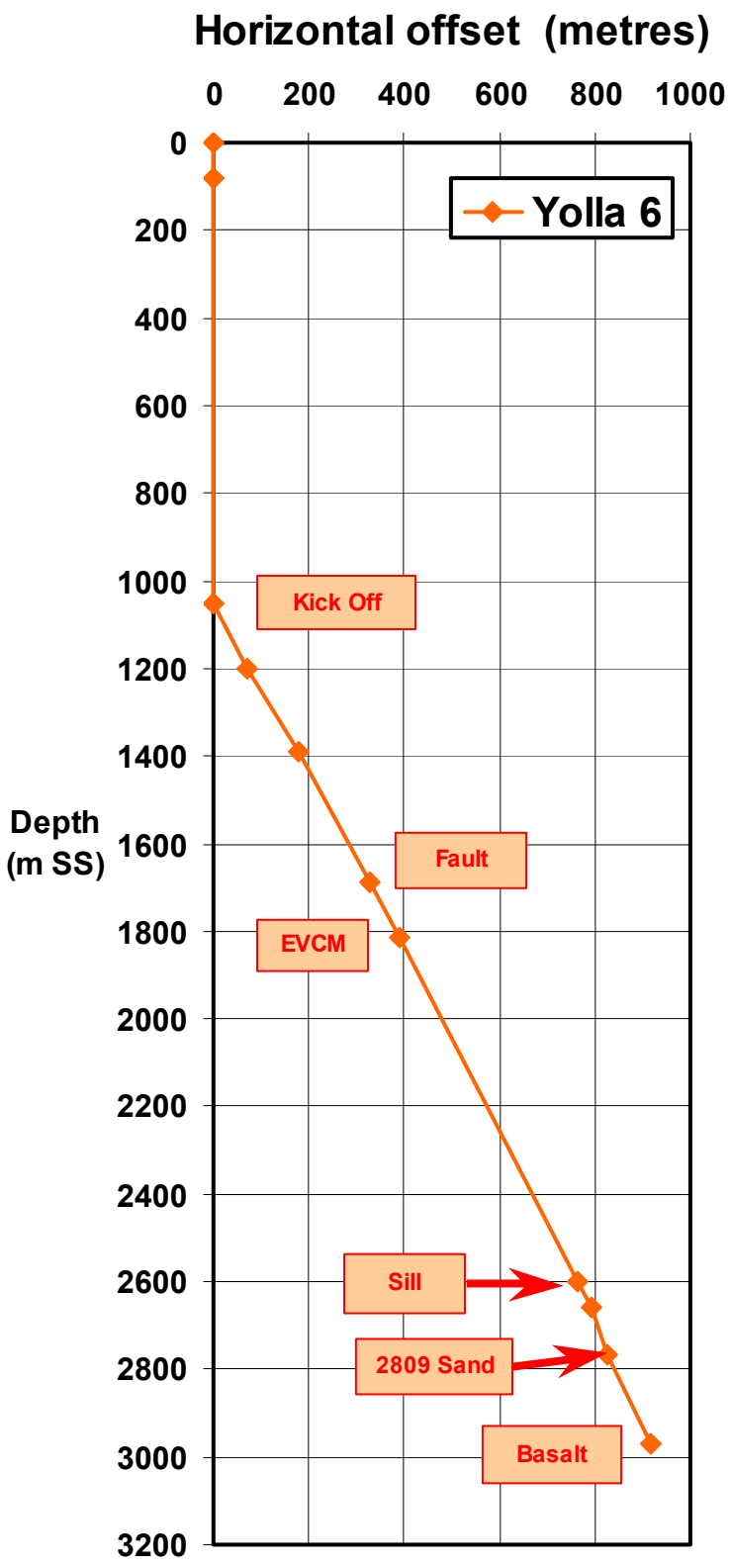

Figure 5.12: Yolla 6 indicative well path.

6 REFERENCES

Bridge J.S & Tye R.S. 2000. Interpreting the dimensions of ancient fluvial channel bars, channels and channel belts from wireline logs and cores. American Association of Petroleum Geologists Bulletin **84** (8) 1205-1228.

Malkewicz-Hueni and Associates 2000, Yolla Gas Field Reserves Review.

Prosser J. & Mahmood T. 1998. Sedimentological interpretation of Formation Micro-scanner (FMS) images from Yolla 2. Report prepared by Z & S (Asia) Ltd for PremierOil.

Taylor, R. (in prep). Yolla 3D 2000 Reprocessing Interpretation Report (Origin Energy Resources Ltd internal report).

APPENDIX 1

SELECTED POROSITY MAPS REALISATIONS FOR GEOLOGICAL MODEL

Porosity map – 2755 Sand

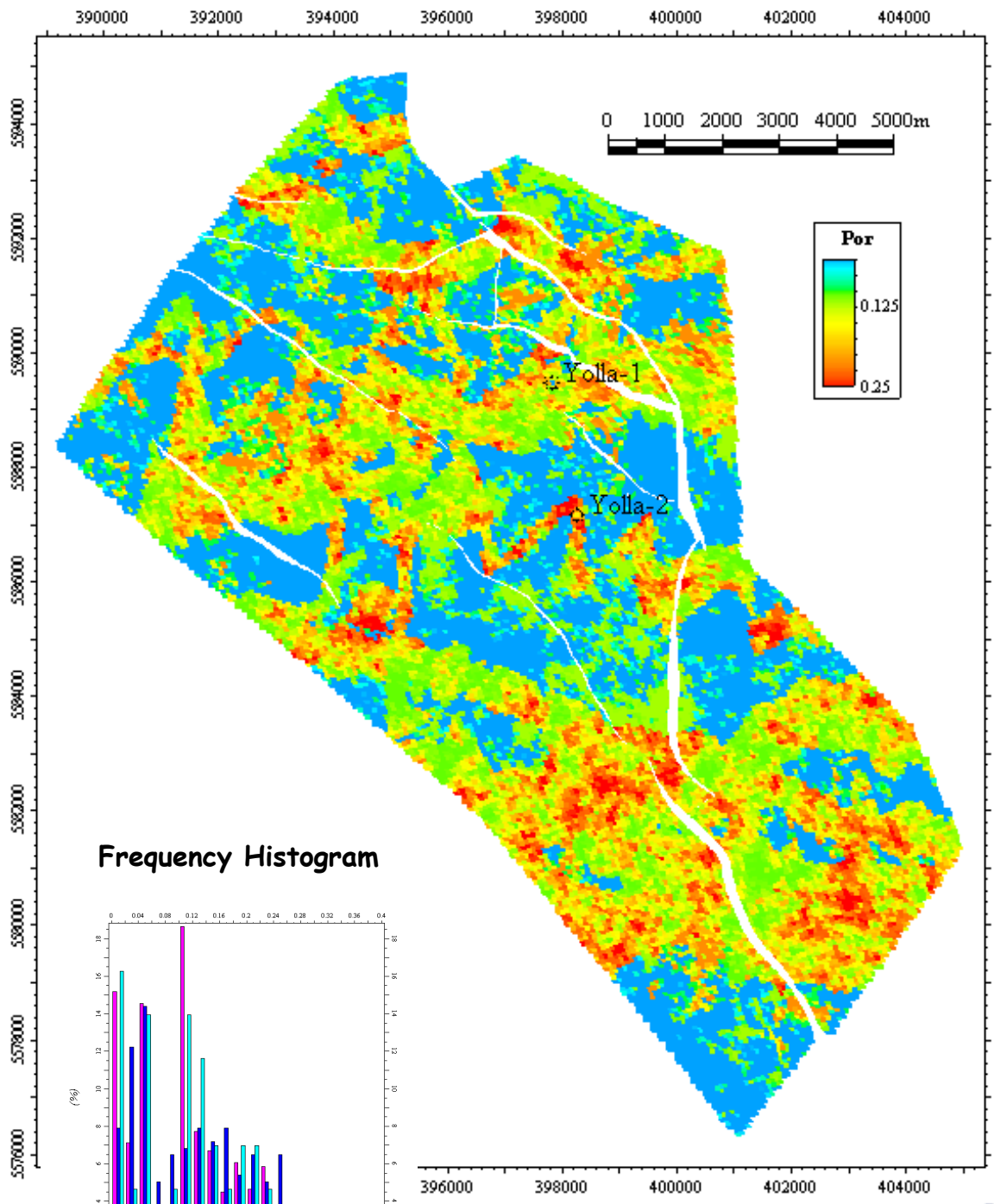

Frequency Histogram

P50 – Realisation 2

Produced with Petrel
3D eLEARNING PC

Porosity map – 2809 Upper Sand

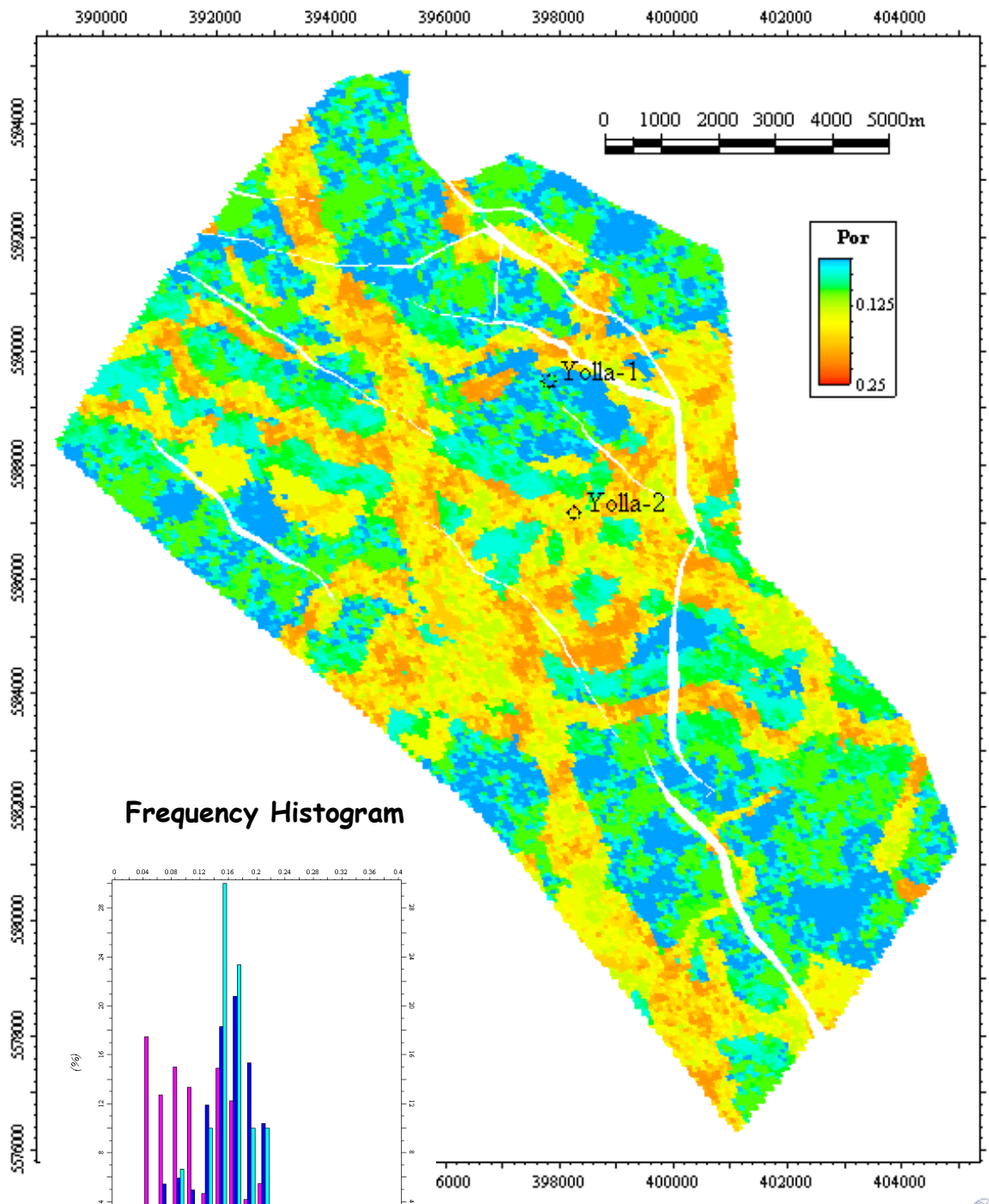

Frequency Histogram

P50 – Realisation 2

Produced with Petrel
3D at its on PC

Porosity map – 2973 Sand

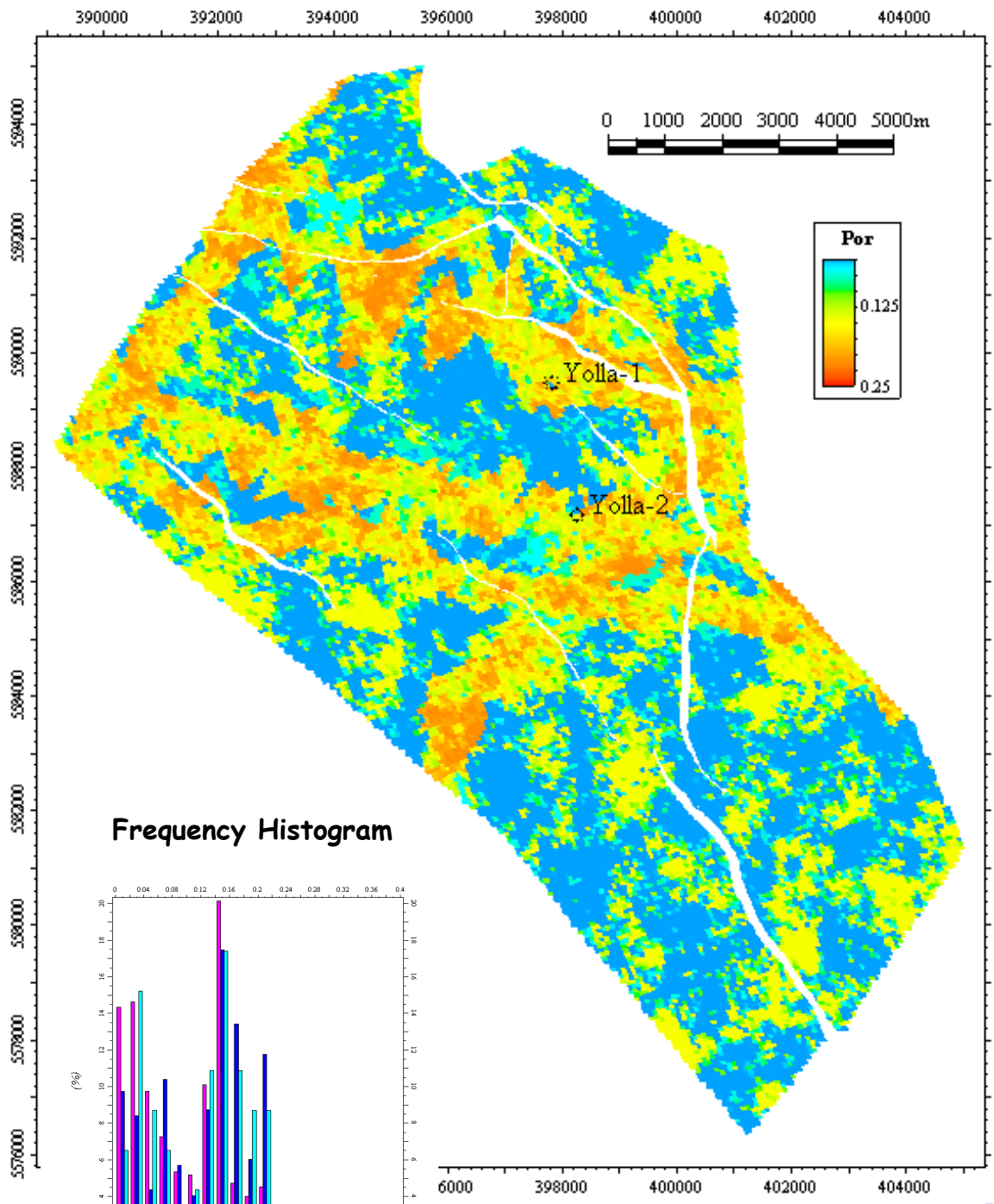

Frequency Histogram

P50 – Realisation 2

Produced with Petrel
3D at its on PC

Porosity map – 2755 Sand

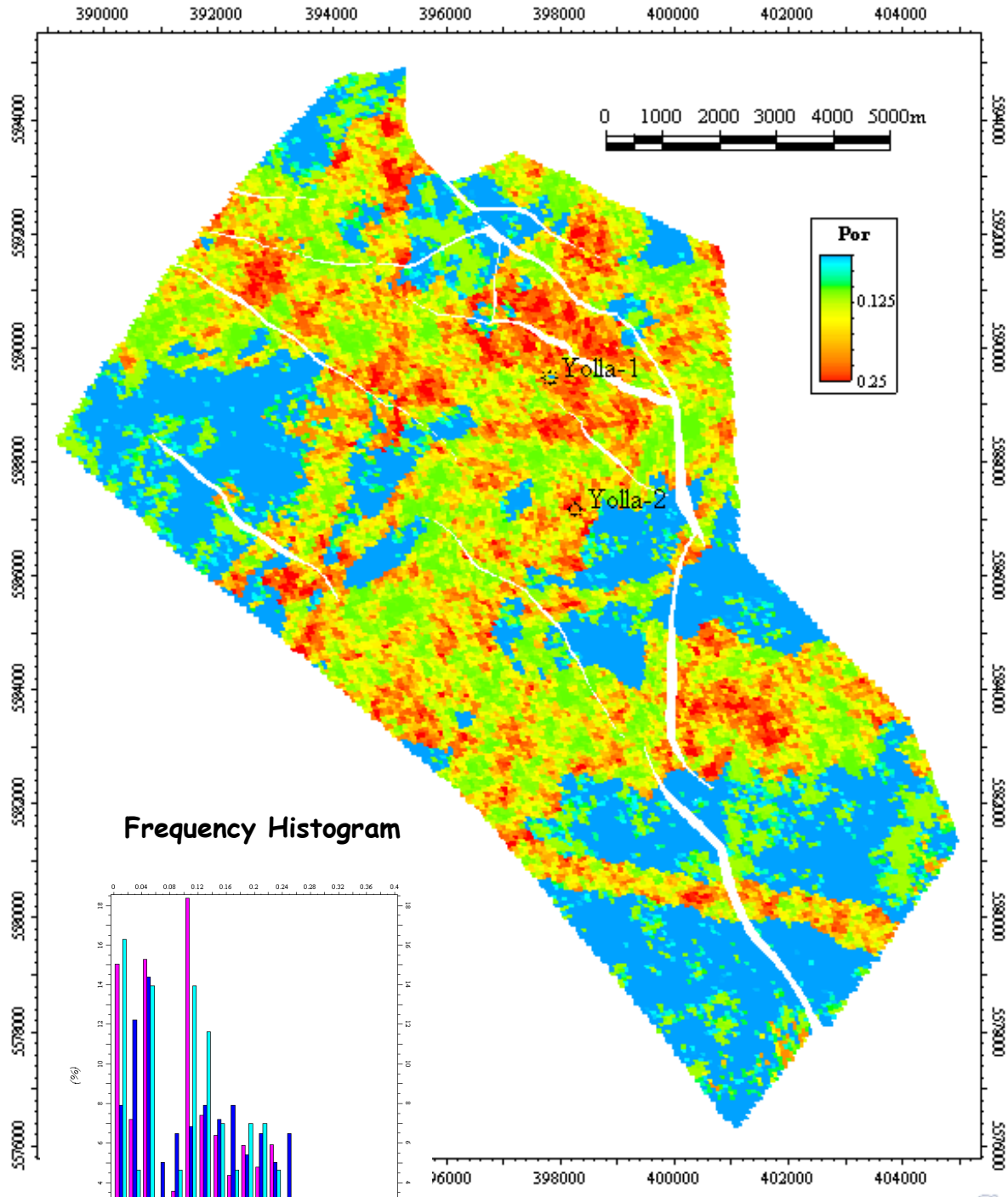

Frequency Histogram

P50 – Realisation 3

Produced with Petrel
3D at its PC

Porosity map – Upper 2809 Sand

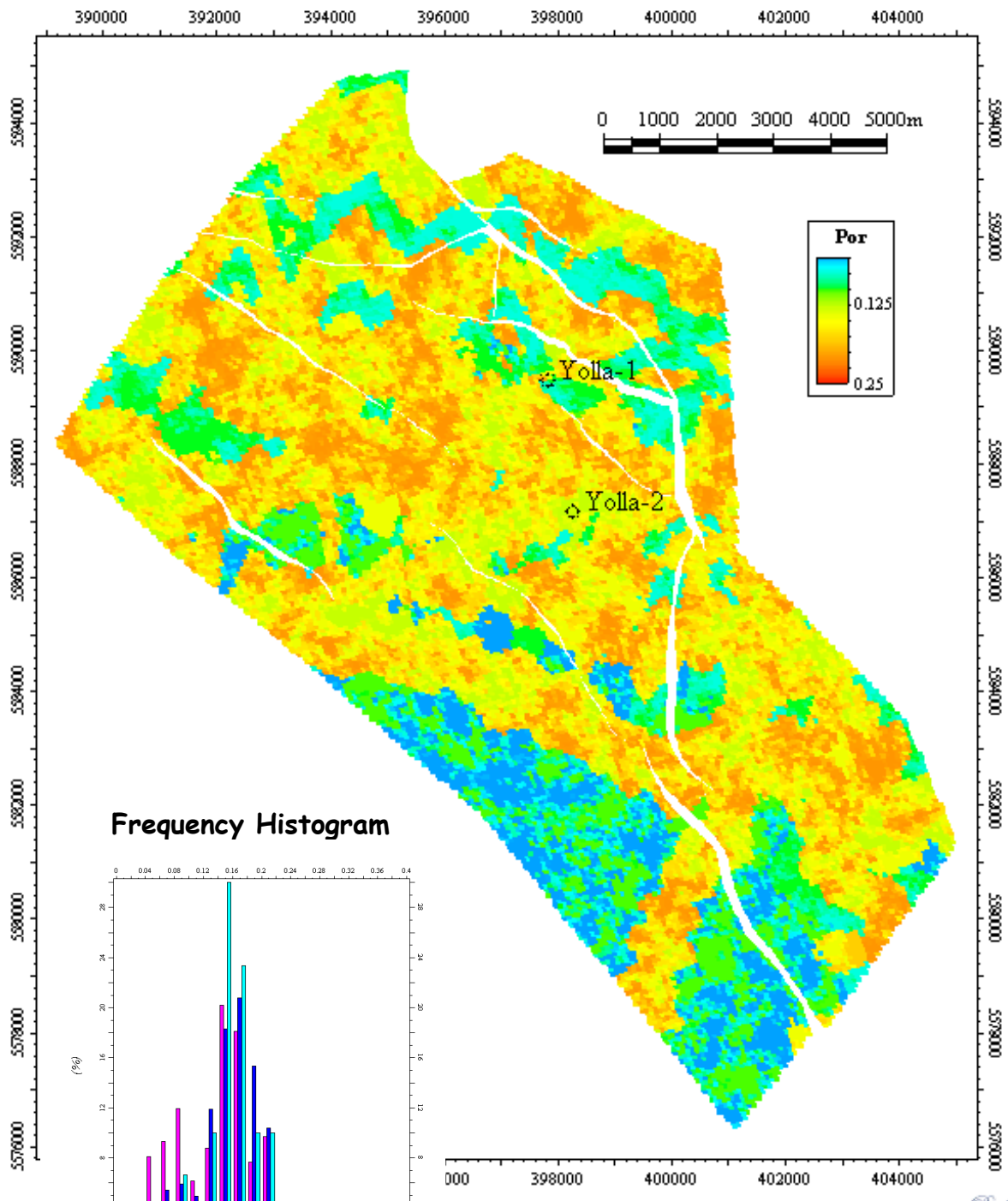

Frequency Histogram

P50 – Realisation 3

Produced with Petrel
3D at its OWN PC

Porosity map – 2973 Sand

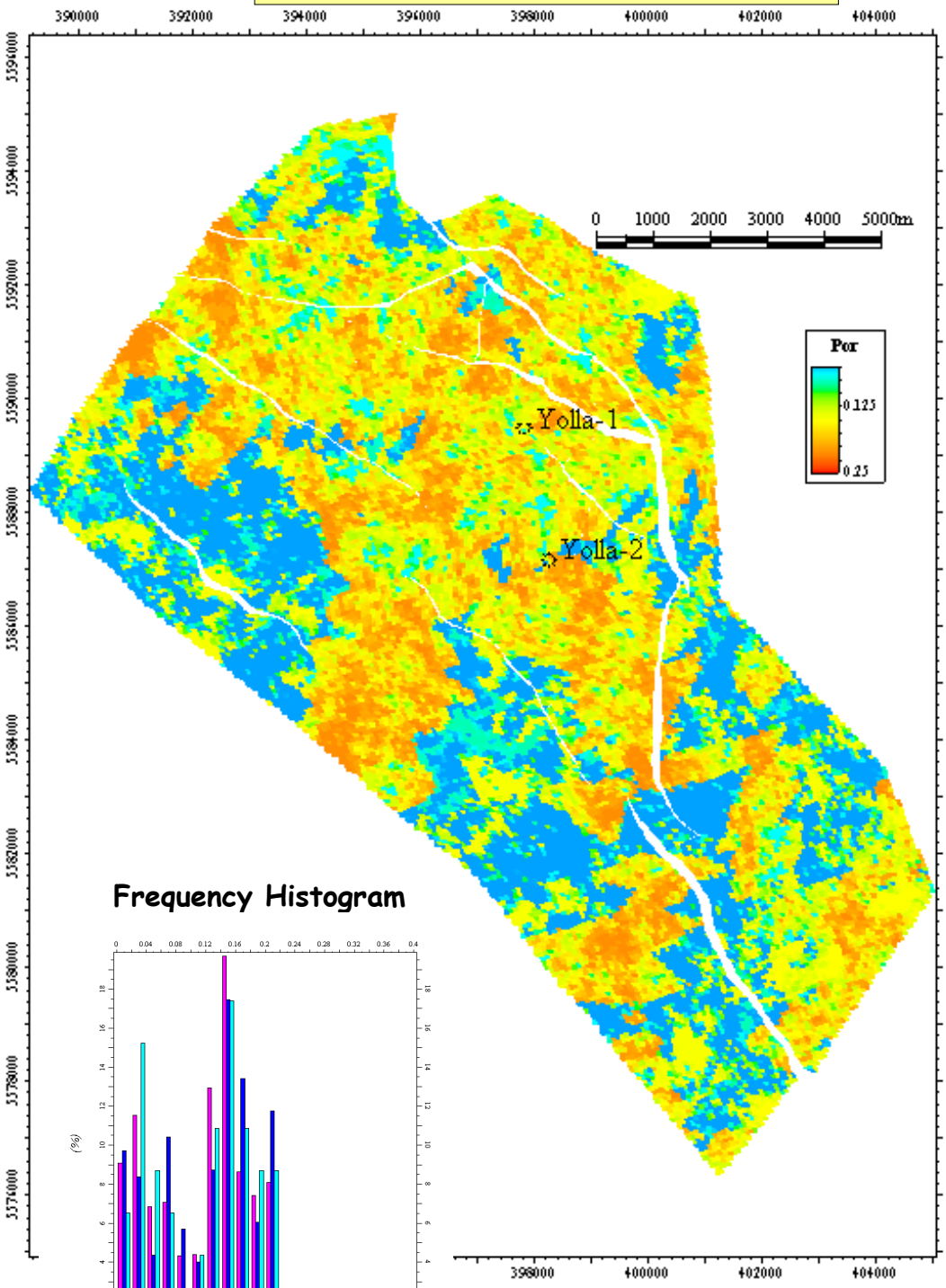

Frequency Histogram

P50 – Realisation 3

Produced with Petrel
3D 4U ON PC

Porosity map – 2755 sand

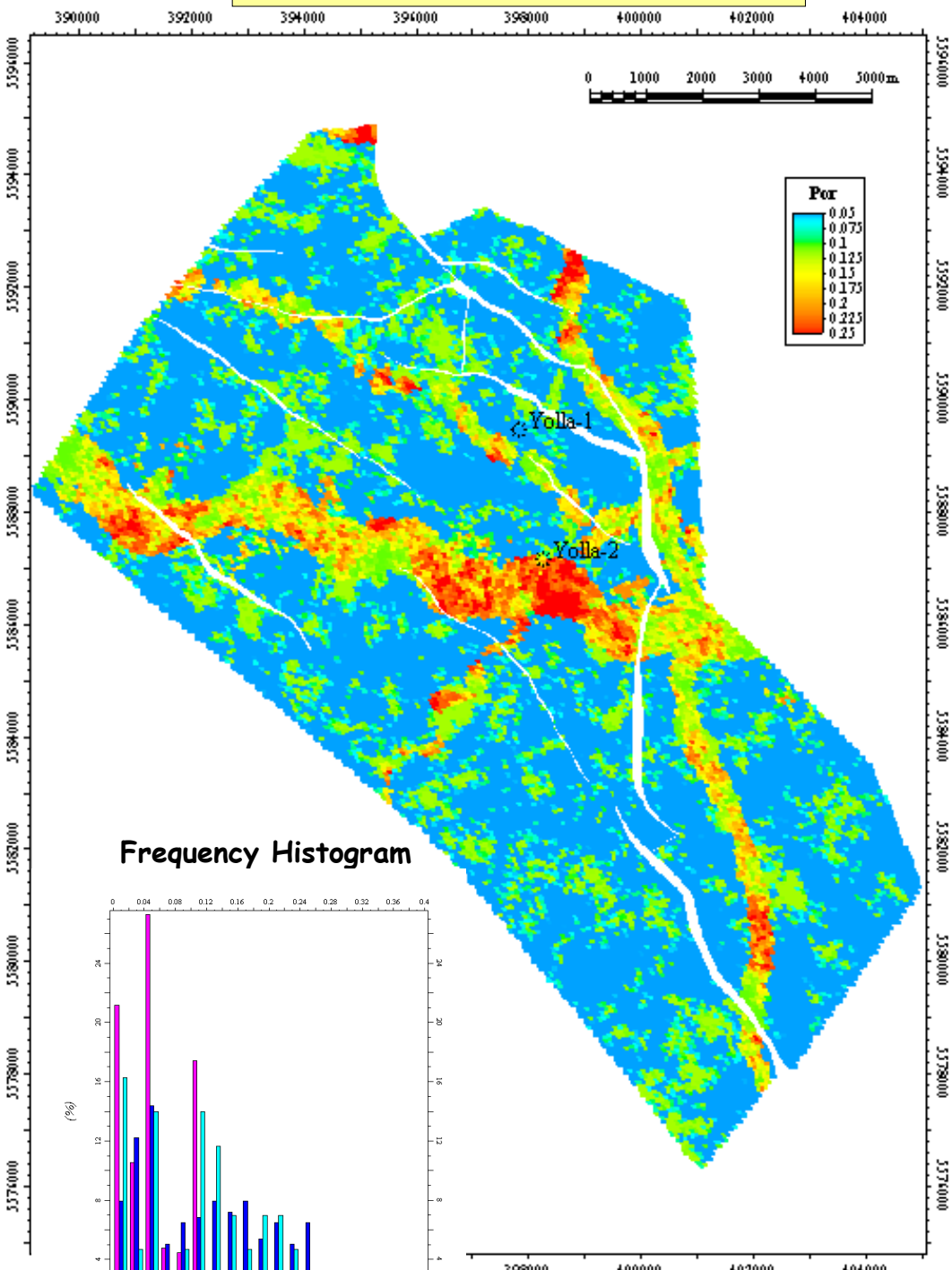

Frequency Histogram

P90 – Realisation 1

Produced with Petrel

Porosity map – Upper 2809 sand

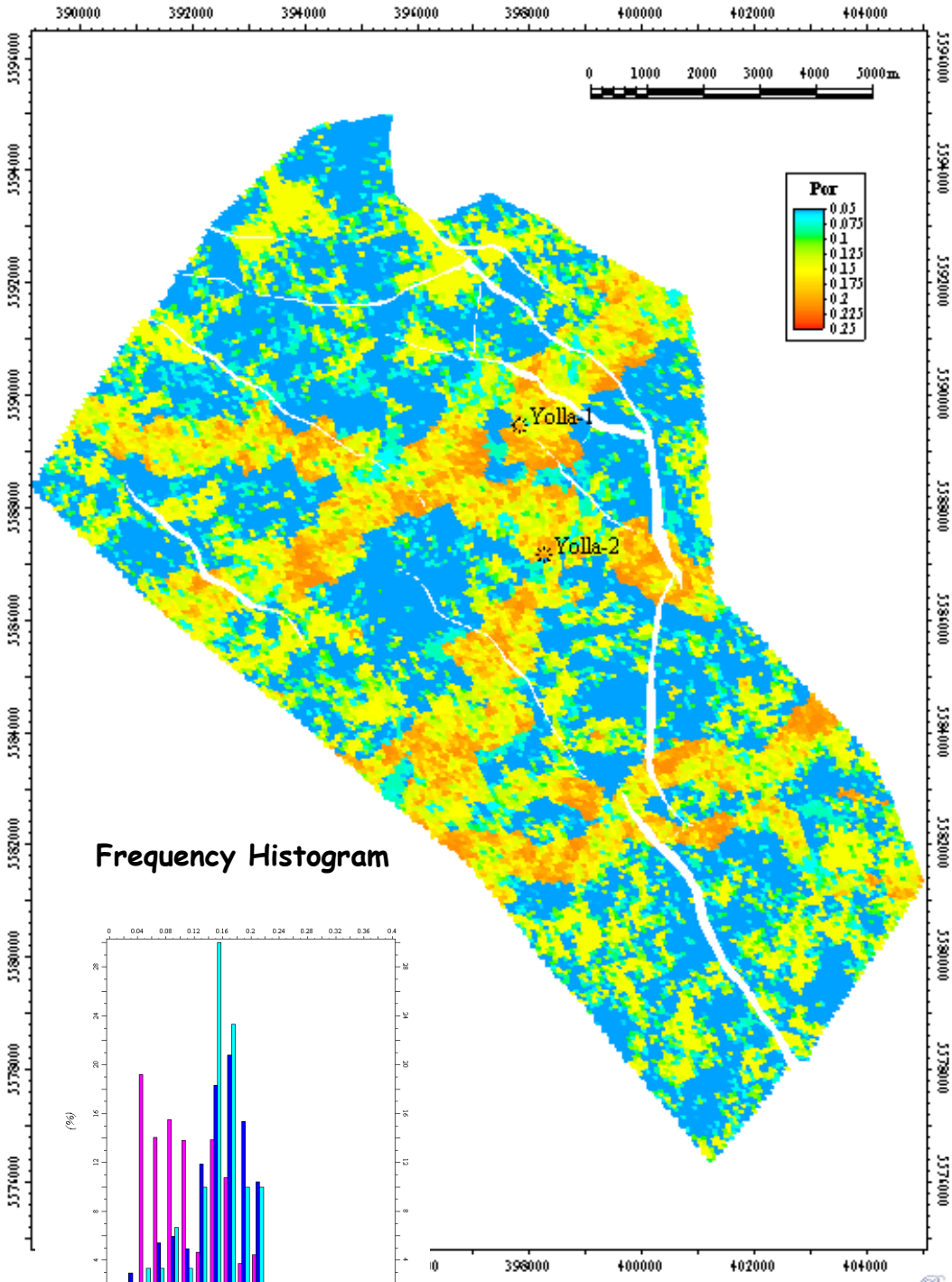

Frequency Histogram

P90 – Realisation 1

Produced with Petrel
3D-4U ON PC

Porosity map – 2973 sand

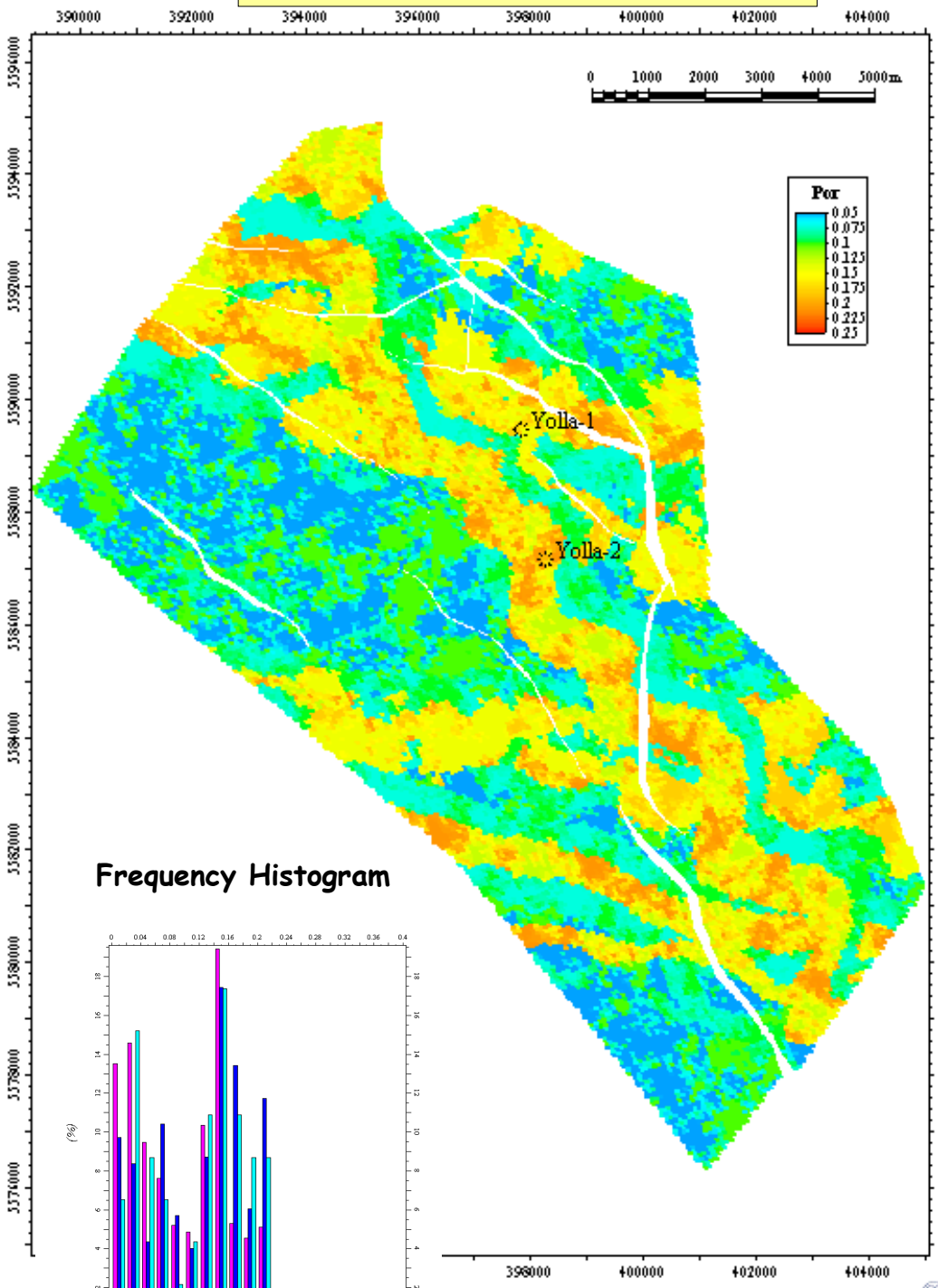

Frequency Histogram

P90 – Realisation 1

Produced with Petrel
3D-4U ON PC

Porosity map – 2755 sand

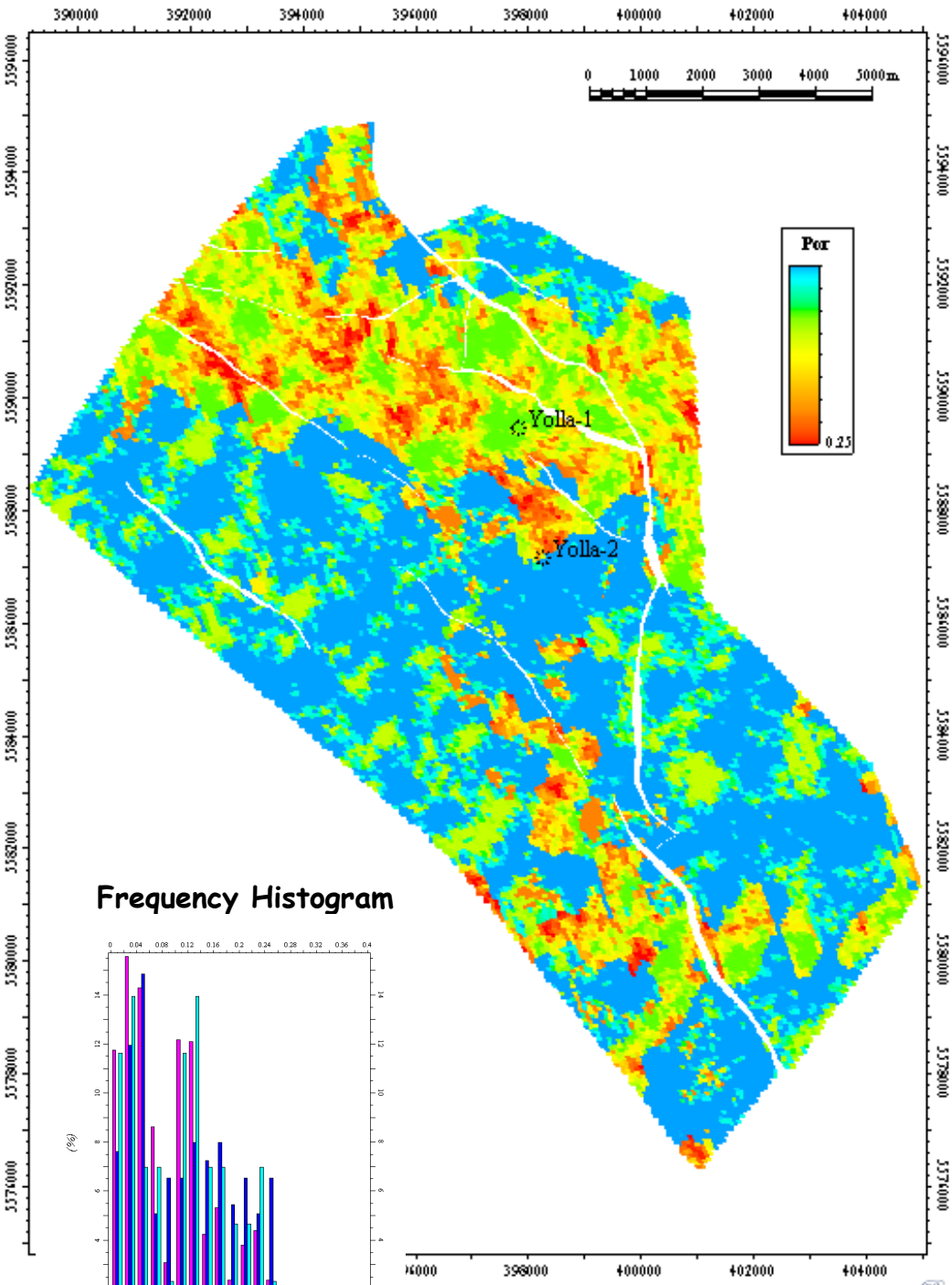

Frequency Histogram

P90 – Realisation 2

Produced with Petrel
3D-4U ON PC

Porosity map – Upper 2809 sand

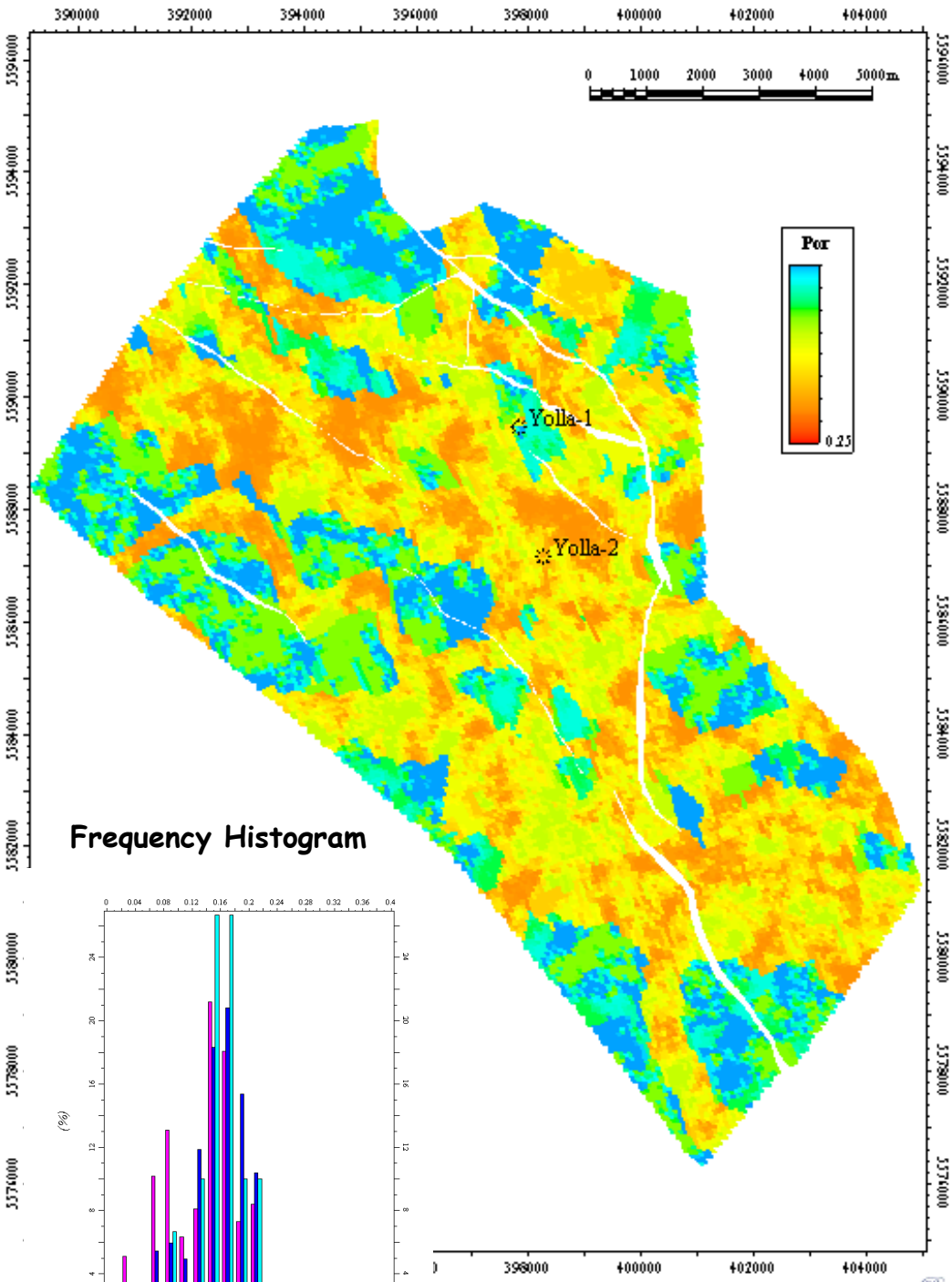

Frequency Histogram

P90 – Realisation 2

Produced with Petrel
3D 4U ON PC

Porosity map – 2973 sand

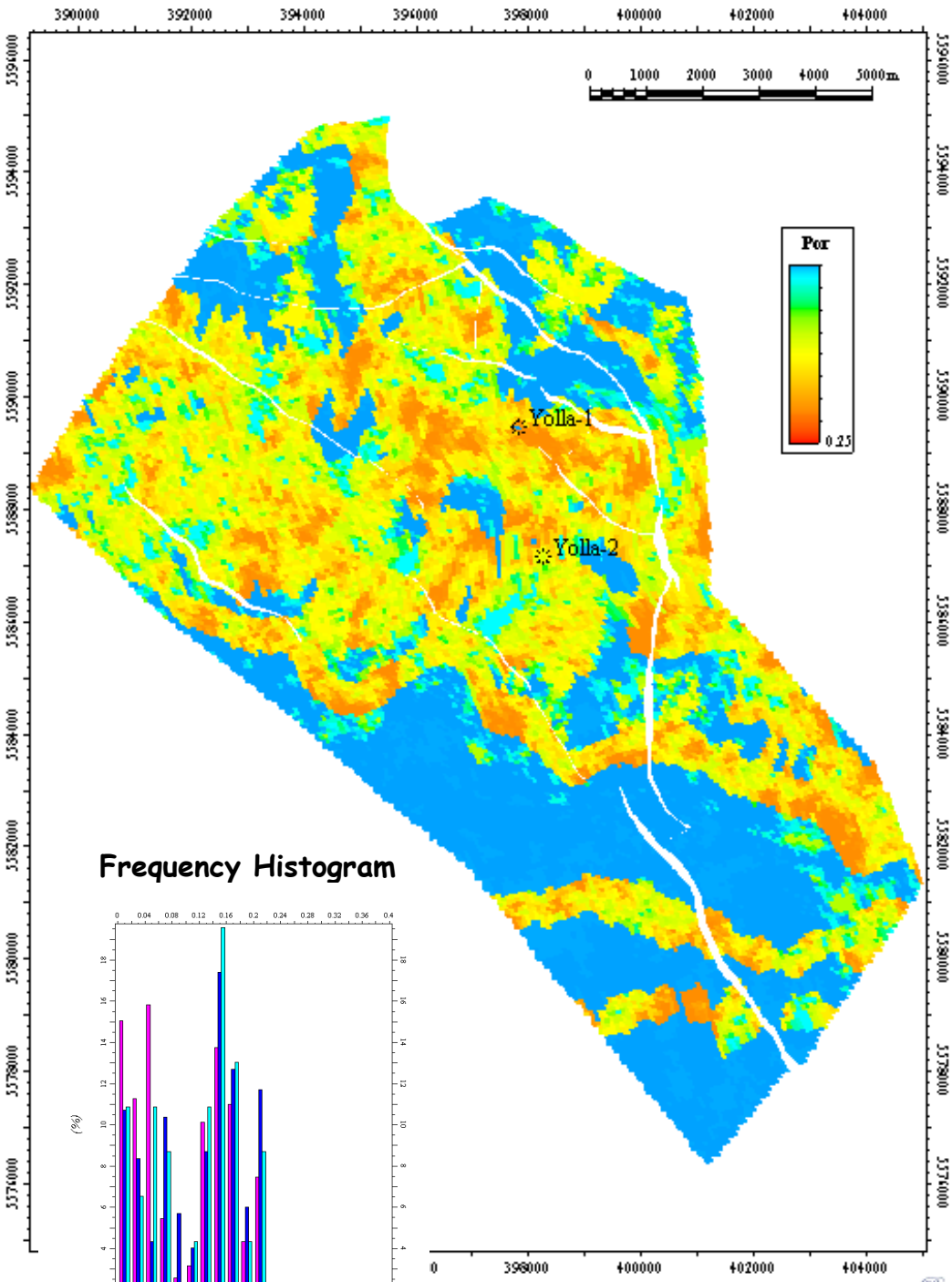

Frequency Histogram

P90 – Realisation 2

Produced with Petrel
3D 4U ON PC

Porosity map – Upper 2809 sand

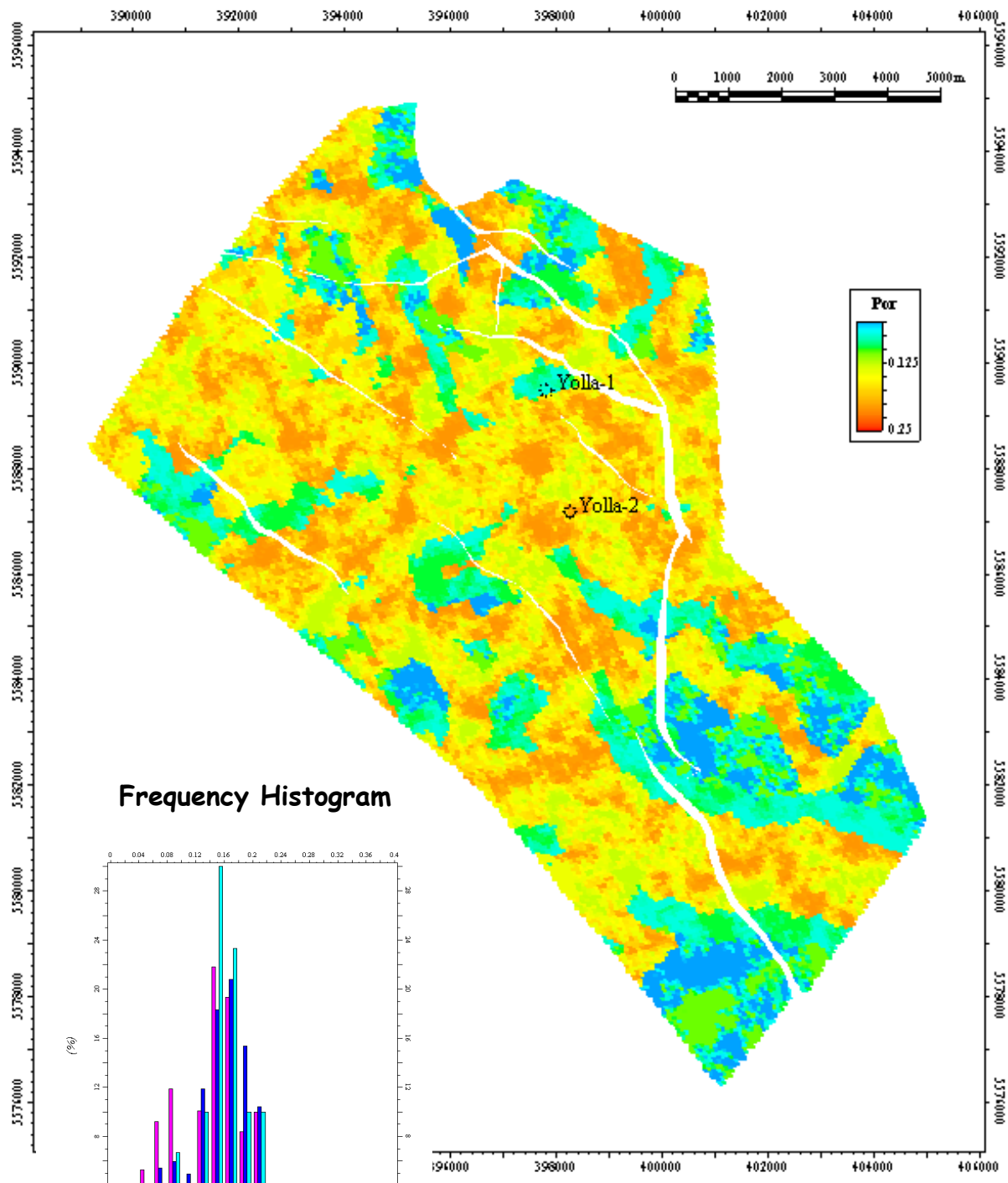

Frequency Histogram

P10 – Realisation 1

Produced with Petrel
3D 4U ON PC

Porosity map – 2755 sand

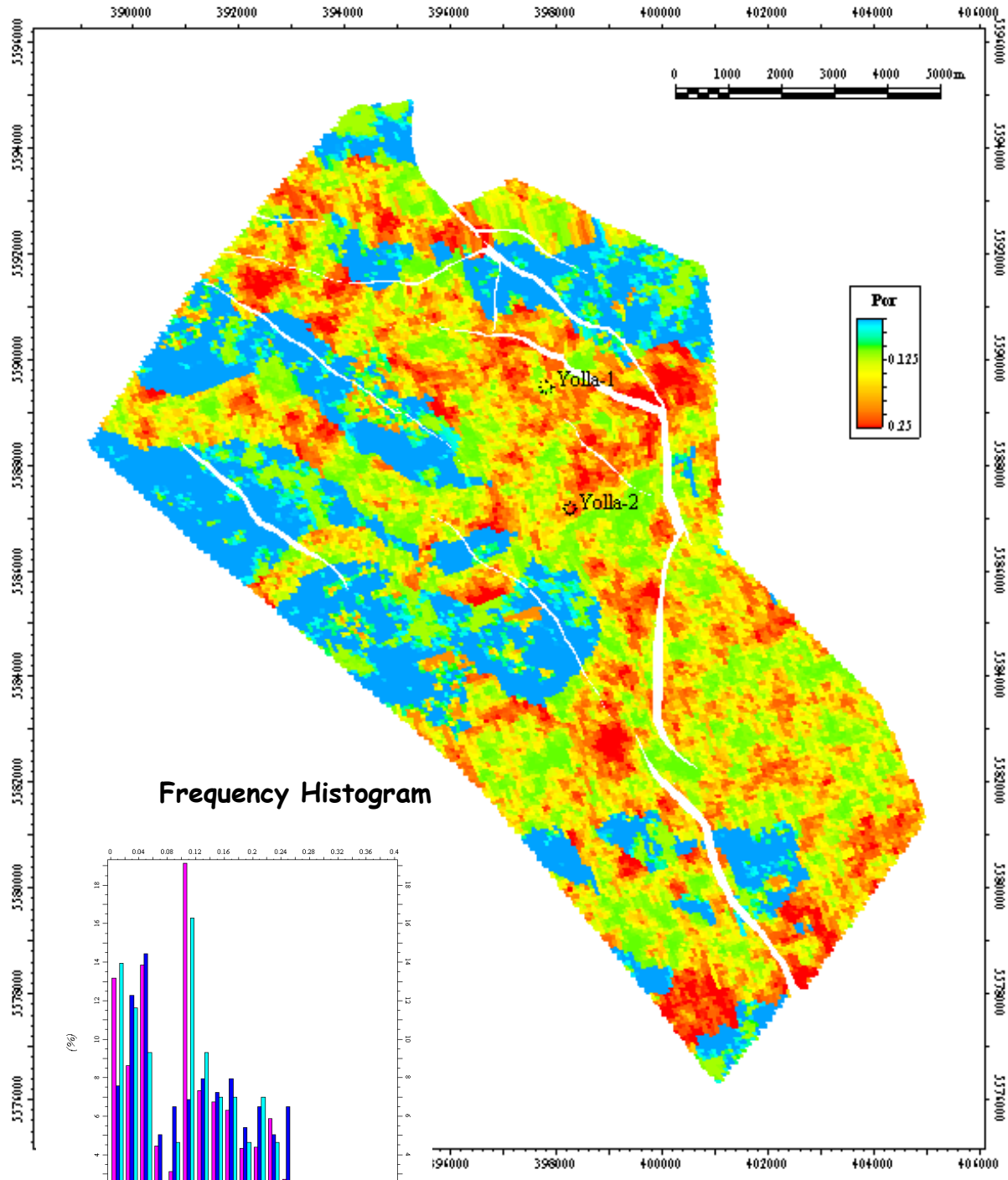

Frequency Histogram

P10 – Realisation 1

Produced with Petrel
3D 4U ON PC

Porosity map – 2973 sand

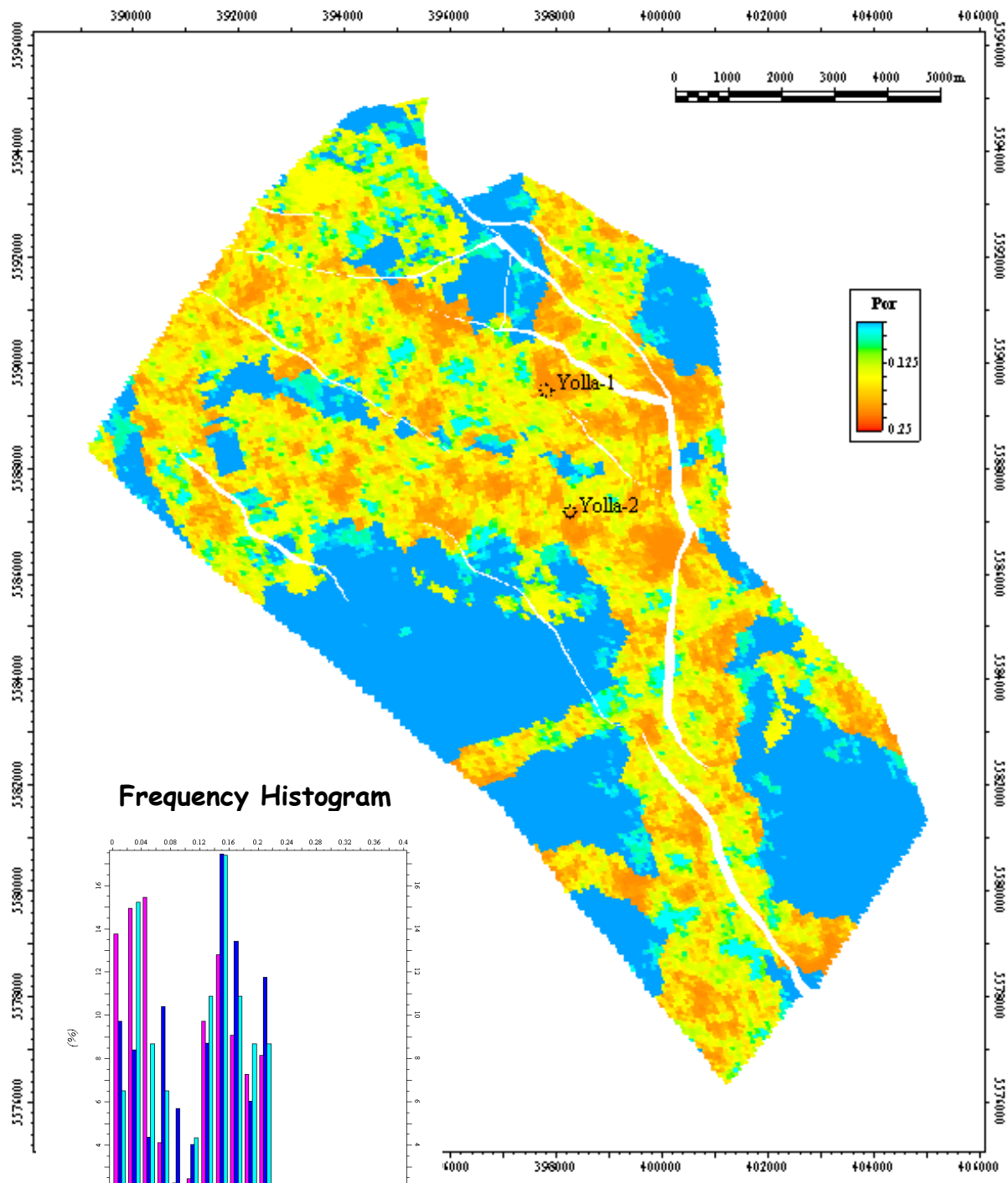

Frequency Histogram

P10 – Realisation 1

Produced with Petrel
3D 4U ON PC